TECHNICAL REPORT HSM-R05-69

NAS8-20336
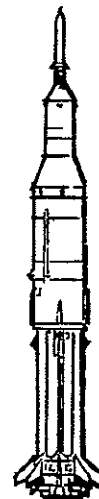
MARCH 7, 1969

APPLICATION OF THE TECHNIQUES FOR EVALUATING THE ACOUSTIC SOURCES OF BACKGROUND NOISE IN WIND TUNNEL FACILITIES

N70-28707

FACILITY FORM 602

(ACCESSION NUMBER)   (THRU)

98

(PAGES)   (CODE)

CR-102623

(NASA CR OR TMX OR AD NUMBER)   (CATEGORY)
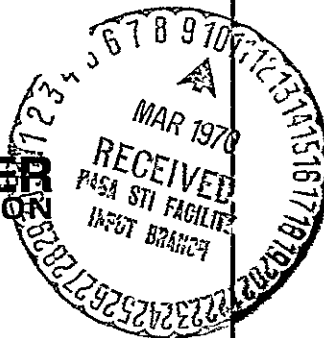
SPACE DIVISION **CHRYSLER CORPORATION**

HUNTSVILLE OPERATIONS

TECHNICAL REPORT HSM-R05-69
NAS8-20336

APPLICATION OF THE TECHNIQUES
FOR EVALUATING THE ACOUSTIC
SOURCES OF BACKGROUND NOISE
IN WIND TUNNEL FACILITIES

By

James R. Boone
George F. McCanless, Jr.

MARCH 7, 1969

SPACE DIVISION **CHRYSLER**
CORPORATION

HUNTSVILLE OPERATIONS

FOREWORD

This report was prepared by the Aero-Space Mechanics Branch, Structures and Mechanics Engineering Department, Huntsville Operations, Chrysler Corporation. The work was authorized by NASA Contract NAS8-20336 which was issued by the Unsteady Aerodynamics Branch, Aerodynamics Division, Aero-Astrodynamics Laboratory, Marshall Space Flight Center in Huntsville, Alabama. The purpose of this study is to establish methods of determining the acoustic sources of background noise in wind tunnels and the effects of background noise on dynamic test data. Suggestions are made for further testing and evaluation in the area of acoustic background noise. This is the second report in a series.

The authors wish to express their appreciation to the people who have assisted in conducting the study program. Personnel who made invaluable contributions are

R. Love	Model Design	Aero Astrodynamics Laboratory (MSFC)
J. Pritchett	Model Instrumentation	Aero Astrodynamics Laboratory (MSFC)
B. Wilbanks	Instrumentation System	Nortronics Division, Northrop
B. Neighbors	Instrumentation System	Aero Astrodynamics Laboratory (MSFC)
H. Bush	Instrumentation System	Aero Astrodynamics Laboratory (MSFC)
E. Simon	Facilities	Aero Astrodynamics Laboratory (MSFC)
S. Mallard	Facilities Operation	Nortronics Division, Northrop
J. Magnan	Facilities Operation	Nortronics Division, Northrop

ABSTRACT

Acoustic calibration tests were planned for the MSFC 14 in. and the
AEDC 16 ft transonic wind tunnels. Acoustic calibration testing has been
conducted in the MSFC 14 in. wind tunnel. The methods used in these tests
are presented. Important results of these tests are discussed and compared
with results obtained by other investigators in similar wind tunnels. Based
on these results the sources of background noise are enumerated. Recommen-
dations are made to eliminate or reduce the pressure fluctuation generated
by these noise sources.

TABLE OF CONTENTS

LIST OF FIGURES

NOMENCLATURE

<u>Symbol</u>

B_1 1/8 in. pressure transducer at M.S. 1.88 on upper flat

B_2 1/8 in. pressure transducer at M.S 2.50 on upper flat

B_3 1/8 in. pressure transducer at M.S. 5.00 on upper flat

B_4 1/8 in. pressure transducer at M.S. 7.50 on upper flat

B_5 1/8 in. pressure transducer at M S. 5.00 on lower flat

$<c_p^2>^{1/2}$ Root mean square pressure coefficient averaged over the transducer on the dynamic calibration device

E_1 Tunnel exhaust to atmosphere

E_2 Tunnel exhaust to vacuum tanks

g Conversion factor = 32.2 ft/sec^2

K_1 1/4 in. pressure transducer in tunnel stilling chamber

K_2 1/4 in. pressure transducer in T.S. nozzle blocks

K_3 1/4 in. pressure transducer in T.S. nozzle blocks and in S.S. window plate

K_4 1/4 in. pressure transducer in center of test section walls (on porous walls in T.S. and in window plate of S.S.)

K_5 1/4 in pressure transducer at M.S. 7.50 on lower flat

K_6 1/4 in. pressure transducer in tunnel exhaust

K_7 1/4 in pressure transducer in tunnel exhaust (K_{7_A} – atmos ; K_{7_V} – vacuum)

L Length of body, ft

ℓ Length on a body, ft

M Mach number $V / \sqrt{\gamma\, gRt_s}$

<u>Symbol</u>

M_1	Calibration cone, Figure 4.3
M_2	Boundary Layer Transition cone, Figure 4.8
p_ℓ	Local static pressure, psf
Δ_{p_ℓ}	Local incremental static pressure, $p_\ell - p_\infty$, psf
p_∞	Free stream pressure, psf
$<p>$	Root mean square pressure, psf
P_o	Stagnation or total pressure
q	Dynamic pressure $= \frac{1}{2}\rho V^2 = \gamma p_\ell\ M^2/2$, psf
R	Gas constant, ft-lbs/lbs°R
R_N	Reynolds number $= \rho V\ell/\mu = V\ell/\nu$
R_N/ft	Reynolds number per foot $= \rho V/\mu = V/\nu$, 1/ft
$R(\tau)$	Correlation function at a specific point
S.S.	Supersonic test section
T_1	Standard Tunnel configuration, Figure 2.2
T_2	Atmospheric inlet at test section (Tunnel test section separate from stilling chamber), Figure 2.3
T_3	Atmospheric inlet at stilling chamber entrance (tunnel stilling chamber separate from valve and storage tank), Figure 2.4
T_4	Standard tunnel configuration with solid walls in place of porous walls
$T_{2,4}$	Atmospheric inlet at test section with solid walls (tunnel test section separate from stilling chamber)

T.S. (B-1)	Transonic test section with transonic nozzle blocks
T.S. (B-2)	Transonic test section with M = 1.45 nozzle blocks
T.S. (B-3)	Transonic test section with M = 1.95 nozzle blocks
t	Time, sec
t_s	Local static temperature, °R
t_o	Stagnation or total temperature, °R
V	Local velocity, ft/sec
x, y, z	Co-ordinates
γ	Ratio of specific heats
δ	Cone half angle, degrees
μ	Absolute coefficient of viscosity, lb $-$ sec/ft^2
ν	Kinematic coefficient of viscosity = μ/ρ, ft^2/sec
ρ	Density, slugs/ft^3
τ	Time, sec
τ_1 through 23	Temperature measuring thermocouples on cooled model, °R

1.0 INTRODUCTION

Prior to this decade the unsteady forces that act on aircraft, missiles, and space vehicles were generally ignored. This was permissible because of the large safety factors that were previously in use. These large safety factors were dictated by the general lack of refinement in the methods of aerospace engineering. However, ever increasing precision is being required in the methods of aerospace engineering. This is caused by the following factors:

- The large cost of the aircraft, missiles, and space vehicles that are built today precludes the earlier procedures of trial and error.

- The competitive nature of the aerospace field requires improvements in performance. This in turn requires that all variables in the system be optimized.

- Commercial transports now carry large numbers of people and space vehicles are now manned. These considerations demand steady improvements in safety.

The increases in design precision imply that the unsteady aerodynamic forces must be established early in the development program. This establishes a basis for designing the structure so that it will withstand the dynamic loading and yet not be excessively heavy. The need for unsteady aerodynamic data is accented by the fact that the structures that are currently being built are larger than those that were fabricated several years ago. The skin of these structures is about the same thickness as those used with the smaller aircraft, missiles, and space vehicles. This combination results in flexible structures that are highly responsive to unsteady aerodynamic excitations.

The unsteady aerodynamic phenomena that must be determined in order to design aircraft, missiles, and space vehicles are briefly described below:

- Boundary Layer Turbulence

  This phenomena can cause fatigue failures and can saturate control sensors. The noise generated by turbulence, especially jet turbulence, can cause discomfort or injury to man. Reducing the turbulent flow area by extending the laminar flow regime will also reduce drag.

- Panel Flutter

  Panel flutter can result in both direct structural failure and fatigue failures.

- Wing or Fin Flutter

  This type of flutter can also result in direct structural failure and fatigue failure.

1

- ### High Angle-of-Attack Buffeting

  This mode of buffeting can result in structural failure.

- ### Transonic Buffeting

  Transonic buffeting can cause any of the problems mentioned above.

- ### Ground Wind Oscillations

  Ground winds cause structures to oscillate. This problem is particularly acute with missiles and space vehicles which can be blown over.

The unsteady aerodynamic loads must be established by experimental testing, because theoretical procedures have not been perfected that are adequate for establishing the vehicle design requirements. Wind tunnel tests have been found to be generally the most satisfactory means of determining the fluctuating pressure environment However, virtually all wind tunnels were designed before the time that the need for unsteady aerodynamic testing was recognized Thus, little or no attempt was made to minimize the background pressure fluctuations that are inherent in fluid flow processes.

Several investigators have measured fluctuations in subsonic, transonic, and supersonic wind tunnels. Mahinder S. Uberoi conducted a study in a subsonic wind tunnel on the behavior of turbulence as it passes from the stilling chamber through the throat of the tunnel. This study is described in Reference 1. The wind tunnel had the blower downstream of the test section and used an open return. Virtually all of the data was obtained with hot wire anemometers. Based on his study, Uberoi states, "Turbulent velocity measurements show that in absolute magnitudes, the longitudinal component decreases and the lateral component increases as the flow accelerates through the contraction " He found that turbulence from the blower was being propagated through the open loop and into the test section. This was eliminated, or stabilized, by installing a honeycomb in the stilling chamber. It was also found that sound waves generated by the blower were being radiated up stream to the test section This conclusion was based on the fact that a correlation coefficient of 0.9 was computed from the measurements of velocity fluctuations across the test section. Uberoi extends his results by stating, "For supersonic nozzles, elementary considerations show that the effects of increase in the mean speed and decrease in density are both beneficial in reducing the flow irregularities."

Tests were conducted by Mark V. Morkovin in the continuous supersonic wind tunnel at John Hopkins University. These tests are described in Reference 2. All tests were at Mach 1.76. He considers three fluctuations modes.

- "Sound mode (variation of pressure, density, and temperature).

2

• Entropy mode (variation of entropy, density, and temperatures).

• Vorticity mode (Variation of the sinusoidal component of the velocity field which is known as turbulence at incompressible speeds)."

He states that, "The entropy and vorticity modes are essentially convected along streamlines so that in a supersonic tunnel they must be traceable.. to conditions in the stilling chamber." He further states that, "The sound disturbances can travel across streamlines so that they come from the settling chamber and from the boundaries of the test section."

Morkovin then classified the sound fluctuations originating at the wall into four types:

a. "Radiation from nascent turbulence...

b. Radiation from developed turbulent boundary layers.

c. Diffraction and scattering of otherwise steady pressure gradients and shock waves (as generated by nozzle contours unintended waviness or roughness, models, supports, etc.) through the turbulent boundary layer.

d. Radiation from unsteady wall vibrations caused by pressure fluctuations in the boundary layer or by the loads on the diffuser associated with the unsteadiness of the terminal shock wave."

From hot wire anomometer data he concluded that the ratio of the rms pressure fluctuations to the free stream static pressure is 0.2 to 0.4. This converts to a rms pressure coefficient of 0.00092 to 0.00185. "For a given wall geometry this sound of category (c) is likely to decrease with Mach number [while that of category (b) may possibly increase]." He concludes that the fluctuations are not convected from the stilling chamber. For this to be significant, he states that the fluctuations in the test section would have to be 114 db, where as in normal operation the noise lvel in the stilling chamber of this continuous flow tunnel was in the range of 70 to 80 db. However, during the starting process (before sonic conditions), large sound levels were present in the stilling chamber which originated in the diffuser. He also concludes that magnitude of sound category (d) is unlikely to reach the intensity of the sound of category (c), i.e., 120-130 db.

J S. Murphy (References 3 and 4) conducted an early study of the pressure fluctuations in the Douglas Trisonic One-Foot Tunnel. This is a blowdown facility with a Mach number range of 0.2 to 1.8. Tests were conducted over this Mach number range using microphone, hot wire anemometers, strain gauge dynamic pressure transducers. It was concluded that the primary cause of the pressure fluctuations in the stilling chamber is a high-intensity sound field

3

that originated in the neighborhood of the control valve. A sound-absorbent muffler was designed, built, and installed in the stilling chamber. At Mach 1.0 it reduced the value of the rms pressure coefficient in the test section from 0.058 to 0.022. The reduction in the ratio of the stilling chamber rms static pressure to stagnation pressure is from 0.025 to 0.005. This proved that a large portion of the fluctuations in the test section are caused by fluctuations either in the entrance to the stilling chamber or upstream of it.

John Laufer conducted a study in 1961 of the fluctuation levels in the 18 x 20 in. supersonic wind tunnel at the Jet Propulsion Laboratory. Reference 5 describes this study. This is a closed circuit, continuous wind tunnel with solid walls in the test section. The tests were conducted over the Mach number range of 1.6 to 5.0. Virtually all data was obtained with a hot wire anemometer. Velocity fluctuations measured in this manner were used to compute the test section static pressure fluctuations. This resulted in a computed value of the rms pressure coefficient of 0.0009 at a Mach number of 1.6. It was concluded that the source of the fluctuations is the turbulent boundary layer on the test section walls. Laufer states that the Reynolds number of the tunnel was lowered to the point that the boundary layer on the walls was laminar. This caused the fluctuation level in the test section to drop by an order of magnitude.

P A. Irani and K. Sridnor Iya (Reference 6) surveyed the general problem area of aerodynamic noise. Their objective was to establish a rational basis for reducing the noise level in the trisonic wind tunnel at the National Aeronautical Laboratory, Bangalore, India. Of special interest is their description of the noise reduction program conducted by R. Westley of the National Aeronautical Establishment, Ottawa, Canada. Westley's objective was to reduce the fluctuation level in the NAE 5 x 5 ft trisonic wind tunnel. This is a blowdown tunnel with a Mach number range of 0.2 to 4.5. A scale model of this tunnel was built with a 5 x 5 in. test section. Stilling chamber pressure fluctuations measuring ±0.023 of the settling chamber static pressure were obtained. This converts to an approximate value of 0.016 for the ratio of the rms static pressure to the stagnation pressure. Dynamic pressure transducers were used to measure the test section pressure fluctuations. These measurements resulted in a rms pressure coefficient of 0.038. External micorphone measurements were made above the wind tunnel. The largest noise levels were measured near the control valve and near the diffuser shock wave. At a Mach number of 1.17, noise levels of approximately 110 db were measured at both locations.

J. S. Murphy, D. A Bies, and W. W. Speaker (Reference 7) conducted studies of boundary layer noise in the previously described Douglas Trisonic One-Foot tunnel. A 26,000 cu ft tank was connected parallel to the 8,000 cu ft reservoir of the tunnel. This facilitated the operation of the tunnel by maintaining the reservoir pressure at the tunnel stagnation pressure. There was no choked flow through a control valve with its associated stilling chamber fluctuations. The stagnation pressure reduces slightly during tunnel operation. However, satisfactory test conditions of 15 sec were obtained. The authors state, "The modification of the blowdown wind tunnel, enabling operation with stagnation pressure equal to reservoir pressure, produced a facility which has satisfactory characteristics (low background noise level) to enable boundary layer noise to be measured

over the Mach range $0.4 \leq M \leq 3.5$ in a single experimental arrangement." Unfortunately, no comparative data is given to show how much (if any) reduction is achieved in the pressure fluctuations in the test section.

Hartmut Bossel conducted a dynamic investigation, which is described in Reference 8, of the Hess 6 in. supersonic wind tunnel This is a continuous, closed-cycle tunnel with a Mach number range of 1.8 to 2.8. Tests were conducted with dynamic pressure transducers in the test section. He found that in the test section "The mean fluctuation from the mean wall static pressure was about 0.3% at Re = 4 x 10^5/in." at Mach number 2.4. This corresponds to a rms pressure coefficient of approximately 0.00075. Spectrum analysis showed peaks at about 260 and 10,000 cps. Observations were made in the stilling chamber of the flow following the last screen. Here erratic jumps occurred in the flow direction of 15 degrees with a frequency of about 5 cps.

Modifications were made in the stilling chamber. The final screen was removed and a 3 in. thick honey comb screen was installed. The stilling chamber flow channel surfaces were smoothed. The static pressure fluctuations were no longer measurable. Hot wire measurements showed that the large low frequency disturbances disappeared. An additional modification was made to the tunnel. It consisted of removing a portion of the boundary layer by suction prior to the nozzle throat. Hot wire anemometer tests were then conducted. The suction was found to be beneficial at high Reynolds numbers and detrimental at low Reynolds numbers.

A sidewall calibration of the AEDC 16 ft transonic tunnel was conducted by the Martin Company during a 6 percent Titan III B Agena model test. This calibration is described in Reference 9. Two pressure microphones were located on the wind tunnel sidewalls. Both microphones were located upstream of the porous tunnel walls. The data from these microphones were presented as sound pressure level versus frequency. In addition, C. D. Riddle conducted cone calibration tests in the AEDC 16 ft transonic and 16 ft supersonic wind tunnels. A description of this calibration is given in Reference 10. The tests in the transonic tunnel covered the Mach number range of 0.6 to 1.4; supersonic tunnel data encompassed the Mach number range of 1.8 to 3.1. The calibration device consisted of a 10° apex angle cone. Two dynamic sensors (a transducer and a microphone) were located longitudinally adjacent to each other at three body stations. The rms pressure coefficient from these tests reached a maximum of 0.028 at Mach number 0.78. Below Mach number 0.70 and above Mach number 0.85 the rms pressure coefficient is less than 0.016.

Data from both of these tests were reduced in terms of power spectral densities by the authors. Reference 11 gives this reduced data. Examination of these power spectral densities reveals a large concentration of fluctuations at frequencies between 500 and 600 cps in the low transonic Mach number regime. This fluctuation concentration reaches a maximum at Mach number 0.75 and decreases both below and above this Mach number. Above the sonic Mach number the fluctuation concentration essentially disappears. The frequency composition remains virtually constant with varying Mach number. Further examination of

5

the reduced data shows that a concentration of fluctuations occurs between approximately 1800 and 2500 cps. Both cone and sidewall calibration data indicate that this concentration of fluctuations is a function of a Mach number between Mach number 0.75 and Mach number 1.30.

Tests were conducted by J. A. B. Wills in a low speed (160 ft/sec max), open circuit, 15 x 10 in. cross section wind tunnel. He describes these tests in Reference 12. He theorized that, "The combination of rapidly-growing boundary layers and comparatively high speeds (in the sonic diffuser) produces intense low-frequency fluctuation which propagate back through the working section as sound waves." He operated the tunnel without the diffuser and observed that the low frequency fluctuations in the test section were greatly reduced. This substantiated his hypothesis.

J. M. Christophe and J. M. Loniewski conducted tests in the transonic test section of the S-2 wind tunnel of the Modane (France) ONERA test center. Reference 13 includes the results of these tests. This facility is a closed circuit, continuous wind tunnel with a 6 x 6 ft cross section. The transonic circuit covers a Mach number range of 0.2 to 1.3. Fluctuations occur in the test section between Mach number 0.62 and 0.91. The frequency of these fluctuations decreased as the Mach number increased from 0.56 to 0.8.

The objective of these tests was to establish the source of the 500-700 cps acoustic perturbations. It was found that there were no fluctuations in the stilling chamber. Changing the second throat had no effect on the test section fluctuation, and altering the plenum chamber volume had only a secondary effect on the fluctuations The investigators found that, "Using a tape to cover completely the perforations of the upper and lower walls led to the elimination of the perturbating frequencies as evidenced simultaneously by the analyzer and by the change in noise from the wind tunnel." The fluctuations were not influenced by variations in the permeability (or porosity) of the lateral walls The authors conclude that the fluctuations in this tunnel can be eliminated by setting the upper and lower walls between 0 and 0.05% permeability.

Currently Chrysler Huntsville Operations is conducting a study of background pressure fluctuations in wind tunnels. The purpose of this study is to present methods to determine the acoustic sources of background noise and their effects on dynamic test data. Methods of reducing these fluctuations and methods of correcting dynamic test data to account for these fluctuations will also be established.

The study was initiated by making a survey of related dynamic wind tunnel evaluations These studies, which have been briefly outlined above, describe numerous mechanisms that can generate fluctuations in test sections. They also gave the amplitudes and, in some cases, the frequency composition of the background pressure fluctuations. The results of these studies were reduced to a similar basis and put in tabular form. This showed the distinct fluctuation characteristics of subsonic, transonic, and supersonic wind tunnels.

Chrysler Huntsville Operations conducted tests in the Marshall Space Flight Center 14 in. trisonic wind tunnel This is a blowdown tunnel with interchangeable transonic and supersonic tests sections. The transonic test section has a Mach number range of 0.2 to 2.5, and the supersonic test section operates from Mach 2.75 to 5.0. The facility consists of a compressor, high pressure storage tank, control valve, stilling chamber with a heat exchanger test section, diffuser, and atmospheric exhaust tower. The transonic test section plenum is normally connected to vacuum tanks

The experimental program conducted by Chrysler was unique in two ways. It made use of extensive instrumentation, including transducers located just down stream of the control valve, down stream of the stilling chamber, on the test section wall, on the test section calibration model, in the diffuser, atmospheric exhaust tower, and in the vacuum tanks. An accelerometer was located on the porous walls. The second unique factor was based on the fact that the Marshall Space Flight Center 14 x 14 in. trisonic wind tunnel can be operated in various configurations. This flexibility of operating modes is ideally suited to identifying the sources of test section fluctuations. Tests were conducted with both the transonic and supersonic test sections. These results give a comparison of their influence on fluctuation levels. Tests were conducted with the transonic test section using solid as well as porous walls. Tests were also conducted using various porosity settings. This indicated the effect of porosity on test section fluctuations. Tests were conducted with the high pressure system and the valve disconnected from the stilling chamber. In this configuration the tunnel was driven by the vacuum tanks. This gave an indication of the effects of the valve flow and its associated upstream turbulence on the test section fluctuations. Tests were conducted with the stilling chamber removed from the facility. Again the tunnel was powered by the vacuum tanks. This showed the effects of the stilling chamber on the fluctuations. These combinations of wind tunnel components show the influence of porous walls, upstream turbulence, and the diffuser flow on the test section fluctuations.

The results of this experimental program indicate that the largest fluctuations occur in the transonic regime. The largest component of test section noise consist of a fluctuation concentration that varies from 6,000 to 12,000 cps, depending on the particular operating conditions of the wind tunnel. This fluctuation is generated by the porous walls. The upstream turbulence apparently has a strong influence on the generation of these fluctuations. This 6,000 to 12,000 cps fluctuations has its counter part in the 16 ft transonic wind tunnel at AEDC and the 5 ft trisonic wind tunnel at ONERA in France. The amplitude of the overall fluctuation level in the MSFC 14 in. transonic test section compares favorably with that measured in the AEDC wind tunnel and with that in the Douglas 1 ft trisonic tunnel and in the NAE 5 ft transonic tunnel.

Based on the results of this study recommendations are made for reducing the background noise in the MSFC 14 in. wind tunnel. Details of the study are given in the following sections.

7

Also as a part of this study, a test program was prepared for the acoustic calibration of the AEDC 16 ft transonic wind tunnel. The instrumentation that will be used for this test is the same as that used for the MSFC 14 in. wind tunnel tests. The calibration model for the AEDC test has been designed. It is geometrically similar to the model used in calibrating the MSFC 14 in. wind tunnel. The transducers have been located so that both the local and unit Reynolds numbers will match at the instrumentation of both calibration models.

2.0 WIND TUNNEL TEST FACILITIES AND SCHEDULES

Two wind tunnel test facilities have been selected for acoustic calibration for background noise phenomena. These wind tunnels are:

- Marshall Space Flight Center 14 in. Trisonic Blowdown Wind Tunnel

- Arnold Air Development Center 16 ft Transonic Continuous, Closed Circuit Wind Tunnel

The following is a brief description of these facilities and the Chrysler Huntsville Operations (CHO) developed test programs.

2.1 WIND TUNNEL TEST FACILITIES

The MSFC 14 in. trisonic wind tunnel can operate from Mach numbers of 0.20 to 5.00. This Mach number range is achieved by using two separate test sections. The transonic test section operates in the Mach number range between 0.2 and 2.5. This Mach number range is covered by operating at points. Four sets of nozzle blocks are used to obtain various Mach numbers. These nozzle blocks are listed in Figure 2.1. This test section is equipped with variable porosity walls. The porosity is continuously variable between 0.5% and 5.40% of the wall area. The porous walls can be replaced with a set of solid walls. Stagnation pressures from atmospheric to 75 psia are possible in the transonic test section. This corresponds to a Reynolds number range of 2.6 to 15.0 million per foot. The supersonic test section operates in the Mach number range between 2.75 and 5.00. These Mach numbers are generated by tipping and translating the single set of nozzle blocks (Figure 2.1). The supersonic test section has solid walls with glass ports in the sidewalls. Stagnation pressures from atmospheric to 110 psia are possible in this test section. This leads to a Reynolds number range of 1 to 18 million per foot.

It is possible to operate the MSFC 14 in. tunnel in three separate configurations in certain Mach number ranges. Each configuration can be operated with both the transonic and supersonic test section. These three configurations are shown in Figures 2.2, 2.3, and 2.4. The Mach number ranges are.

- Standard Configuration (Figure 2.2) 0.2 to 5.0

- Atmospheric Inlet at Test Section Inlet (Stilling Chamber Removed) (Figure 2.3) 0 2 to 0.95 and 1.46 to 5.00

- Atmospheric Inlet at Stilling Chamber Inlet (High Pressure Tank and Valve Removed) (Figure 2.3) 0.2 to 0.95 and 1.46 to 5.00

Each configuration was operated in the acoustic calibrations.

9

Test Section	Nozzle Blocks	Mach Number Range
Transonic	M = 1.0 Nozzle Blocks	0.2 to 1.3
	M = 1.46 Nozzle Blocks	1.46
	M = 1.96 Nozzle Blocks	1.96
	M = 2.50 Nozzle Blocks	2.50
Supersonic	Standard	2.75 - 5.00

FIGURE 2.1. MSFC 14 IN. TRISONIC TUNNEL OPERATING MACH NUMBER RANGE
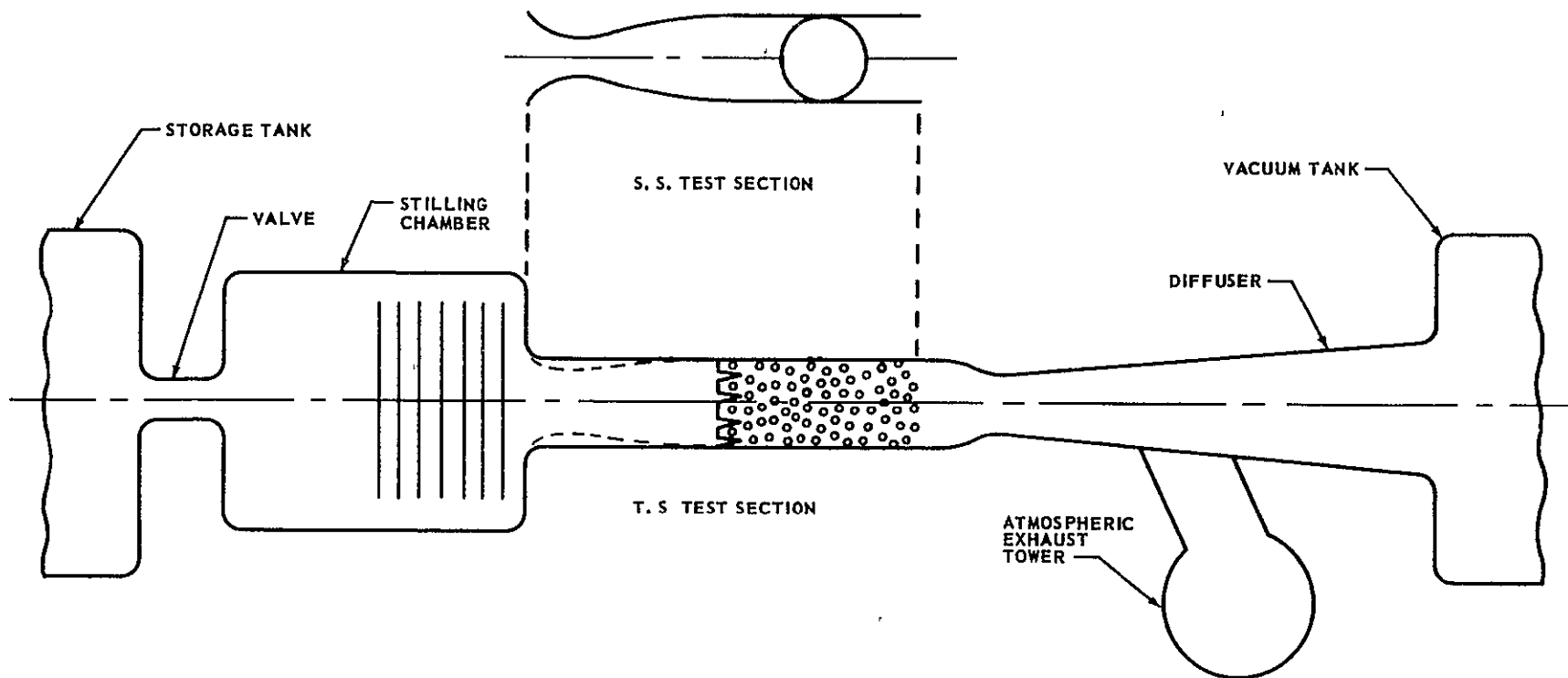
FIGURE 2.2. MSFC 14 IN. WIND TUNNEL IN STANDARD OPERATION (CONFIGURATION T_1)

VALVE

STILLING
CHAMBER

S. S. TEST SECTION

VACUUM TANK

DIFFUSER
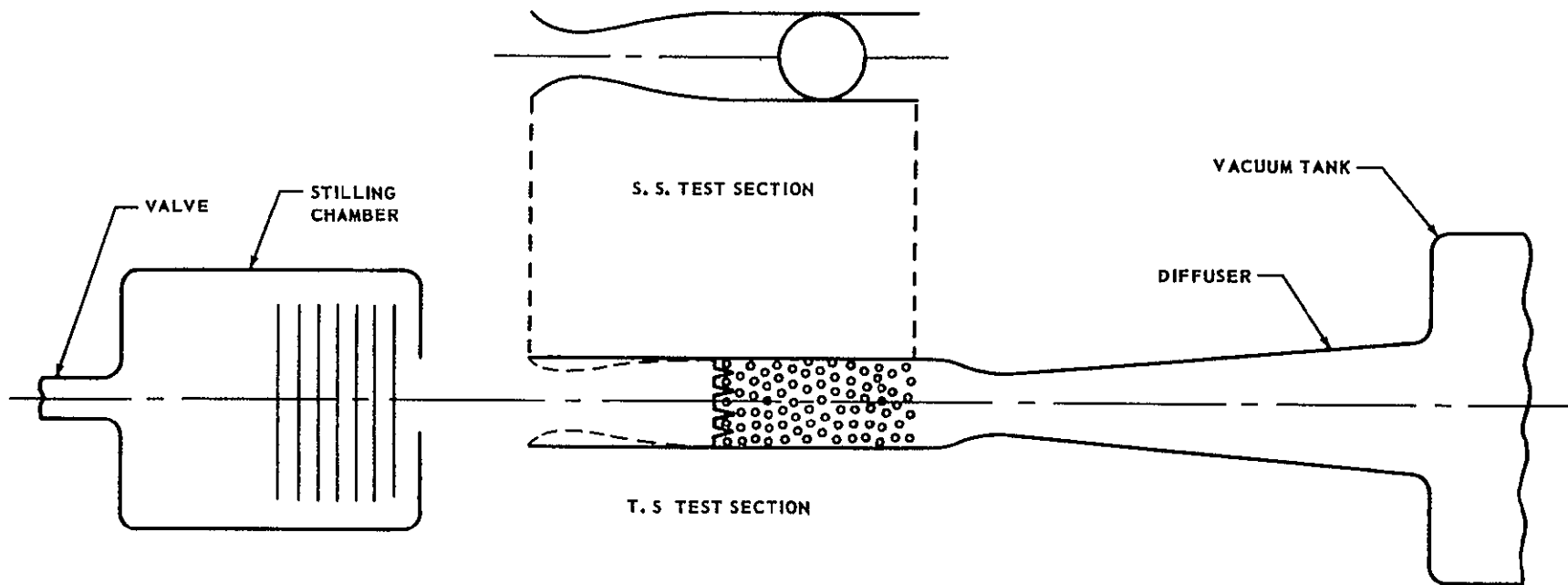
T. S TEST SECTION

FIGURE 2.3. MSFC 14 IN. WIND TUNNEL WITH
ATMOSPHERIC INLET AT TEST SECTION
(CONFIGURATION T_2)

STORAGE TANK

VALVE

STILLING
CHAMBER

S. S. TEST SECTION

VACUUM TANK

DIFFUSER

T. S. TEST SECTION
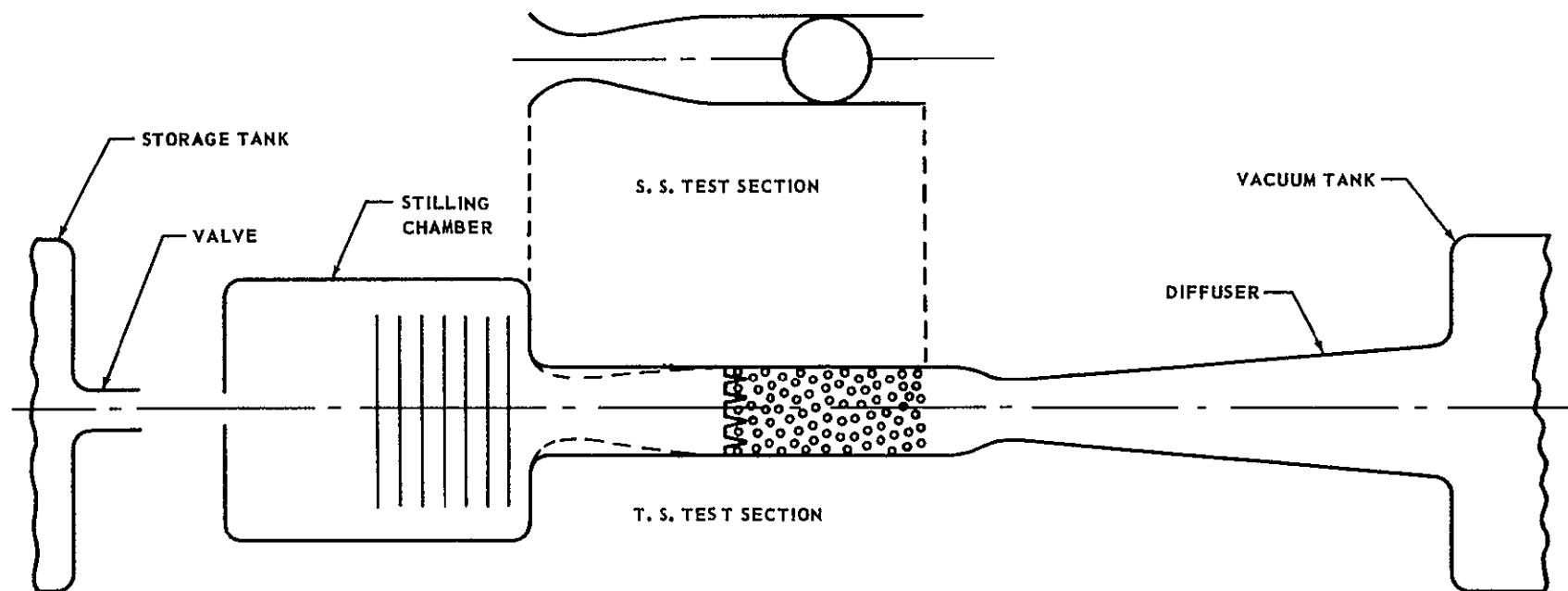
FIGURE 2.4.   MSFC 14 IN WIND TUNNEL WITH
              ATMOSPHERIC INLET AT STILLING
              CHAMBER ENTRANCE (CONFIGURATION T_3)

Additional information concerning the MSFC 14 in. trisonic tunnel can be found in References 14 or 15.

The AEDC 16 ft transonic wind tunnel can operate from Mach numbers of 0.5 to 1.6. The Mach number is continuously variable over this range. This tunnel is equipped with fixed porosity walls. The porosity is 6.0% of the wall area. Removable plates are provided for viewing of the model under test conditions. Stagnation pressures up to 28 psia can be achieved under most test conditions. This will provide Reynolds numbers of up to 8.4 million under most test conditions. Additional information concerning the AEDC 16 ft transonic tunnel can be found in Reference 16.

2.2 WIND TUNNEL TEST SCHEDULES

The MSFC 14 in. wind tunnel trisonic test program is presented as Figure 2.5. This schedule is segmented into three parts. The first part is a static calibration of the MSFC 14 in. tunnel. The static calibration was performed for nonstandard test conditions required for the acoustic calibration part of the test schedule. The static calibration device is described in Section 4.0 of this report. The second part of the test program is the acoustic calibration of the tunnel. The objective of this series of test is to determine the background pressure fluctuations in the various sections of the wind tunnel. This portion of the program is planned so that the test data will be useful in determining the interrelationship between the background fluctuations in the various sections of the tunnel. The effects of Mach number, porosity, stagnation temperature, tunnel exhaust, tunnel diffuser, solid walls, control valve, and stilling chamber are investigated during this test schedule. The third part of the program was to investigate the possibility of delaying laminar to turbulent boundary layer transition in the MSFC wind tunnel facility. The surface of the model was to be lowered in temperature. This has been shown to, under favorable circumstances, delay boundary layer transition (Reference 17). Unfortunately, scheduling problems have prevented this portion of the test program from being conducted.

The tentative test schedule for the AEDC 16 ft wind tunnel is presented as Figure 2.6. The AEDC 16 ft tunnel test schedule is organized to yield as much comparative data between the AEDC 16 ft tunnel and the MSFC 14 in. tunnel as possible. Wherever possible, both unit Reynolds number (Reynolds number per foot) and local Reynolds numbers are matched between the AEDC and MSFC test schedules. Some test conditions are included that match those used by other investigators who have conducted acoustic tests in this tunnel. Test points which will match some of this test data were also included. The test is also set up to provide information concerning the interrelationship between pressure fluctuations in various sections of the wind tunnel. The effects of Mach number, stagnation pressure, stagnation temperature, tunnel diffuser, tunnel compressor, and scaling on the background pressure fluctuation will be investigated with the results of this test program.

14

FACILITY: _____

TEST NO : _____

MODEL

SCORE: PART I, STATIC CALIBRATIONS _____

TYPE TEST: _____   DATE: _____

PROJECT _____   ENGINEER _____

COST NO : I _____   APPROVED: _____

RUN	CONFIGURATION	MACH	POR	EXH.	P_o	t_o	AUX. VAC.		REMARKS
1	T1, T S (B-1), P	0.60	0 50%	E2	ATM	530	Yes		
2			0.75%						
3			2.50%						
4			5 40%						
5			0.50%						
6		0 90	0.75%						
7			2.50%		-				
8			5.40%						
9		0.70	2.50%						
10		0.80							
11		0 95							
12		1.15	2.50%	E1	22.0				
13			5.40%	E2					
14	T2, T.S. (B-1), P	0.90	2.50%		ATM				
15		0.60							
16		0.90	5.4 %						
17	T1, T S (B-1), P								
18	T4, T S (B-1), P		Solid						
19	T2,4, T.S (B-1) P								
20	T4, T S (B-1), P	0.60							
21	T1, T.S. (B-1), P	0.95	0.50%						
22			0.75%						
23			5.40%						
24	T2, T S (B-3), P	1 95	2 50%				No		
25	T1, T.S. (B-3), P								
26	T1, T.S. (B-2), P	1.45							
27			0.75%						
28			5.40%						
29			0.50%						
30	T2, T S (B-2), P		2 50%						
31			5.40%						
32	T1, T.S (B-1), P	0 90	5.40	E1	22.0		Yes		
33		1.15							
34		0.90		E2			No		
35		0.95	STD						
36	T2, T.S. (B-1), P	0.60	2.50%		ATM				
37		0.90	5.40%						
38		0. 95	2.50%						
39		0.80							
40	T4, T S. (B-1), P	0.60	Solid						

SPECIAL INSTRUCTIONS:

FIGURE 2.5   MSFC 14 IN. WIND TUNNEL TEST PROGRAM

EXPERIMENTAL TEST PROGRAM

FACILITY: _____

TEST NO : _____

MODEL: _____

SCOPE   PART I. STATIC CALIBRATION _____

TYPE TEST: _____   DATE: _____

PROJECT _____   ENGINEER: _____

COST NO I _____   APPROVED _____

RUN	CONFIGURATION	MACH	POR.	EXH.	P_o	t_o	AUX. VAC.		REMARKS
41	T4, T.S. (B-1), P	0.90	Solid	E2	ATM	530	No		
42	↓	0.95							
43	T2, 4, T S (B-1), P	0.90							
44	T4, T S (B-2), P	1.45							
45	T2, 4, T S.(B-2), P	↓	↓						
46	T2, T S (B-1), P	0 90	0 75%						
47	T1, T.S. (B-1), P	0.95	2.50%		-				
48	T2, T S (B-1), P	0.90	↓	↓	↓	↓	↓		

SPECIAL INSTRUCTIONS:

FIGURE 2.5. MSFC 14 IN WIND TUNNEL TEST PROGRAM

MSFC - Form 668 (October 1960)

GEORGE C MARSHALL SPACE FLIGHT CENTER

EXPERIMENTAL TEST PROGRAM

FACILITY: _____

TEST NO : _____

MODEL: _____

SCOPE **PART II, ACOUSTIC CALIBRATIONS**

TYPE TEST: _____   DATE: _____

PROJECT _____   ENGINEER: _____

COST NO :[1] _____   APPROVED: _____

RUN	CONFIGURATION	MACH	POR	EXH	P_O	t_O	RN/ft x10^{-6}	tw/ts	REMARKS
1	T4, T.S. (B-1)	0 60	Solid	E2	ATM	530	3.54	INS	7, 8, 9, 2
2		0.90					4.45		7, 8, 9, 2
3		0 95					4 54		7, 8, 9, 2
4	T1, T S. (B-1)	0.60	0.50%				3.54		2
5		0.90					4.45		2
6		0 95					4.54		2
7	T1, T S (B-1)M1	0 40	2 50%		-		2.56		1, 3
8		0 60					3.54		1, 2, 3, 8, 9
9			0 75%						1, 2, 3, 8, 9
10			5 40%						1, 2, 3, 8, 9
11		0.70	2.50%				3.91		1, 3
12		0.80					4.20		1, 3, 9
13		0.90					4.45		1, 2, 3, 8, 9
14			0 75%						1, 2, 3, 8, 9
15			5 40%						1, 2, 3, 8, 9
16		0 95					4.54		1, 2, 3, 9
17			0.75%						1, 2, 3, 9
18			2.50%						1, 2, 3, 9
19		0.40	5.4%	E1	22.0		3.83		1, 3
20		0.60					5.30		1, 3
21		0 80					6.30		1, 3
22		0.85					6 48		1, 3, 5
23		0.90					6.66		1, 2, 3, 5
24			0.75%						1, 2, 3
25		0 95	5.40%				6.80		1, 3, 5
26		1 00	0 50%				6.90		1, 3, 5
27		1 05	0 75%				7.04		1, 3, 5
28		1.10	1.10%				7.18		1, 3, 5
29		1.15	2 50%				7.10		1, 2, 3
30			5 40%						1, 2, 3
31		1.20					7.12		1, 3
32		1.30	STD				7 12		1, 3
33		0 90	5.40%			590	5.78		4
34		1 15	2 50%				6.14		4
35		0 90	5 40%			640	5.20		4
36		1 15					5.56		4
37		0.60			28.0	530	6.75		1, 3
38		0.90					8.48		1, 3, 5
39		1.00	0.50%				8.78		1, 3
40		1.15	2,50%				9.03		1, 3

SPECIAL INSTRUCTIONS:

FIGURE 2 5 MSFC 14 IN WIND TUNNEL TEST PROGRAM

EXPERIMENTAL TEST PROGRAM

FACILITY: _____

TEST NO : _____

MODEL: _____

SCOPE: __PART II. ACOUSTIC CALIBRATIONS_____

TYPE TEST: _____   DATE: _____

PROJECT: _____   ENGINEER: _____

COST NO :[1] _____   APPROVED: _____

RUN	CONFIGURATION	MACH	POR.	EXH.	P_o	t_o	RN/ft	$\times 10^{-6}$	tw/ts	REMARKS
41	T1, T.S (B-1)M1	0.9	5 40%	E2	28.0	530	8 48		INS.	5
42							5.20			5
43		0.95	STD		22 0		6.80			5
44	T1, T S (B-3)M1	1.95		E1	28 0		7 55			1,3
45			2.50%	E2	ATM		3.96			9
46	T1, T.S (B-2), M1	1 45	STD	E1	28 0		8 94			1,3
47					22.0		7.00			1,3
48			2.50%	E2	ATM		4.68			1,2,3,8,9
49			0.75%							1,2,3,8,9
50			5.40%							1,2,3,8,9
51			0 50%							2
52	T4, T.S. (B-2),		Solid							7,8,9,2
53	T2,4 TS (B-2),									2,7,9
54	T2, TS (B-2),M1		2 50%							2,9
55			5.40%							2,9
56	T2,4, T.S (B-1)	0 90	Solid				4 45			2,7,9
57	T2, T S (B-1), M1	0.60	2.50%				3 54			9
58		0.80					4.20			9
59		0.90					4.45			2,9
60			5.40%							2,9
61		0 95	2.50%				4.54			9
62	T2, T S (B-3), M1	1 95					3.96			9
63	T3, T S (B-3), M1									8
64	T3, T S (B-2), M1	1 45					4 68			2,8
65			5.40%							2,8
66	T3, T S (B-1), M1	0.6	2.50%				3.54			8
67		0 9					4.45			2,8
68			5.40%							2,8
69	T1, S.S , M1	3.0	N.A.				2.24			1,3,8,9
70		4.0					1.25			1,3,8,9
71		5.0					0.72			1
72		3.0			65.0		9.90			3
73		4.0					5.43			3
74		3.0		E1			9.90			3,5
75				E2	82.5		12.60			3,4,6
76		4.0					7.03			3,4,6
77		3.0			ATM		2.24			Repeat
78	T2, S S M1	3.0					2.24			9
79		4.0					0.72			9

SPECIAL INSTRUCTIONS:

FIGURE 2 5. MSFC 14 IN. WIND TUNNEL TEST PROGRAM

GEORGE C MARSHALL SPACE FLIGHT CENTER

EXPERIMENTAL TEST PROGRAM

FACILITY: _____

TEST NO : _____

MODEL: _____

SCOPE   PART III, BOUNDARY LAYER TRANSITION STUDIES _____

TYPE TEST: _____   DATE: _____

PROJECT _____   ENGINEER: _____

COST NO : [1] _____   APPROVED _____

RUN	CONFIGURATION	MACH	POR.	EXH	P_o	t_o	RN/ft x 10^{-6}	tw/ts	REMARKS
1	T1,T.S (B-1), M2	0.6	STD	E1	22 0	530	5.30	INS.	10
2								0.90	
3								0.80	
4								0 70	
5								0.60	
6		0 8					6.30	INS.	
7								0.95	
8								0.80	
9								0 70	
10								0.60	
11		0.95					6 80	INS	
12								1.00	
13								0 85	
14								0.75	
15								0.65	
16		1.05					7.04	INS.	
17								1 00	
18								0 85	
19								0 75	
20								0.65	
21		1.30					7 12	INS.	
22								1.05	
23								0 85	
24								0 75	
25								0.65	
26	T1,T.S.(B-3), M2	1.95					5.93	INS.	
27								1.60	
28								1 50	
29								1.40	
30								1.30	
31	T1,S.S., M2	2.74	N.A.	E2			3 92	INS	
32								2.10	
33								2.00	
34								1.95	
35								1.90	
36		3.50					2 57	INS	
37								2 90	
38								2.60	
39								2.45	
40								2 30	

SPECIAL INSTRUCTIONS:

FIGURE 2.5 MSFC 14 IN. WIND TUNNEL TEST PROGRAM

REMARKS

1   For Evaluation of the Effect of Mach No. on Fluctuating Pressure

2   For Evaluation of the Effect of Porosity on Fluctuating Pressure

3   For Evaluation of the Effect of Stagnation Pressure on Fluctuating Pressure

4   For Evaluation of the Effect of Stagnation Temperature on Fluctuating Pressure

5   For Evaluation of the Effect of Tunnel Exhaust on Fluctuating Pressure

6   For Evaluation of the Effect of Diffuser Setting on Fluctuating Pressure

7   For Evaluation of the Effect of Solid Walls in Test Section on Fluctuating Pressure

8   For Evaluation of the Effect of Valve on Fluctuating Pressure

9   For Evaluation of the Effect of Valve and Stilling Chamber on Fluctuating Pressure

10   For Evaluation of the Effect of Temperature Ratio on Boundary Layer Transition

FIGURE 2.5 MSFC 14 IN. WIND TUNNEL TEST PROGRAM

Run No.	Mach No.	P_0(psi)	$t_0(^{O}R)$	Plenum Suction	Purpose	Similar Test In MSFC Tunnel
1	0.50	22.00	530	Standard	Match Unit Reynolds No.	
2	0.60					Yes
3	0.65					
4	0.70					
5	0.75					
6	0.80					
7	0.90					Yes
8	0.95					Yes
9	1.00					Yes
10	1.05					Yes
11	1.15					Yes
12	1.20					Yes
13	0.60	28.00			Effects of P_0	Yes
14	0.70					Yes
15	0.75					
16	0.80					
17	0.90					
18	1.00					Yes
19	1.15					Yes
20	0.50	14.70				Yes
21	0.60					
22	0.65					Yes
23	0.70					
24	0.75					Yes
25	0.80					
26	0.90					Yes
27	0.95					Yes
28	0.50	8.23			Match Local Reynolds No.	Yes
29	0.60					Yes
30	0.65					Yes
31	0.70					Yes
						Yes

FIGURE 2.6.   AEDC 16 FT. WIND TUNNEL TEST PROGRAM

Run No.	Mach No.	P_o (psi)	t_o (°R)	Plenum Suction	Purpose	Similar Test In MSFC Tunnel
32	0.75	8.23	530	Standard	Match Local	Yes
33	0.80				Reynolds No.	Yes
34	0.90					Yes
35	1.00					Yes
36	1.05					Yes
37	1.15					Yes
38	1.30					Yes
39	0.70	22.00	590		Effects of	Yes
40	0.90				Temperature	
41	1.15					
42	1.20					
43	0.70		640			
44	0.90					
45	1.15					
46	1.20					
47	0.60	11.10	530		Match AEDC	
48	0.75				Cone Tests	
49	0.80				Match MSFC	
50	0.90				Cone Tests	
51	1.00				Match AEDC	
52	1.10				Cone Tests	
53	1.20					
54	0.90	22.00		S_1	Effects of	
55				S_2	Plenum Suction	
56				S_3		
57	1.15			S_1		
58				S_2		
59				S_3		
60	1.30			S_1		
61				S_2		
62				S_3		

FIGURE 2.6. AEDC 16 FT. WIND TUNNEL TEST PROGRAM

3.0 INSTRUMENTATION

Three types of data are required in the acoustic calibration of a wind tunnel. They are:

- Mean static pressure

- Fluctuations in the static pressure

- Model surface temperature

Three types of instrumentation systems were assembled to obtain these data. The mean static pressures were recorded by two of these three systems. Scheduling difficulties prevented the cooled model tests from being conducted. These tests were to have established the effects of wall cooling on boundary layers.

The instrumentation used is referenced by manufactures name and model number. A list of the instrumentation and the manufacturer is provided as Figure 3.1. Further information concerning the instrumentation can be obtained from the manufactures specification report. However, these specification reports are performance quotations obtained under ideal conditions.

Overall instrumentation system characteristics were requested by Chrysler Huntsville Operations. The only measure of overall instrumentation system characteristics that can practically be obtained is the instrumentation noise floor. It is assumed that the overall system has linear response from approximately 100 cps to 20,000 cps. Data to substantiate this are presented wherever it is available.

3.1 INSTRUMENTATION FOR STATIC PRESSURE DATA

Static pressure orifices are connected to a scani-valve through approximately 15 ft. of tygon tubing. The scani-valve system has eight valves with 11 ports each. The valves can be stepped from port to port every second. This yields data reading times of 0.97 seconds. A Statham Instruments, Inc., Model PM 131 static pressure transducer is calibrated with a constant pressure source. The electrical signal from the transducer is input to a Systems Engineering Labs., Model 600 digital data acquisition system. Data are stored in this system and read out in a pre-programmed manner at the command of the tunnel operator. This system was utilized for all static data generated from the wind tunnel static calibrations.

Static pressures measured during the acoustic calibration testing were recorded on magnetic tape. The static orifices are connected to Statham Instruments, Inc., Models PM 131 and PA 208, pressure transducers. The Model PM 131 transducer is used in conjunction with the transonic test section and the Model PA 208 transducer is used in conjunction with the supersonic test section.

23

Item Name	Manufacturer	Model
D. C Pressure Transducer	Statham Instruments, Inc	PM 131
D. C Pressure Transducer	Statham Instruments, Inc.	PA 208 TC
Digital Data Acquistion System	Systems Engineering Labs	600
Calibration Source	Photocon Research Products	PC-125
A. C. Pressure Transducer	Schaevitz-Bytrex	HFD-2
A. C. Pressure Transducer	Schaevitz-Bytrex	HFD-25
A. C Pressure Transducer	Kistler Instrument Corp.	601L
A C. Pressure Transducer	Kulite Semiconductor Products	CPL 070-5
Charge Amplifier	Kistler Instrument Corp.	566
Charge Amplifier	Kistler Instrument Corp	553
Low Level Amplifier	Tektronic, Inc	RM-122
Signal Generator	Hewlett Packard	203A
Voltage Controlled Oscillator	Data Control System	GOV-4
Oscilloscopes	Tektronic, Inc.	502
Tape Recorder	Consolidated Electrodynamics Corp	VR-3600
True RMS Voltmeter	Ballantine Laboratories, Inc	320A
Subcarrier Demodulator	Data Control Systems, Inc	6F0-13
Correlator	Princeton Applied Research	100 or 101
Copper Constanten Thermocouples	MSFC	
Signal Conditioning Module	Endevco Corp	4400
Low Level Galvanometers	Honeywell	M-100-120A
Oscillograph	Honeywell	1612

FIGURE 3.1. INSTRUMENTATION USED IN MSFC 14 IN.
WIND TUNNEL CALIBRATION

24

The transducer output is fed to a Data Control System, Inc., Model GOV-4, voltage controlled oscillator. The voltage controlled oscillator converts the signal into a frequency modulated signal. This signal is then recorded on a Consolidated Electrodynamics Corp., Model VR-3600 tape recorder. This system has nine FM channels on each data track. This system is diagramed in Figure 3.2

3.2 INSTRUMENTATION FOR FLUCTUATIONS IN STATIC PRESSURE

All fluctuating pressures are recorded by the system diagramed in Figure 3.2. This system has as input the output of three types of pressure transducers. These transducers are:

- Schaevitz - Bytrex Corp., Models HFD-2 and HFD-25

- Kulite Corp., Model CPL-070-5

- Kistler Instrument Corp., Model 601L

All acoustic transducers were calibrated using a 1000 cps signal from a Photocon Research Products, Model PC 125, calibrator. Both the Schaevitz-Bytrex Corp., Model HFD transducer, and the Kulite Corp., Model CPL-070-5, transducer are strain gauge transducers. A part of the strain gauge is located outside the transducer as a compensation module. The Tektronic, Inc., Model RM 122, low level amplifiers are used to amplify the output of both these transducers. The Kistler Instrument Corp., Model 601L, transducer is a Quartz crystal transducer. The Kistler Instrument Corp., Model 553, charge amplifier is used to amplify the output signal of the Kistler transducers. The amplified transducer output is then input to a Data Control Systems, Inc., Model GOV-4, voltage controlled oscillator which converts the output to a FM signal. The FM signal is then recorded on one of the nine channels of a Consolidated Electrodynamics Corp., Model VR-3600, tape system. Each of the nine channel has a $\pm$ 40 KC range and a FM separation of 80 KC. These data are presented in Figure 3.3. A monitor station is provided between the amplifier and the voltage controlled oscillators. This is illustrated in Figure 3.2. A Ballantine Laboratories, Inc., Model 320A, true rms voltmeter and a Tektronic, Inc., Model 502, oscilloscope are provided at the tunnel monitor station.

Noise floor data was taken on the instrumentation used in the tests at the MSFC 14 in. tunnel. Only a portion of this data has been reduced into correlation functions. The data given in Figure 3 4 are noise floor data for few data channels and tracks.

The natural frequency of various Bytrex pressure transducers used in the MSFC 14 in. tunnel tests can be determined from the data in Figure 3.5. A low frequency oscillation also occurs in the damping curves of Figure 3.5. This oscillation is not mentioned in the manufacturers performance specifications.
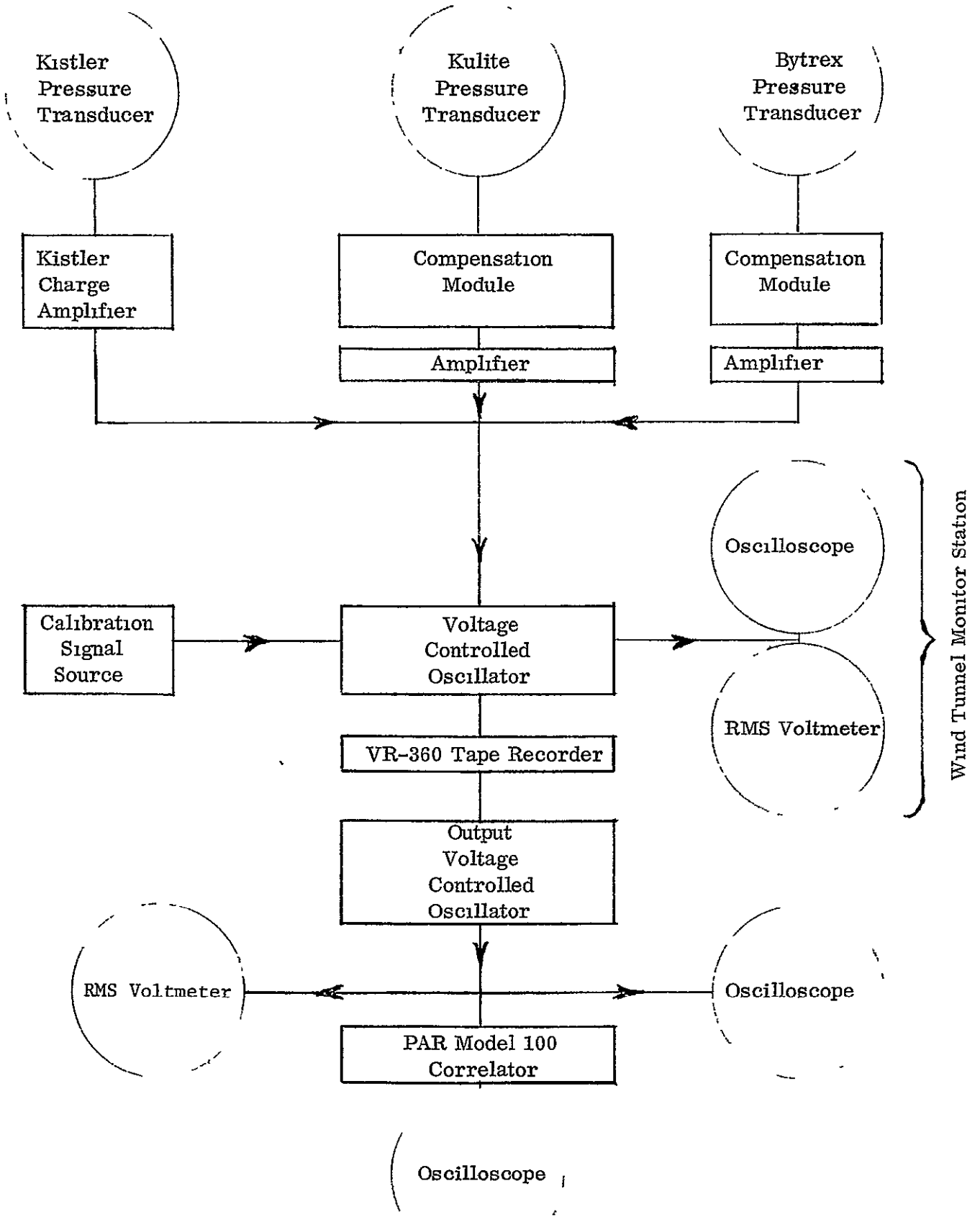
25

Kistler
Pressure
Transducer

Kulite
Pressure
Transducer

Bytrex
Pressure
Transducer

Kistler
Charge
Amplifier

Compensation
Module

Compensation
Module

Amplifier

Amplifier

Oscilloscope

Calibration
Signal
Source

Voltage
Controlled
Oscillator

RMS Voltmeter

VR-360 Tape Recorder

Wind Tunnel Monitor Station

Output
Voltage
Controlled
Oscillator

RMS Voltmeter

Oscilloscope

PAR Model 100
Correlator

Oscilloscope

FIGURE 3.2 INSTRUMENTATION BLOCK DIAGRAM FOR MSFC 14 IN.
WIND TUNNEL CALIBRATION

26

Channel	Track 4 Transducer	Track 6 Transducer	Track 8 Transducer	Track 10	Track 14	FM Frequency Band
1	B1	K1	B3	Blank		160 ± 40 KC
2	B2	K2	B4	Cone Surface Pressure		320 ± 40 KC
3	B3	K3	B5	Cone Cavity Pressure		480 ± 40 KC
4	B4	K4	K1	Cone Base Pressure	Voice	640 ± 40 KC
5	K2	K5	K2	Blank		800 ± 40 KC
6	K3	K6	K5	Tunnel Storage Tank Pressure		960 ± 40 KC
7	K4	K7	K6	Blank		1120 ± 40 KC
8	Blank	A1	Blank	Blank		1280 ± 40 KC
9	Blank	Blank	Blank	Blank		1440 ± 40 KC

FIGURE 3.3, TAPE CHANNEL INSTRUMENTATION ORGANIZATION
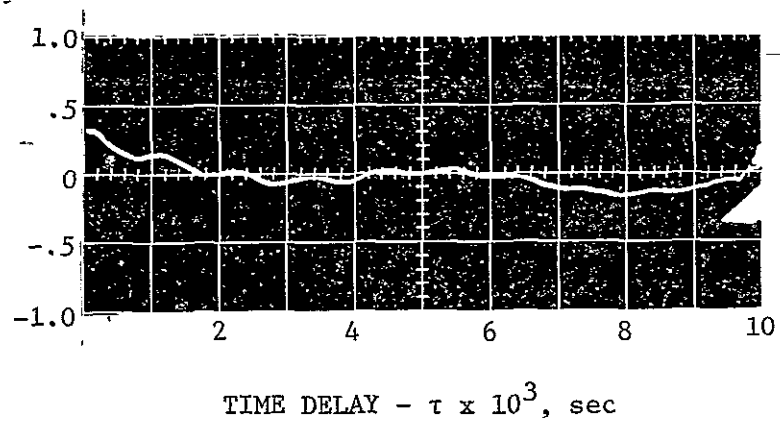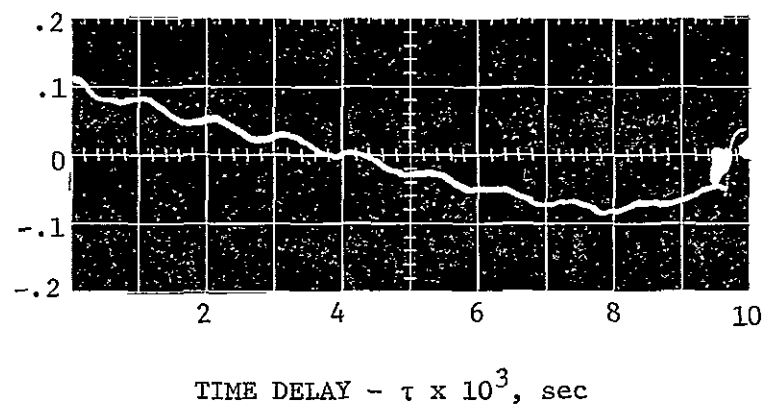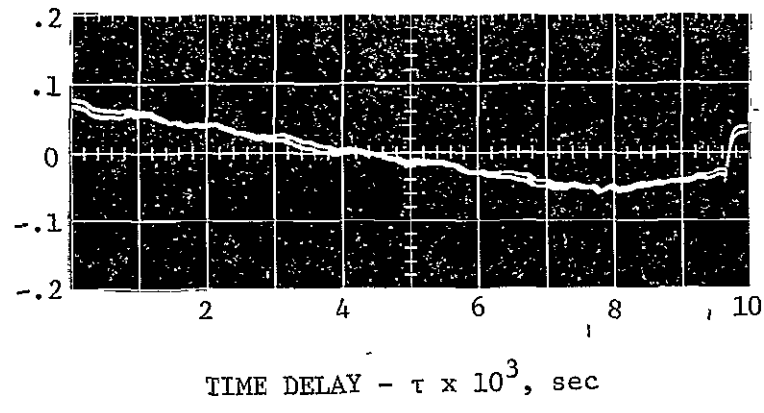
FIGURE 3.4. OVERALL INSTRUMENTATION NOISE FLOOR

28

FIGURE 3.4.   OVERALL INSTRUMENTATION NOISE FLOOR

29

FIGURE 3.4.   OVERALL INSTRUMENTATION NOISE FLOOR
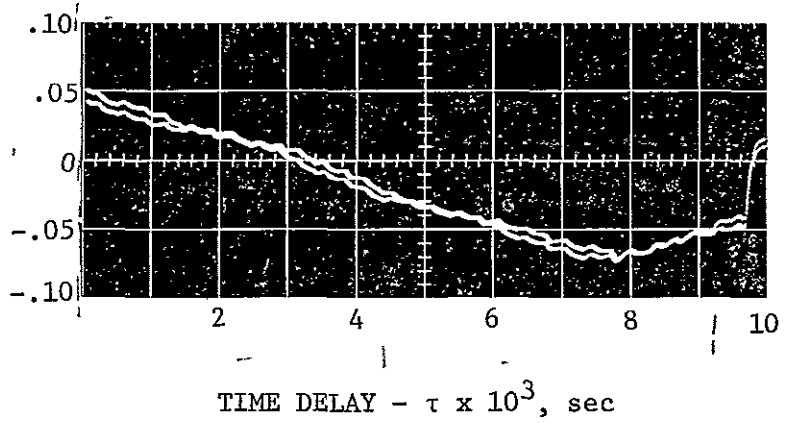
30
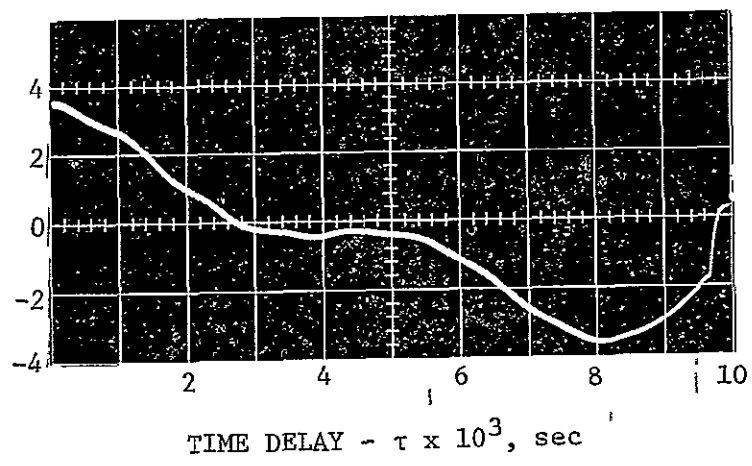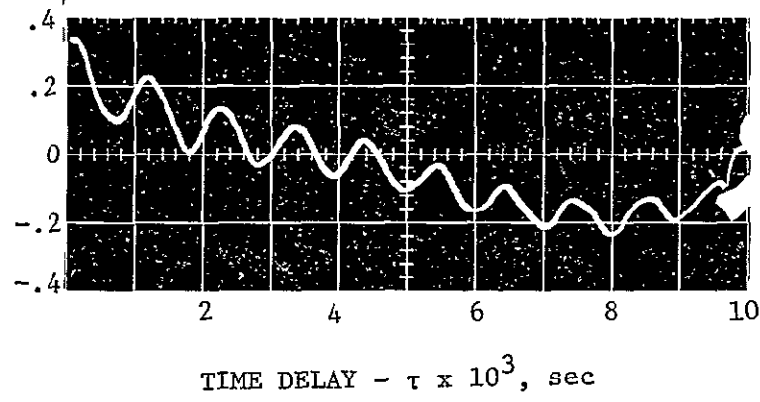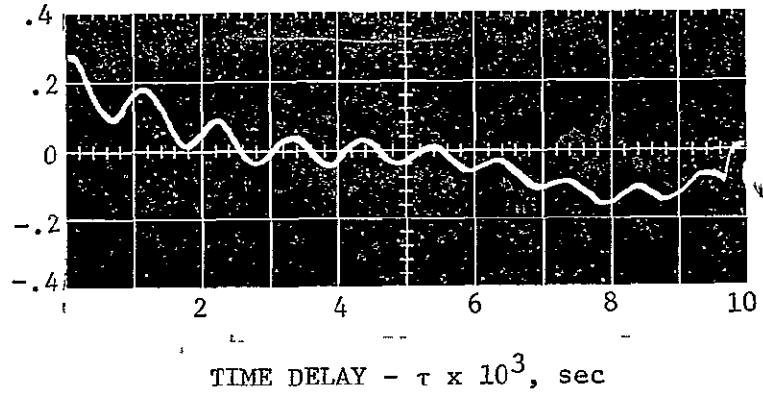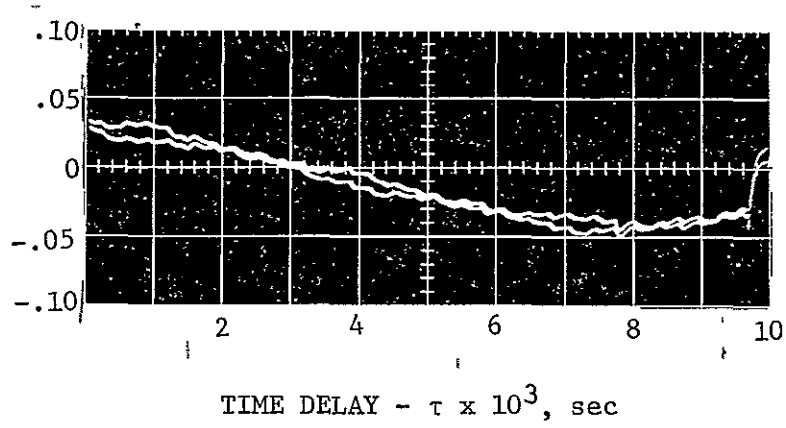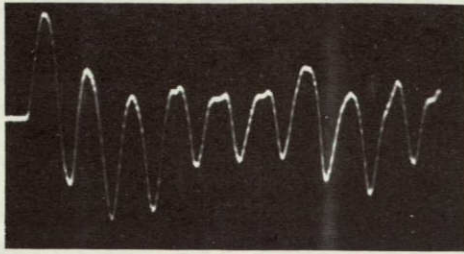
RESPONSE, 2 mv/cm

SWEEP, 20 microsec/cm

TRANSDUCER B1

RESPONSE, 2 mv/cm

SWEEP, 20 microsec/cm

TRANSDUCER B2

RESPONSE, 2 mv/cm

SWEEP, 10 microsec/cm

TRANSDUCER B3

RESPONSE, 2 mv/cm

SWEEP, 10 microsec/cm
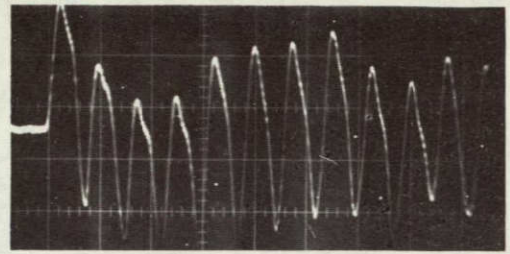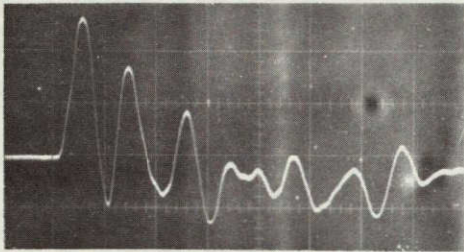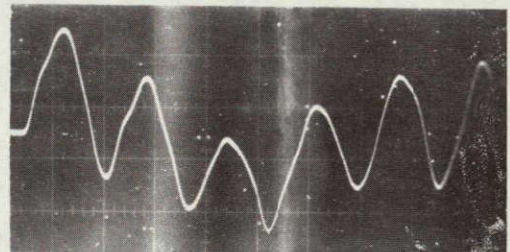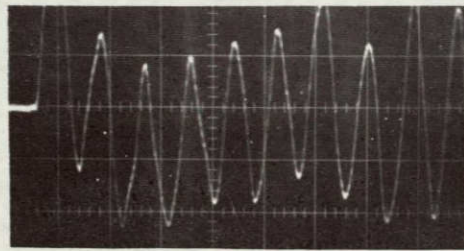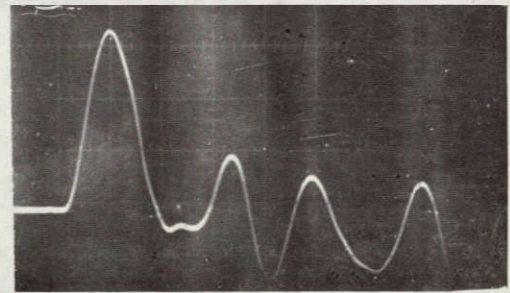
TRANSDUCER B4

RESPONSE, 2 mv/cm

SWEEP, 20 microsec/cm

TRANSDUCER B5

RESPONSE, 200 mv/cm

SWEEP, 5 microsec/cm

TRANSDUCER K5

FIGURE 3.5.   RESPONSE OF CONE MOUNTED TRANSDUCER TO IMPULSE EXCITATION

3.3 INSTRUMENTATION FOR MODEL SURFACE TEMPERATURE

Surface temperature measurements were to be made in the MSFC 14 in.
trisonic tunnel on a cooled model. Copper constanten thermocouples were
silver soldered into a 1/16 in. thick wall. The output of the thermocouples
was to have been passed through a Honeywell Corp., Model M-100-120-A, low
level, galvanometer. This would then pass through a Endevco Corp., Model
4400, signal conditioning module to a Honeywell Corp., Model 1612, oscillo-
graph. These tests were not performed due to time limitations.

3.4 DATA REDUCTION INSTRUMENTATION

Preliminary data reduction was conducted. The equipment used in this
data reduction was similar to that used in the data acquisition. Tapes were
played on a Consolidated Electrodynamics Corp., Model VR-3600, tape system
through output voltage controlled oscillators. The output was monitored and
rms voltages recorded using a Ballantine Laboratories, Inc., Model 320A, true
rms voltmeter. A Tektronic, Inc., Model 502, oscilloscope was also used a
a tape monitor. The output of selected data was also played through a
Princeton Applied Research, Model 100 and 101 correlator. The correlator out-
put was stored in the memory unit. This was then input into a Tektronic, Inc.,
Model 502, oscilloscope and a Polaroid photograph was taken of the resulting
correlation function. This system is diagramed in Figure 3.2.

4.0 CALIBRATION DEVICES AND INSTRUMENTATION LOCATION

In Reference 11 it was shown that several types of calibration devices have been used in wind tunnel acoustic testing. A brief evaluation of each type of calibration device is presented in Reference 11. It was shown in this evaluation that the most acceptable pressure fluctuation data can be obtained from a combination of calibration devices. This combination was shown to be a slender cone with flat surfaces for mounting instrumentation and sidewall mounted instrumentation. It was also shown, that if the instrumentation is submerged under a turbulent boundary layer, the boundary layer fluctuation are recorded in addition to the background noise that is to be investigated. For this reason it was decided to attempt to establish a laminar boundary layer over a device of identical external geometry to that of the dynamic calibration cone. If a laminar boundary layer could be established over this model, then a device can be designed to obtain acoustic measurements under a laminar boundary layer. Therefore, a slender cone calibration device was designed for use in boundary layer transition studies. The calibration devices and instrumentation locations on these calibration devices are described in detail in the following paragraphs.

4.1 STATIC CALIBRATION DEVICE FOR THE MSFC 14 IN. TUNNEL

The static probe is the MSFC standard probe described in Reference 14 or 15. A photograph of this static calibration device installed in the 14 in. wind tunnel is presented as Figure 4.1. This device is designed to collect mean static pressure along the wind tunnel centerline. It is a 47.938 in. long cone cylinder with a cone apex angle of 10 degrees. Twenty five static ports are spaced one in. apart from model station 3 15/16 forward. This model station corresponds to wind tunnel station 8.   The cone cylinder juncture is prior to the wind tunnel test section to allow the static pressure to return to stream static pressure after the cone cylinder juncture. Instrumentation has been described in Section 3.0.

4.2 DYNAMIC CALIBRATION CONE FOR THE MSFC 14 IN. TUNNEL

Fluctuating pressures existing in the frequency range between approximately 8 cps and 20,000 cps were recorded at several stations on a slender calibration cone device. This cone is shown in Figures 4.2, 4.3, and 4.4. It is 10 in. in length with a 10° apex angle and two flat surface. The flat surfaces are for flush mounting pressure transducers. The apex angle between the flat surfaces is 9.24^o. This is shown on Figure 4.2. Also shown in Figure 4.2 is the instrumentation location, type and serial number. The Bytrex pressure transducers used on this model must be vented to a pressure source that is relatively free from pressure fluctuations, and is at the same or similar pressure as the transducer face. These transducers are vented into the internal cavity shown in Figure 4.2. The internal cavity pressure is equalized to the external pressure through 7.75 ft of tygon and metal tubing. It is shown in Reference 11 that external pressure fluctuations are essentially damped out by this arrangement. The Bytrex transducers are, therefore, properly vented. The Kistler transducers do not require venting. The
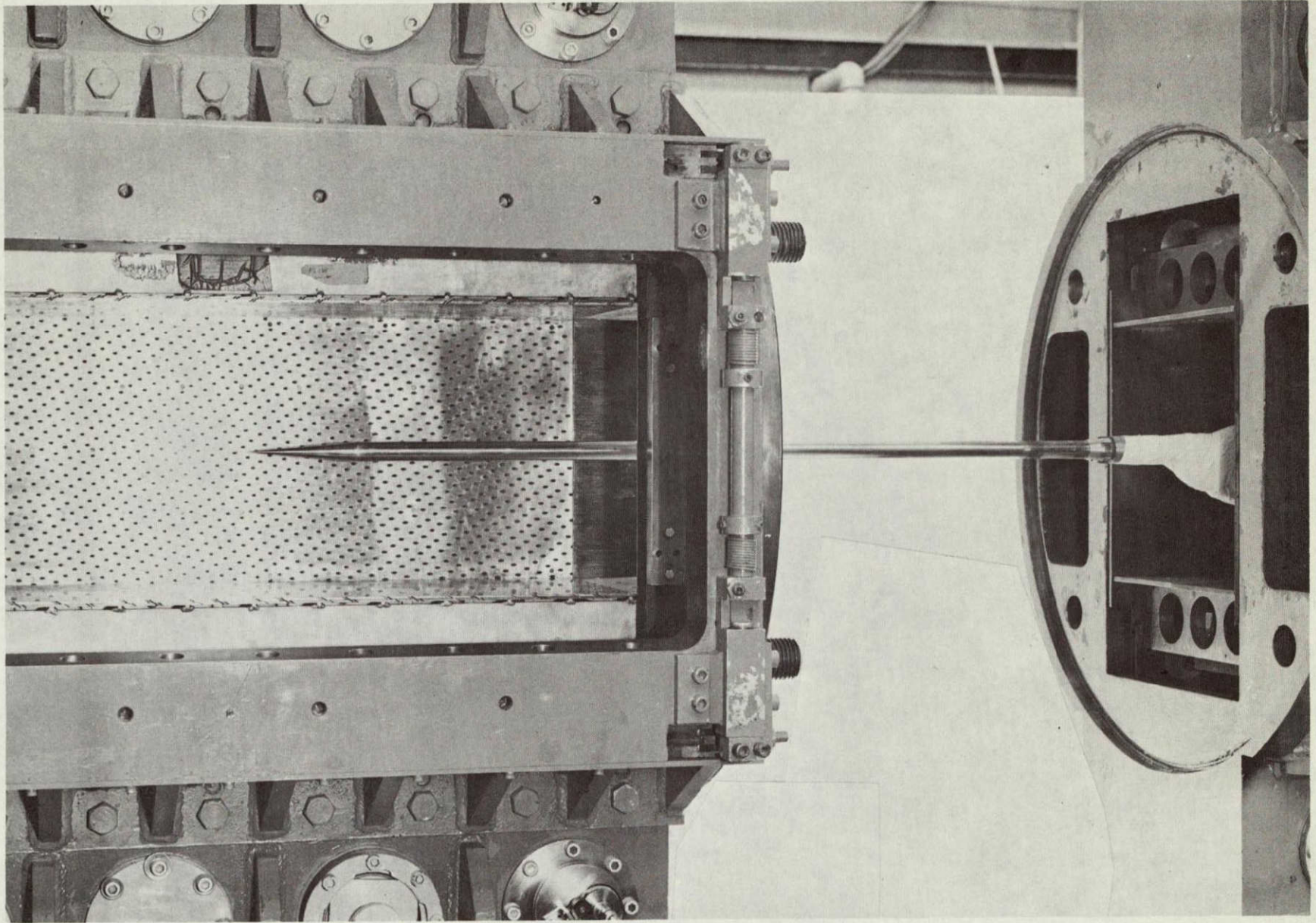
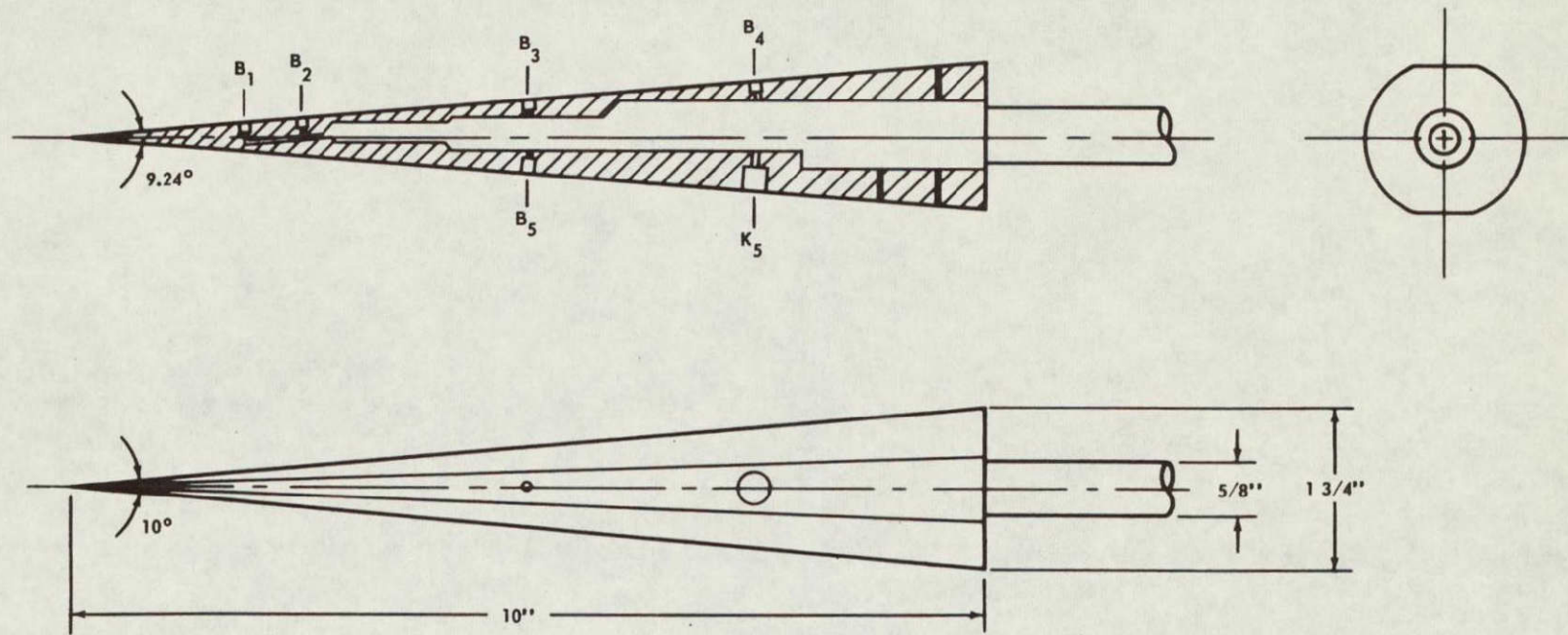FIGURE 4.1. STATIC CALIBRATION PIPE INSTALLED IN MSFC 14 IN. WIND TUNNEL

34

FIGURE 4.2. DYNAMIC CALIBRATION CONE FOR MSFC 14 IN. WIND TUNNEL

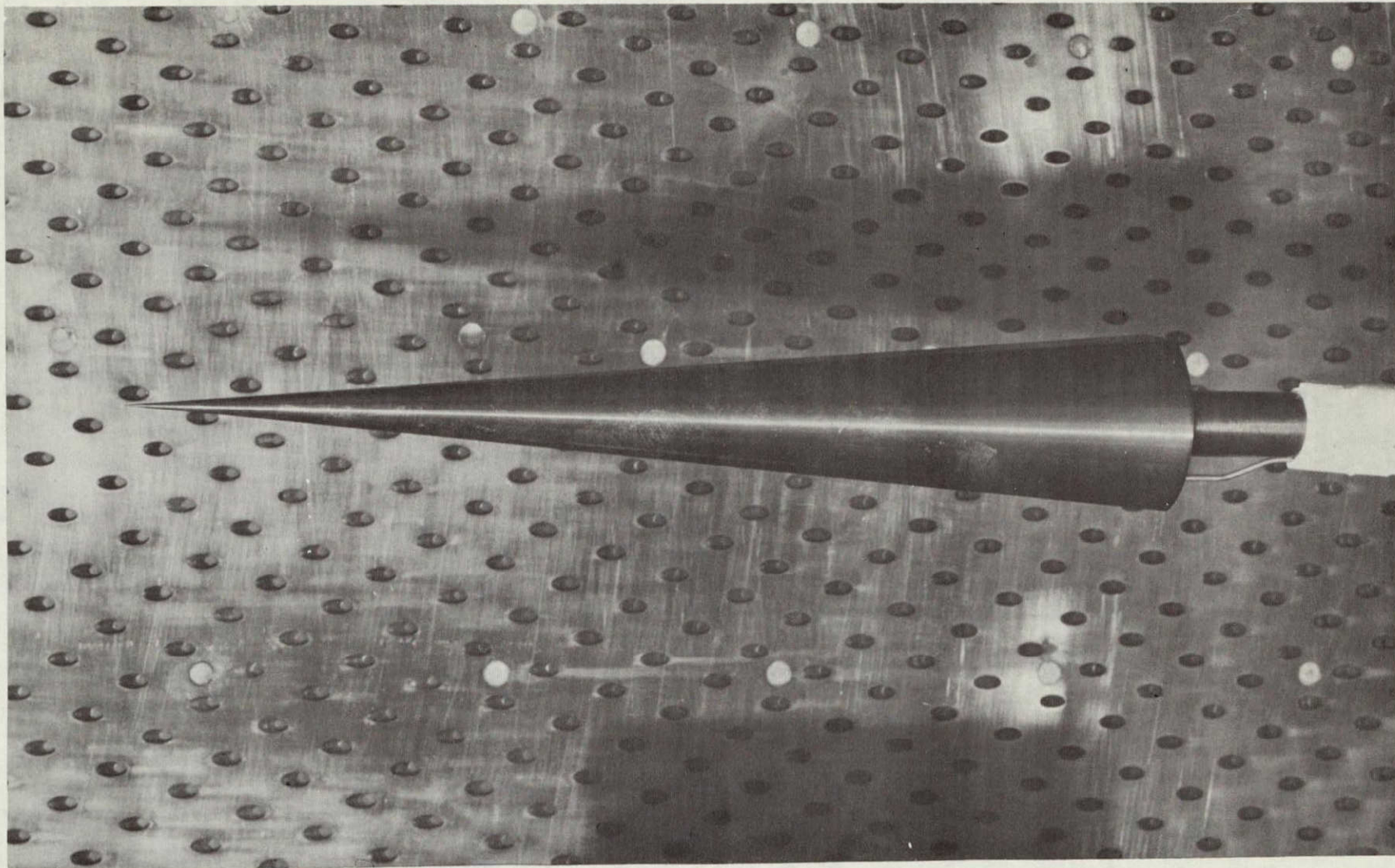FIGURE 4.3. DYNAMIC CALIBRATION CONE INSTALLED IN MSFC 14 IN. WIND TUNNEL

36

BOUNDARY LAYER CONE
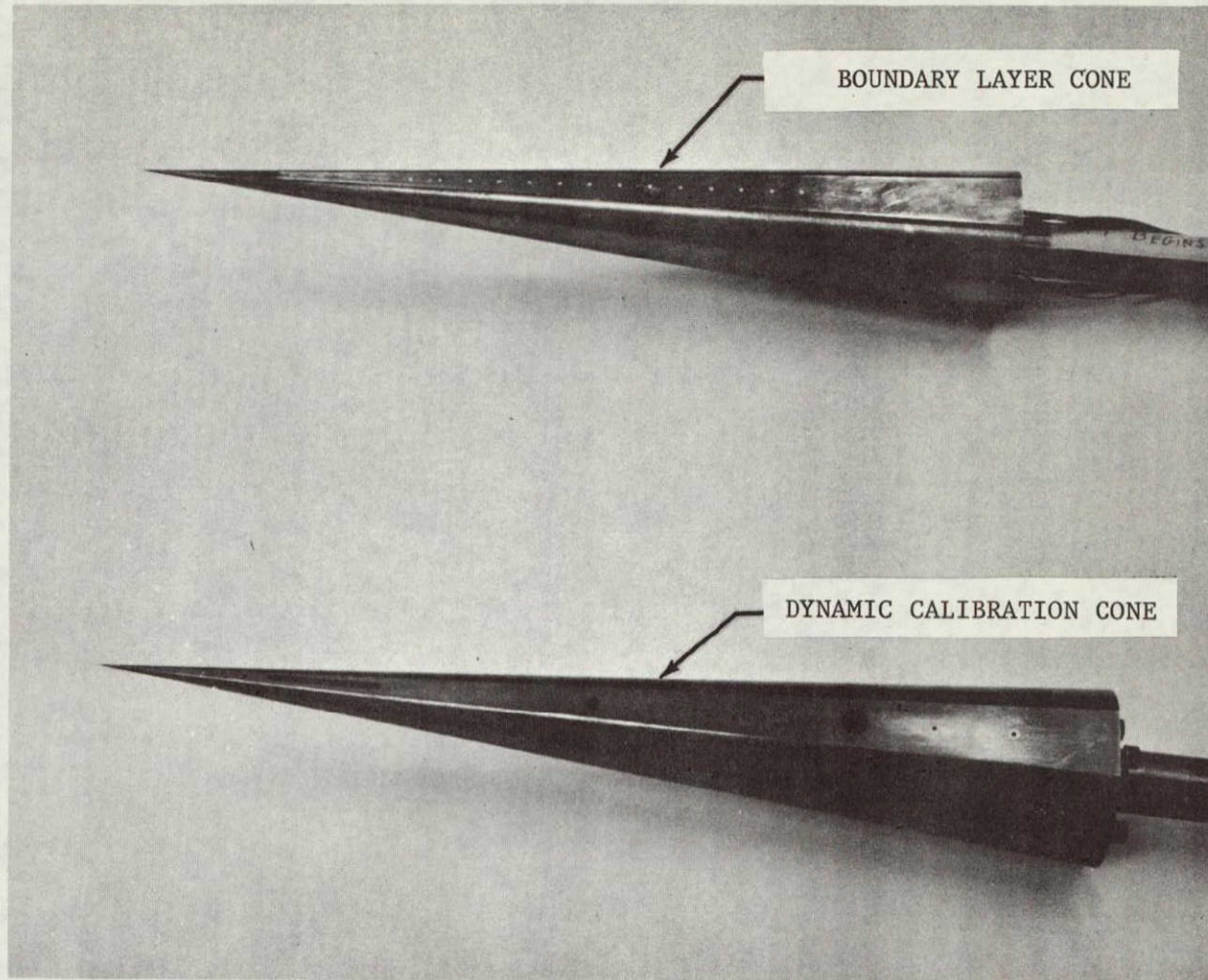
DYNAMIC CALIBRATION CONE

FIGURE 4.4. CALIBRATION MODELS FOR MSFC 14 IN. WIND TUNNEL

37

model as installed in the wind tunnel is shown in Figure 4.3. As shown in
this figure, the base of the dynamic calibration cone is located at tunnel
station 15. The flat surfaces are mounted facing the upper and lower walls.
Pressure transducers were located on the upper and lower cone flat surfaces to
determine if similar fluctuations exit on the upper and lower portion of the
tunnel. No measurements were made to compare the fluctuations radiated from
the sidewalls. The lower flat surface of the cone is shown in Figure 4.4 along
with the boundary layer transition cone.

4.3 DYNAMIC CALIBRATION SIDEWALL MOUNTED INSTRUMENTATION FOR THE MSFC 14 IN.
    TUNNEL

As previously stated, both a cone device and wall mounted instrumentation
were shown to be useful in the collection of fluctuating pressure data. Data
in the frequency range between 8 and 20,000 cps were recorded by wall mounted
instrumentation. Wall mounted instrumentation was located at several stations
along the wind tunnel. The exact location of this instrumentation is shown in
Figure 4.5. Dimensions are given from the tunnel centerline and the zero station
of the tunnel test section. All sidewall pressure transducers are the Kistler
transducer described in the instrumentation section of this report. An accel-
erometer was also attached to the wind tunnel walls. The location of this
accelerometer is also shown in Figure 4.5.

4.4 DYNAMIC CALIBRATION CONE FOR THE AEDC 16 FT TRANSONIC TUNNEL

The AEDC dynamic calibration cone is geometrically similar to the MSFC
dynamic calibration device. Instrumentation to be installed will be capable
of measuring fluctuating pressures in the same frequency range as measured in
the MSFC 14 in. tunnel. Figure 4.6 is a scaled drawing of this calibration
device. As can be seen, three different types of transducer are to be used.
The instrumentation location and type are shown in Figure 4.6. The Bytrex and
Kolite transducers require venting. The same system used in the MSFC 14 in.
tunnel dynamic calibration device will be used. The area and shape of the
venting cavity will be identical with that of the MSFC 14 in. dynamic cali-
bration cone. The flat surfaces of the cone will be mounted facing the upper
and lower walls of the tunnel. A ring of transducer is provided at dimension-
less model station 0.75 to determine the ring correlation. This will indicate
to what extent symmetry exist in the measured fluctuating pressures.

4.5 DYNAMIC CALIBRATION SIDEWALL MOUNTED INSTRUMENTATION FOR THE AEDC 16 FT
    TUNNEL

Wall mounted transducers will be used in the AEDC tests to determine the
sources of fluctuating pressures and the interdependance of the fluctuating
pressures in various sections of the wind tunnel. The tentative locations of
this instrumentation is shown in Figure 4.7. The exact location cannot be
called out until a pretest conference has been held. The transducers to be
used along the walls are the Kistler transducers described in Section 3.0 of
this report. It is the current intention that enduced accelerometers will be
placed at the location of each transducer. These locations are shown in
Figure 4.7.

X KISTLER TRANSDUCER

— 3/16 THICK

TRANSDUCERS LOCATED
ON CENTER LINE OF
LOWER NOZZLE BLOCK

TRANSDUCER LOCATED
ON TUNNEL CEILING
5 1/8" FROM WEST WALL

29 5/8 — 91

X

X

X

50 1/8

87 7/8

4 3/4

3/4 THICK

1 5/8 THICK

STATION 0

1/2 THICK

X

65 3/4

TRANSONIC TEST SECTION

GROUND
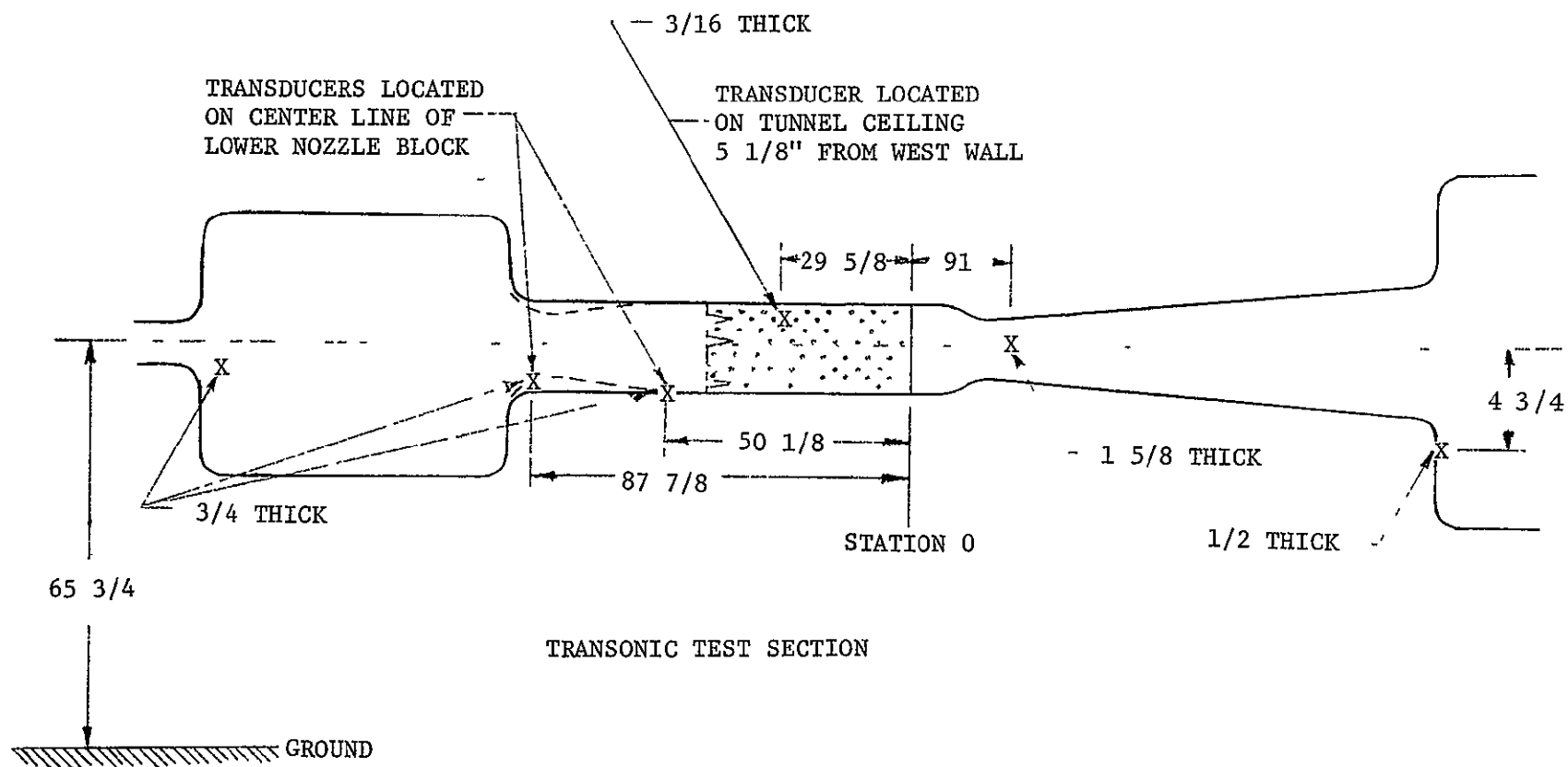
FIGURE 4.5.   SIDEWALL INSTRUMENTATION LOCATIONS IN THE MSFC 14 IN.
WIND TUNNEL

X KISTLER TRANSDUCER
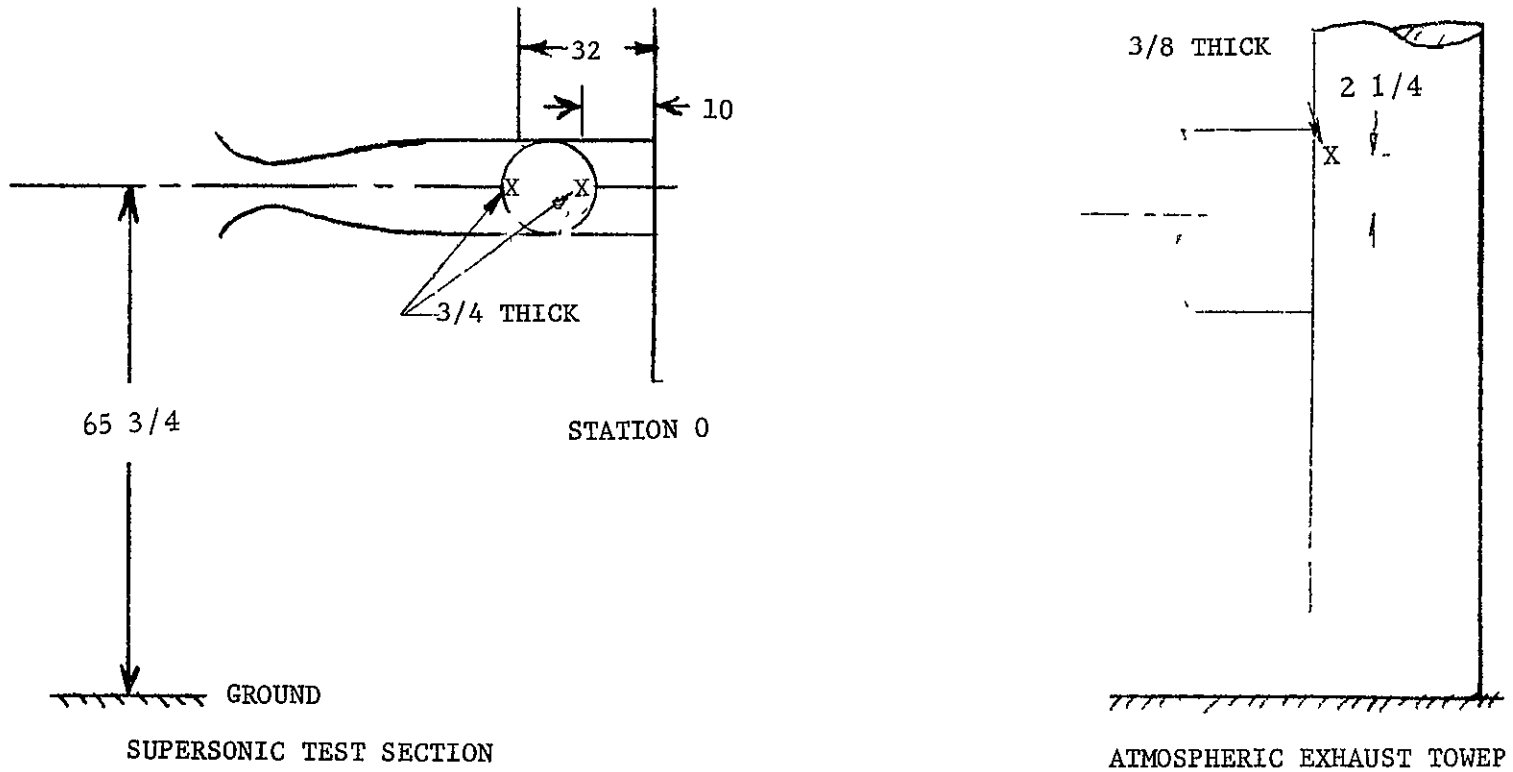
←32→

←─ 10

3/8 THICK

2 1/4

X

X

X

3/4 THICK

65 3/4

STATION 0

GROUND

SUPERSONIC TEST SECTION

ATMOSPHERIC EXHAUST TOWEP

FIGURE 4.5. SIDEWALL INSTRUMENTATION LOCATIONS IN THE MSFC 14 IN.
WIND TUNNEL

B BYTREX TRANSDUCER

ʎ KISTLER TRANSDUCER

Q KULITE TRANSDUCER

19 90

13 30

2 50

1 88

B

Q

5 00

7 50

K

26 60

RING OF 8 Q

4 65 Dɪa
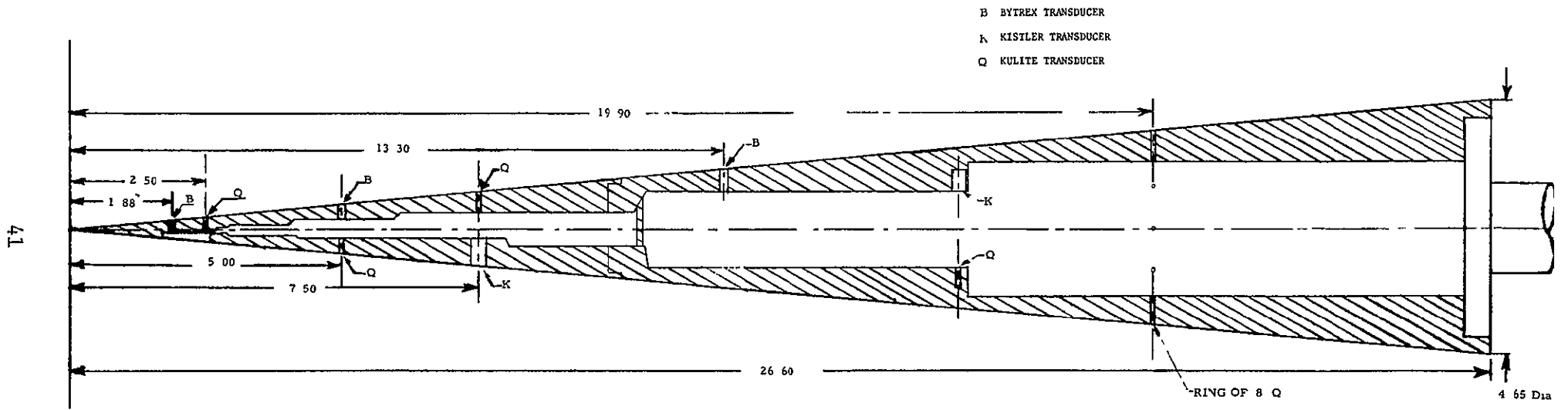
FIGURE 4.6. DYNAMIC CALIBRATION CONE FOR AEDC 16 FT WIND TUNNEL
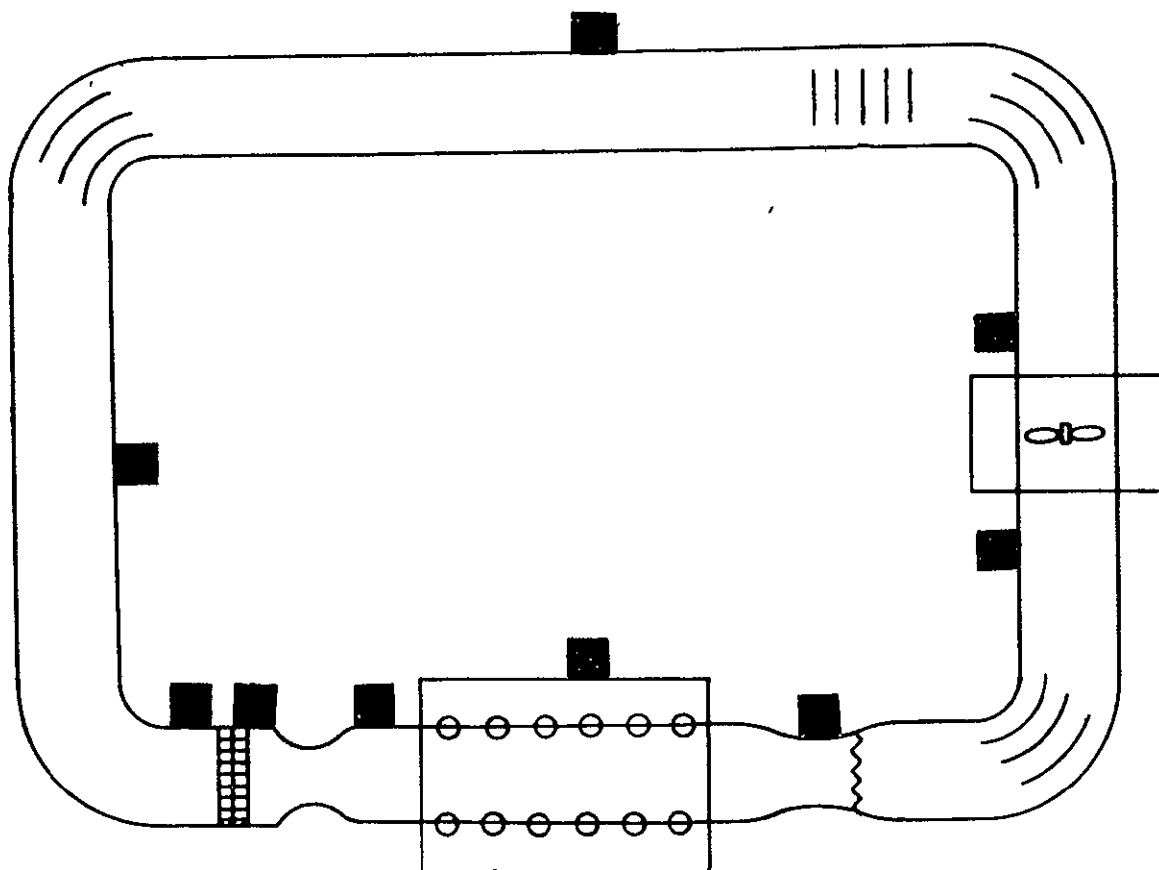
■ Location of Pressure Transducer

FIGURE 4.7. TENTATIVE SIDEWALL INSTRUMENTATION LOCATIONS IN THE
AEDC 16 FT. WIND TUNNEL

4.6 BOUNDARY LAYER TRANSITION CONE DEVICE

This model was designed for the MSFC 14 in. wind tunnel. Its purpose was to determine the feasibility of obtaining a laminar boundary layer over a dynamic calibration cone in the MSFC wind tunnel. The model is shown in Figure 4.8. The external dimensions are identical to the dynamic calibration device for this tunnel. Thermocouples are mounted along the upper flat surface. The location and type of thermocouples are indicated in Figure 4.8. Cold gaseous nitrogen is used to cool the model to temperatures of -230°F. The temperature distribution and the cooling system are described in Reference 18.

τ INDICATES THERMOCOUPLE LOCATION
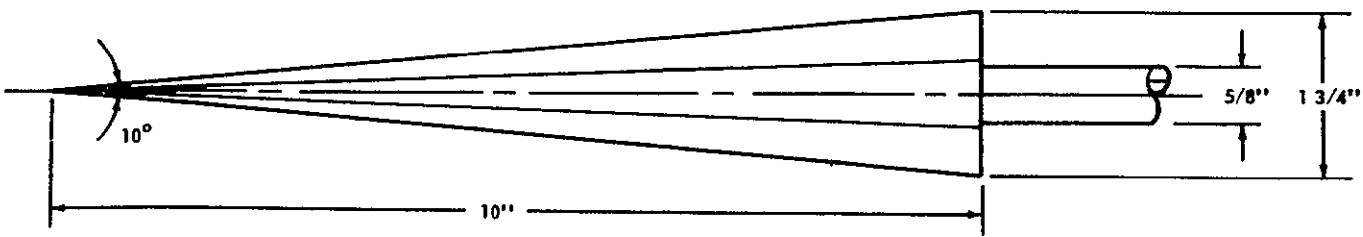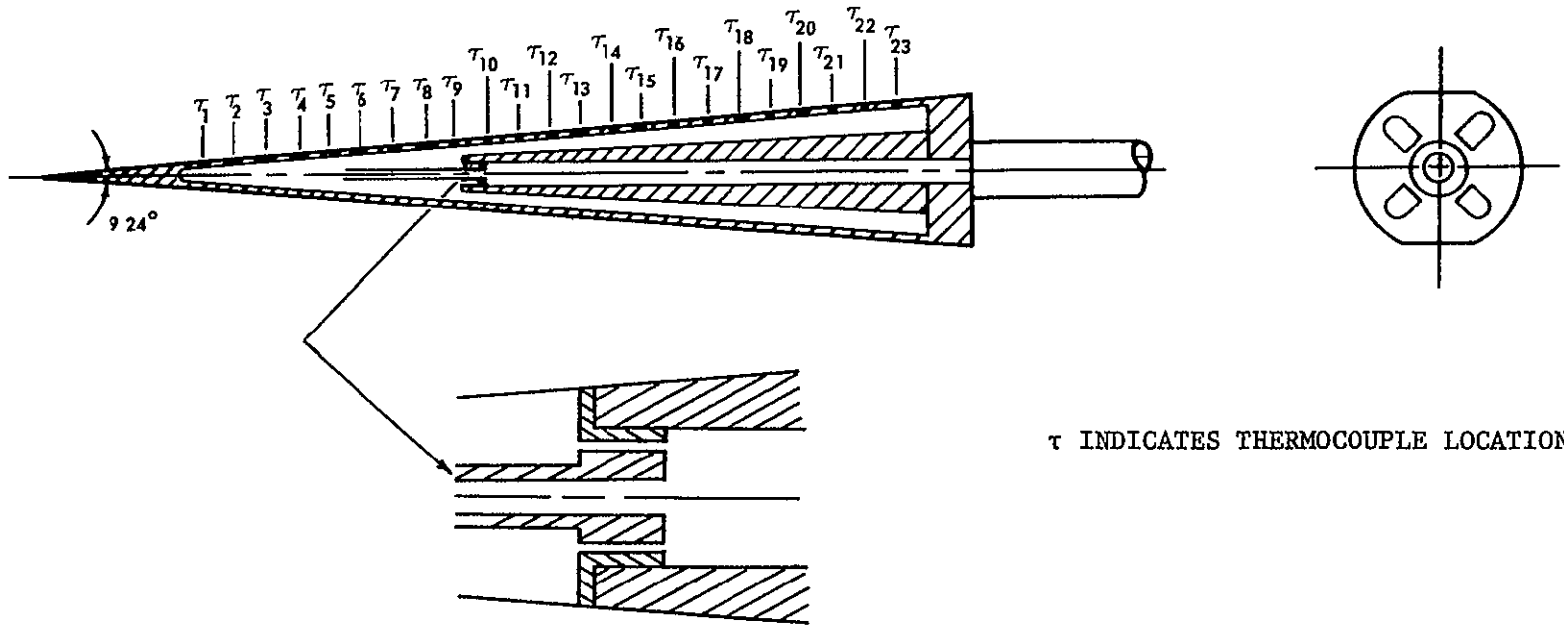
FIGURE 4.8.   BOUNDARY LAYER TRANSITION CONE FOR THE MSFC 14 IN. WIND TUNNEL

5.0 REDUCTION OF MSFC 14 IN. WIND TUNNEL
ACOUSTIC DATA

The magnitude of the fluctuations in the 14 in. tunnel were established with a rms voltmeter. All acoustic data recordings were reduced in this fashion. Analysis of the rms pressures indicated that certain data would yield significant correlation functions and power spectral densities. The selected data were then analyzed with a Princeton Applied Research, Model 100, correlator. A summary chart of data reduced in the form of correlation functions is shown in Figure 5.1. This data reduction of the background pressure fluctuations has indicated the existence of concentrations of fluctuations at specific frequencies. From this data reduction the general tunnel location at which these concentrations of fluctuations originate has been indicated. The concentrations of fluctuations at specific frequencies are:

- Another concentration of fluctuations appears primarily in the wind tunnel test section. These fluctuations are of the narrow band random type and exist in a frequency range between 6,000 and 12,000 cps.

- As the porosity is increased in the wind tunnel test section, a concentration of fluctuations of the narrow band random type appears between 100 and 200 cps.

- A concentration of fluctuations, which appears primarily in the wind tunnel diffuser, exists at a frequency of approximately 555 cps. In the transonic and subsonic Mach number range the concentration of fluctuations is strongly periodic with random noise superimposed.

- A concentration of fluctuation appears in the data prior to the wind tunnel test section. Under restricted conditions this concentration occurs in the test section. This concentration of fluctuation appear between 500 and 1750 cps.

Each of these concentrations of fluctuations is discussed in detail and substantiating data is given in Section 6.0 of this report.

Based on this analysis of background noise in the MSFC 14 in. wind tunnel, it is recommended that the following power spectral densities and autocorrelation studies be performed. A summary of the data reduction requirements is presented in Figure 5.2.

Power Spectral Densities

Type 1

50 cps to 500 cps   – 50 cps bandwidth
500 cps to 1,800 cps – 10 cps bandwidth

PHOTO NO.	RUN NO	TRANS- DUCER	MACH NO.	P_o(psi)	POR. (%)	VACUUM EXHAUST	τ RANGE (sec)	CORREL. GAIN G_A	CORREL. GAIN G_B	OSCILLO- GRAPH SCALE (mv/cm)
1/30	II,28	K1	1 10	22 0	Stand	No	0.010	1.0	1.0	50.
2/30	Cal.Sig.									↓
3/30	II,22	K1	0.85	22.0	Stand	No				
4/30	II,28	K2	1.10	↓	↓	↓				200.
5/30	Cal.Sig									1000
6/30	II,22	K2	0 85	22.0	Stand	No	↓			200.
7/30	↓	K2	0.85				0 005			
8/30	II,28	K3	1.10				0 001			
9/30	↓	K3	1 10	↓	↓	↓	0.002			
10/30		K3	1 10				0.005			↓
11/30	Cal.Sig						0.001			1000.
12/30	II,28	K5	1 10	22 0	Stand	No	↓	↓	↓	200
13/30		K5	1.10				0.005	0.2	0 2	20
14/30		K6	1.10				0 010			100
15/30		K4	1.10				0.001			200.
16/30		K4	1.10				0.005	↓	↓	10
17/30		A1	1 10				0 001	1.0	1 0	200
18/30		B1	1.10				↓	0 5	0.5	100.
19/30	II,22	B1	0 85				↓	↓	↓	↓
20/30	↓	K6	0 85				0.005	0.2	0 2	200
21/31	II,28	K2	1.10				0.001			50.
22/31		K7A	1.10				↓			100
23/31		K7A	1.10				0.005			50
24/31		K6-K7A	1.10				1.000			10
25/31		K6-K7A	1.10				0.100			20
26/31		K6-K7A	1.10				0.005			50
27/31		B1					0.005			↓
28/31		B3								
29/31	↓	B5					↓			10.
30/31	↓	B4					↓			50.
31/31	69	K6	2 99	14 7		Yes	0 010	1.0	1.0	20.
32/31	↓	↓	↓			↓	0 005	↓	↓	↓
33/31							↓	0.2	0.2	50.
34/31	Noise	Eq.On					0.010	5.0	5.0	↓
35/1	Floor	Eq.Off								
36/1		Eq On								20.
37/1		Eq.Off								
38/1		Eq.On								
39/1		Eq.Off								
40/1	↓	Eq.On								200.
41/1	Noise	Eq.On								10.
42/1	Floor	Eq Off								
43/1		Eq.On								
44/1		Eq.Off								
45/1		Eq.On&Off					0,050	↓	↓	↓
46/1	↓	Eq.On					0.010			5.

FIGURE 5.1.   TABLE OF COMPUTED CORRELATION FUNCTIONS FROM
MSFC 14 IN. WIND TUNNEL CALIBRATION

PHOTO NO	RUN NO.	TRANS-DUCER	MACH NO.	P_o(psi)	POR (%)	VACUUM EXHAUST	τ RANGE (sec)	CORREL. GAIN G_A	CORREL. GAIN G_B	OSCILLO-GRAPH SCALE (mv/cm)
47/1	Noise	Eq On					0 010	5.0	5.0	5.
48/1	Floor	Eq.On								
49/1	Correl. Memory									
50/6	68	K1	0.90	ATM	Stand	Yes	0 005	0.5	0 5	100
51/6		K2		Inlet						
52/6								2 0	2.0	
53/6							0 050			
54/6							0 001			
55/6		K3					0.001	1.0	1.0	
56/6							0 005			50
57/6		K4								100
58/6		K5						0.5	0.5	20.
59/6		A1								
60/6							0.001			50
61/6		K6					0.005		0 5	
62/6							0.001			
63/6		B1					0.005			
64/6							0.001			20
65/6		B3					0.005			50.
66/6										
67/6		A1					0 001			
68/6	65	K6	1 46				0.005			
69/6	64									
70/6	63		1.96					1.0	1.0	20.
71/6	61									50.
72/6	45			ATM				0.5	0.5	
73/6	44			28.0		No		0.1	0.1	
74/6	45/1			ATM		Yes	0 5	0.5	0.5	20.
75/6	48/0		1.46							50.
76/6	48/1									
77/6	48/2									
78/6	52	K2								
79/6	50				Solid		0.020			
80/6		K4						0.2	0.2	
81/6	52	K4					0.001			
82/6		K6					0 005			20.
83/7		K3					0.010	1.0	1.0	
84/7		K7					0 005	0.2	0.2	10.
85/7	53	K2								50
86/7		K4					0.010	1.0	1.0	20.
87/7		K4					0 005	0 2	0 2	10
88/7		K6								20.
89/7	56	K2	0.90					0.1	0.1	
90/7		K3					0 050	1.0	1.0	10
91/7		K4					0.005	0.2	0.2	
92/7		K6								20.
93/7	2	K2					0.010	0.5	0.5	50.

FIGURE 5.1.   TABLE OF COMPUTED CORRELATION FUNCTIONS FROM
MSFC 14 IN. WIND TUNNEL CALIBRATION

47

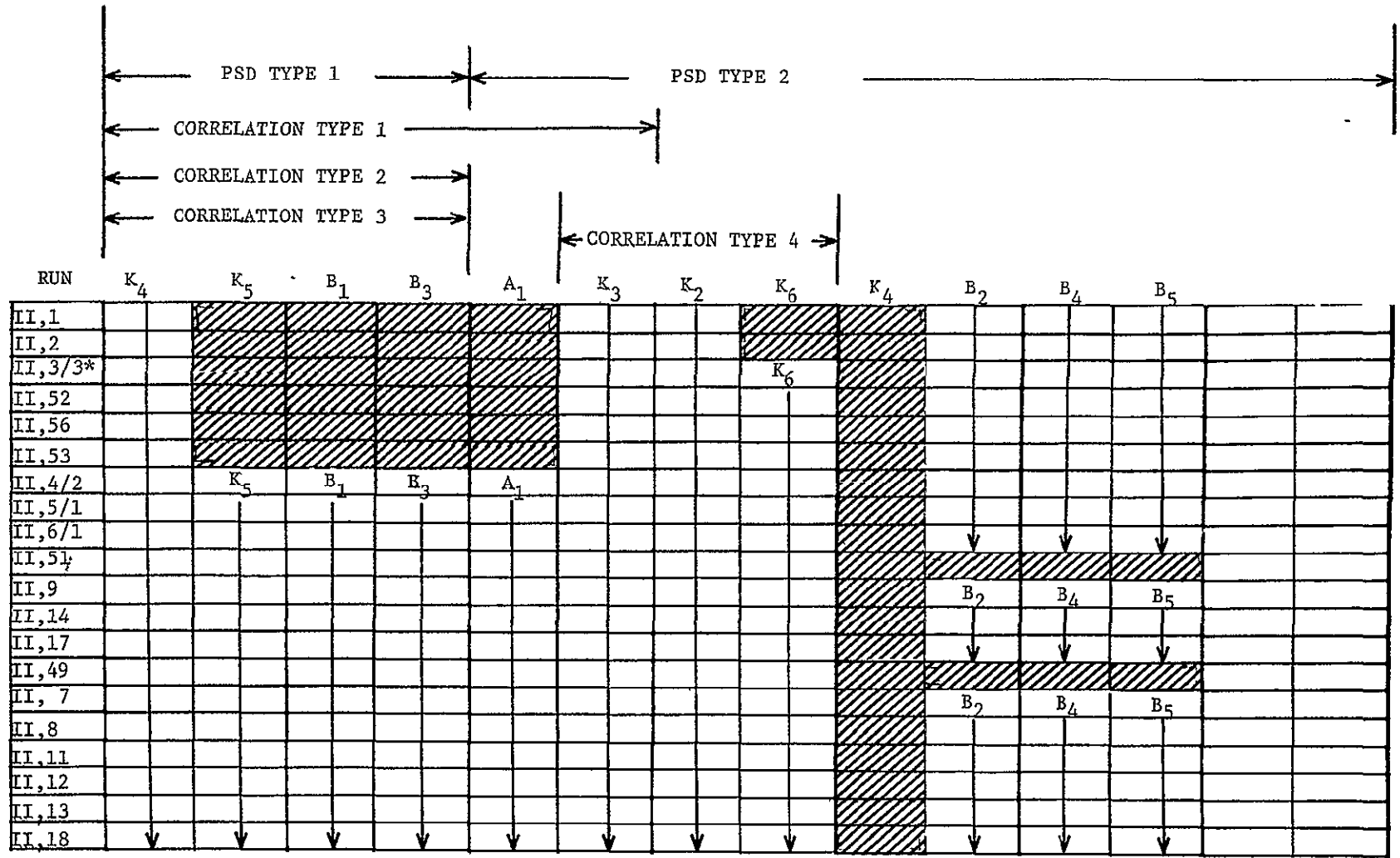| PHOTO NO	RUN NO	TRANS-DUCER	MACH NO	P_o(psi)	POR. (%)	VACUUM EXHAUST	τ RANGE (sec)	CORREL GAIN G_A	CORREL. GAIN G_B	OSCILLO-GRAPH SCALE (mv/cm)
94/7	2	K3	0 90	ATM	Solid	Yes	0.005	0 5	0 5	20
95/7		K4						0.2	0 2	50
96/7		K6						0 1	0.1	
97/7	3	K2	0.95					0.5	0 5	
98/7		K3								10
99/7		K4						0.2	0 2	50
100/7		K6						0.1	0.1	
101/7	1	K2	0.60					0.5	0 5	
102/7		K3								20
103/7		K4						0.1	0 1	
104/7		K6					0 010			50
105/7a		B4			2.50		0 050	0.5	0.5	20.
105/7b	8						0 010			10
105/7c							0.001			
106/7a		B5					0.050			
106/7b							0.010			5.
107/7a		K1					0 010			10
107/7b							0 050			5.
108/7		K2					0 010			20.
109/7		B1								
110/8		K3								
111/8		K6								
112/8	9	K2			0.75					
113/8		K3								
114/8		K4								
115/8		K5								
116/8		B1								
117/8a		B3					0.001	0.2	0.2	
117/8b							0.005			10
118/8		K6								
119/8	4	K2			0 50					
120/8		K3								
121/8		K4								
122/8		K5								
123/8		B1								
124/8a		B3								20.
124/8b										10.
125/8		K6								
126/8	8	K4			2 50					
127/8		K5								
128/8		B3					0 001	0 5	0.5	50
129/8							0.005			20.
130/8							0.020			
131/8	5		0.90		0.50		0.001			
132/8							0 005			
133/8							0.020			
134/8	14				0 75		0.001	0.2	0.2	50.
135/8							0.005			

FIGURE 5.1.   TABLE OF COMPUTED CORRELATION FUNCTIONS FROM
MSFC 14 IN. WIND TUNNEL CALIBRATION

PHOTO NO	RUN NO.	TRANS-DUCER	MACH NO.	P_O(psi)	POR. (%)	VACUUM EXHAUST	τ RANGE (sec)	CORREL GAIN G_A	CORREL GAIN G_B	OSCILLO-GRAPH SCALE (mv/cm)
136/8	14	B3	0.90	ATM	0.75	Yes	0 020	0.2	0.2	50.
137/8	13	↓	↓	↓	2 50	↓	0.001	↓	↓	↓
138/8	↓						0 005			
139/8	↓				↓		0 020			10.
140/8	15				5 40		0 001			50.
141/8	↓						0 005			↓
142/8	↓	↓	↓	↓	↓	↓	0.020	↓	↓	20
143/8	19	K6	0.40	22.0		No	0.005	0.1	0.1	50
144/8	20		0 60							
145/8	21		0 80							100.
146/8	23		0 90							↓
147/8	25		0 95		↓					↓
148/8	22		1 00		0.50					50.
149/8	27		1.05		0.75					100.
150/8	28		1.15		2 50					50.
151/8	31		1 20		5.40					
152/8	32		1.30							
153/8	↓	↓	1.45				↓	↓	↓	
154/8	19	B3	0 40				0.050	0.5	0.5	
155/8	↓		↓				0 010	↓	↓	
156/8			1 30				0.001	0.1	0.1	
157/8	20		0.60				0.050	0 5	0 5	↓
158/8	↓		↓				0 010	↓	↓	
159/8							0.001			20
160/9	21		0.80				0 050	0 2	0.2	↓
161/9	↓		↓				0.010	↓	↓	
162/9							0.001	0.1	0.1	50
163/9	23		0 90				0.050	0.2	0 2	20.
164/9	↓		↓				0.010	↓	↓	↓
165/9							0.001	0.1	0.1	50
166/9	25		0 95				0.050	0 2	0 2	20.
167/9	↓		↓				0.010	0.1—	0.1	10.
168/9							0.001			50.
169/9	28		1.00		0 50		0.050			20.
170/9	↓		↓		↓		0.005			↓
171/9							0 001			50.
172/9	27		1.05		0 75		0.050			20.
173/9	↓		↓		↓		0.010			↓
174/9							0.001			50.
175/9	29		1.15		2.50		0.050			20.
176/9	↓		↓		↓		0 005			↓
177/9							0.001			50.
178/9	33		1.20		5 40		0.050			20.
179/9	↓		↓				0.010			50.
180/9							0.001			↓
181/9	32		1.30				0.050			20.
182/9	↓		↓				0.010			↓
183/9	↓	↓	↓	↓	↓	↓	0.001	↓	↓	50.

FIGURE 5.1. TABLE OF COMPUTED CORRELATION FUNCTIONS FROM MSFC 14 IN. WIND TUNNEL CALIBRATIONS

FIGURE 5 2. SUMMARY OF RECOMMENDED FINAL REDUCTION OF MSFC 14 IN WIND TUNNEL
CALIBRATION DATA

50

PSD TYPE 1   PSD TYPE 2

CORRELATION TYPE 1

CORRELATION TYPE 2

CORRELATION TYPE 3

CORRELATION TYPE 4

RUN	K_4	K_5	B_1	B_3	A_1	K_3	K_2	K_6	K_1	B_2	B_4	B_5		
II,19/1*														
II,20/1														
II,21														
II,22					A_1			K_6	K_1					
II,23														
II,25														
II,26														
II,27														
II,28	K_4				A_1				K_1	B_2				
II,29														
II,31														
II,32														
II,47	K_4				A_1				K_1					
II,33										B_2	B_4			
II,34												B_5		
II,35	K_4													
II,36														
II,42/4	K_4				A_1				K_1					
II,43/2														
II,37/1														

Crosshatched Areas Indicate No Useful Data

*/Indicates Specific Data Tape of Given Run

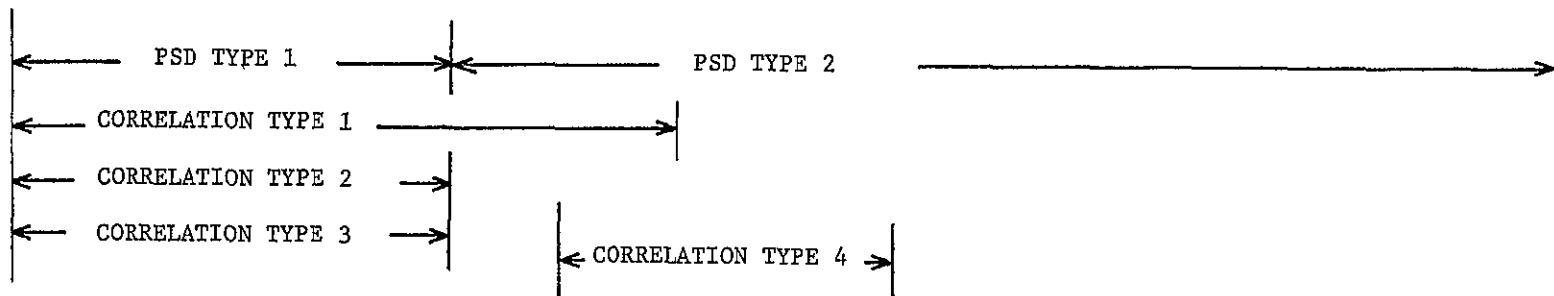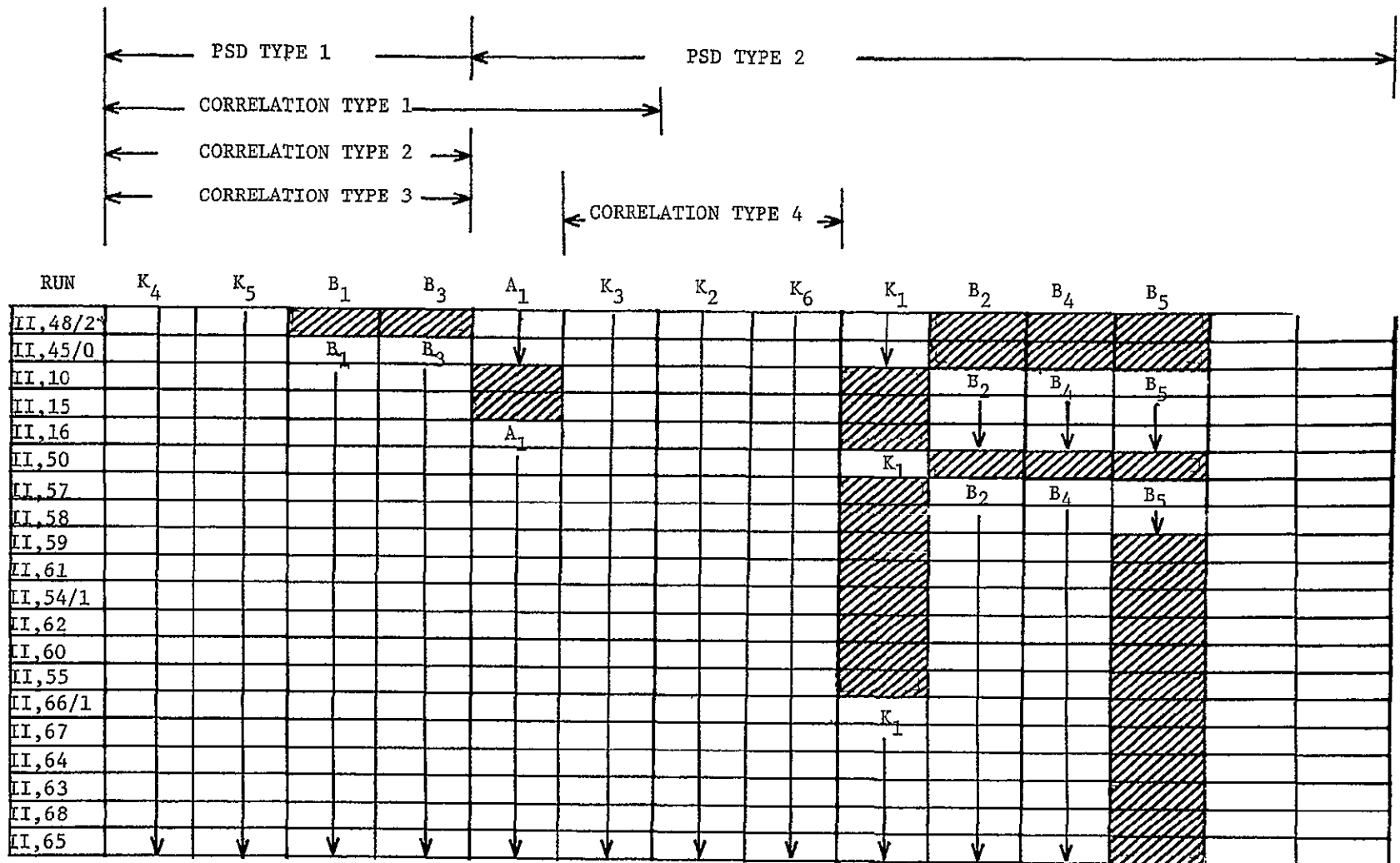FIGURE 5 2   SUMMARY OF RECOMMENDED FINAL REDUCTION OF MSFC 14 IN WIND TUNNEL CALIBRATION DATA

PSD TYPE 1 | PSD TYPE 2

CORRELATION TYPE 1

CORRELATION TYPE 2

CORRELATION TYPE 3

← CORRELATION TYPE 4 →

RUN	K_4	K_5	B_1	B_3	A_1	K_3	K_2	K_6	K_1	B_2	B_4	B_5		
II,38/1														
II,39/2														
II,35/1														
II,46														
II,41/5														
II,69														
II,70/1														
II,71/2														
II,77														
II,78														
II,79														
II,72														
II,73														
II,74														
II,75														
II,76														
II,24								K_2			B_2	B_4	B_5	
II,30	K_4								K_6					
II,44/1	K_4				A_1					K_1				
II,19/2														
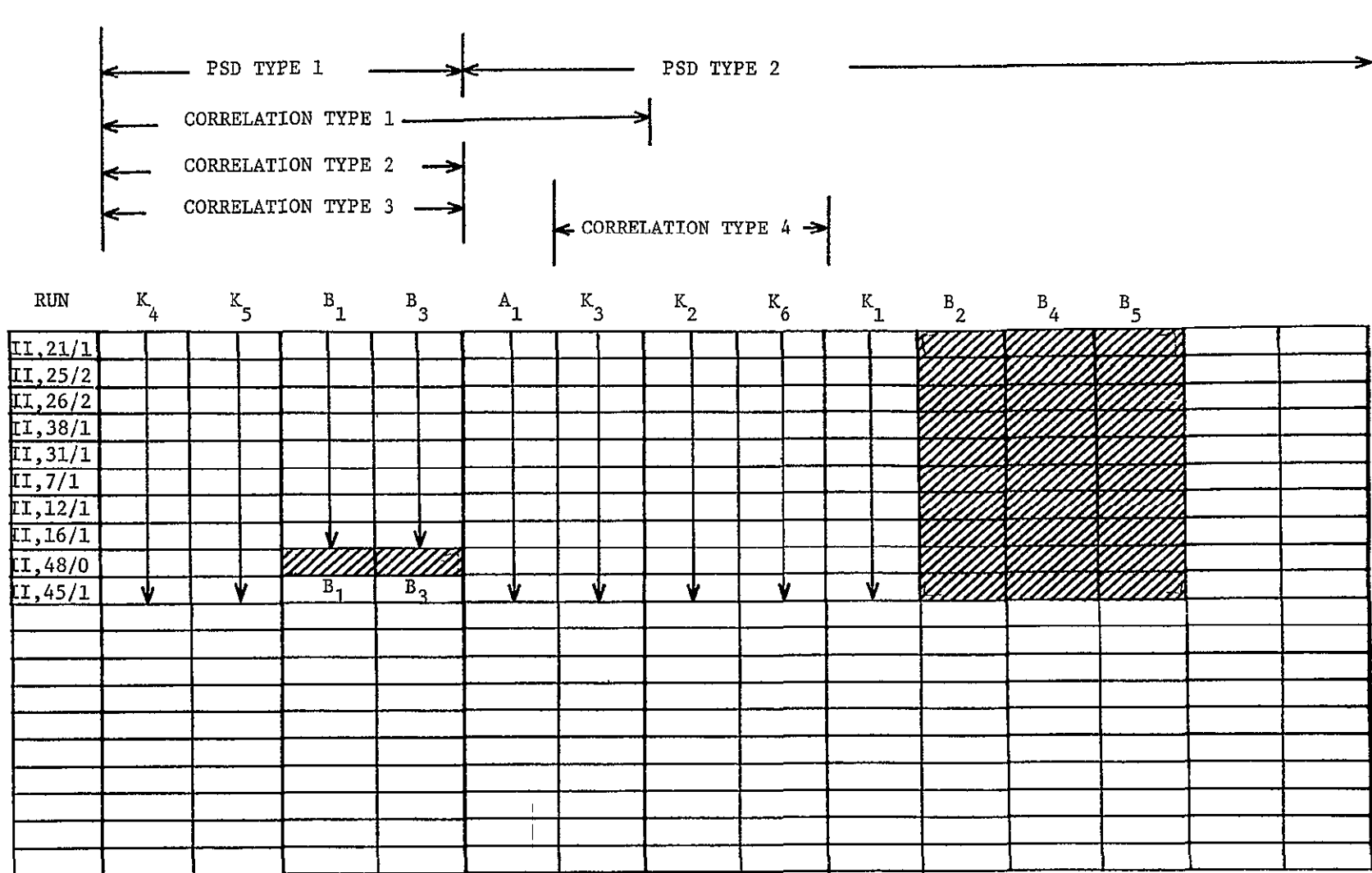
Crosshatched Areas Indicate No Useful Data

*/Indicates Specific Data Tape of a Given Run

FIGURE 5 2. SUMMARY OF RECOMMENDED FINAL REDUCTION OF MSFC 14 IN. WIND TUNNEL CALIBRATION DATA

PSD TYPE 1 — PSD TYPE 2

CORRELATION TYPE 1

CORRELATION TYPE 2

CORRELATION TYPE 3

CORRELATION TYPE 4

RUN	K_4	K_5	B_1	B_3	A_1	K_3	K_2	K_6	K_1	B_2	B_4	B_5		
II,48/2*			/////	/////						/////	/////	/////		
II,45/0			B_1	B_3	A_1				K_1	/////	/////	/////		
II,10					/////				/////	B_2	B_4	B_5		
II,15					/////				/////					
II,16					A_1				/////	↓	↓	↓		
II,50									K_1	/////	/////	/////		
II,57									/////	B_2	B_4	B_5		
II,58									/////			↓		
II,59									/////			/////		
II,61									/////			/////		
II,54/1									/////			/////		
II,62									/////			/////		
II,60									/////			/////		
II,55									/////			/////		
II,66/1									/////			/////		
II,67									K_1			/////		
II,64									↓			/////		
II,63												/////		
II,68												/////		
II,65	↓	↓	↓	↓	↓	↓	↓	↓	↓	↓	↓	/////		

Crosshatched Areas Indicate No Useful Data

*/Indicates Specific Data Tape of Given Run

53

FIGURE 5.2   SUMMARY OF RECOMMENDED FINAL REDUCTION OF MSFC 14 IN WIND TUNNEL
CALIBRATION DATA

PSD TYPE 1 — PSD TYPE 2

CORRELATION TYPE 1

CORRELATION TYPE 2

CORRELATION TYPE 3

CORRELATION TYPE 4

RUN	K_4	K_5	B_1	B_3	A_1	K_3	K_2	K_6	K_1	B_2	B_4	B_5		
II,21/1														
II,25/2														
II,26/2														
II,38/1														
II,31/1														
II,7/1														
II,12/1														
II,16/1														
II,48/0														
II,45/1			B_1	B_3										

Crosshatched Areas Indicate No Useful Data

*/Indicates Specific Data Tape of a Given Run

54

FIGURE 5.2.   SUMMARY OF RECOMMENDED FINAL REDUCTION OF MSFC 14 IN WIND TUNNEL
CALIBRATION DATA

1,800 cps to 7,000 cps - 1/3 octave bandwidth
7,000 cps to 11,000 cps - 50 cps bandwidth
11,000 cps to 20,000 cps - 1/3 octave bandwidth

Type 2

50 cps to 1,800 cps   - 50 cps bandwidth
1,800 cps to 7,000 cps   - 1/3 octave bandwidth
7,000 cps to 11,000 cps   - 50 cps bandwidth
11,000 cps to 20,000 cps   - 1/3 octave bandwidth

Autocorrelation Functions

Type 1

Narrow band from 7,000 cps to 11,000 cps

Type 2

Narrow band from 500 to 1,800 cps

Type 3

Narrow band from 150 to 500 cps

Type 4

Narrow band from 100 to 1,800 cps

This data reduction consists of 326 PSD of Type 1, 502 PSD of Type 2, 486 autocorrelations of Type 1, 330 autocorrelations of Type 2 and 3, and 253 autocorrelations of Type 4.

However, if the MSFC 14 in. trisonic wind tunnel is to be modified as recommended in Section 7.0 of this report, it is not advisable to complete the final data reduction outlined above. It would be more useful to modify the tunnel based on the information at hand. This data was reduced on a PAR correlator. A final detailed calibration should then be conducted of the Quiter Facility. This final data should then be reduced into final form and be useful in correcting dynamic tests conducted in the MSFC 14 in. facility.

6.0 RESULTS

Tests were conducted in the MSFC 14 in. trisonic wind tunnel. The significant results of these tests are described in this section. These results are also compared with those obtained in other wind tunnel facilities.

The initial series of tests were conducted with the standard MSFC 14 in. wind tunnel configuration using the transonic test section. The effects of three stagnation pressure levels were investigated. A porosity setting of 5.40% was used below Mach 1.00 and above Mach 1.20. Between Mach 1.00 and Mach 1.20 the standard porosity settings for normal operation of the wind tunnel were used. The effects of these porosity settings and the effects of stagnation pressure on the test section fluctuations are given in Figure 6.1. A series of tests were also made, below Mach 1.00 and above Mach 1.30, with a reduced porosity of 2.50%. The effects of this porosity setting is also given in Figure 6.1. For comparative purposes, the results of a calibration of the AEDC 16 ft transonic wind tunnel is given in this figure. This tunnel has a fixed porosity of 6.00%.

Figure 6.1 shows that increasing the stagnation pressure causes the rms pressure coefficient in the test section to increase. It also shows that, in the subsonic regime, reducing the porosity of the walls increases the magnitude of the fluctuations. The maximum fluctuations occur between Mach 1.00 and 1.20 when the wind tunnel is operating with its standard settings. The region of maximum fluctuation is precisely the region where the porosity is reduced below 5.40%. The fluctuation level in the test section is generally comparable to that measured in the AEDC 16 ft transonic wind tunnel. However, the maximum fluctuations in that tunnel occur between Mach 0.65 and 0.75. It is significant that the wall porosity is not reduced just above Mach 1.00 in the AEDC wind tunnel. Instead a constant porosity of 6.00% is used throughout the Mach number range.

Measurements of the pressure fluctuations were made in the stilling chamber of the MSFC 14 in. wind tunnel. One transducer was located just down stream of the control valve in the entrance of the stilling chamber. Another was located downstream of heat exchanger at the exit of the stilling chamber. Data from some of these measurements is given in Figure 6.2. The pressure fluctuations are shown to be roughly proportional to the operating stagnation pressure and essentially independent of Mach number or flow rate. Also the passage of the air through the stilling chamber, which contains a heat exchanger, is shown to reduce the pressure fluctuations to approximately 15% of their original magnitude.

Tests were conducted using the transonic test section with the standard wind tunnel configuration. Additional tests were carried out with the stilling chamber removed and with the supply tank and control valve removed. The results are given in Figure 6.3. It is evident that atmospheric entrance into the test section generates as much fluctuation in test section pressure as the normal
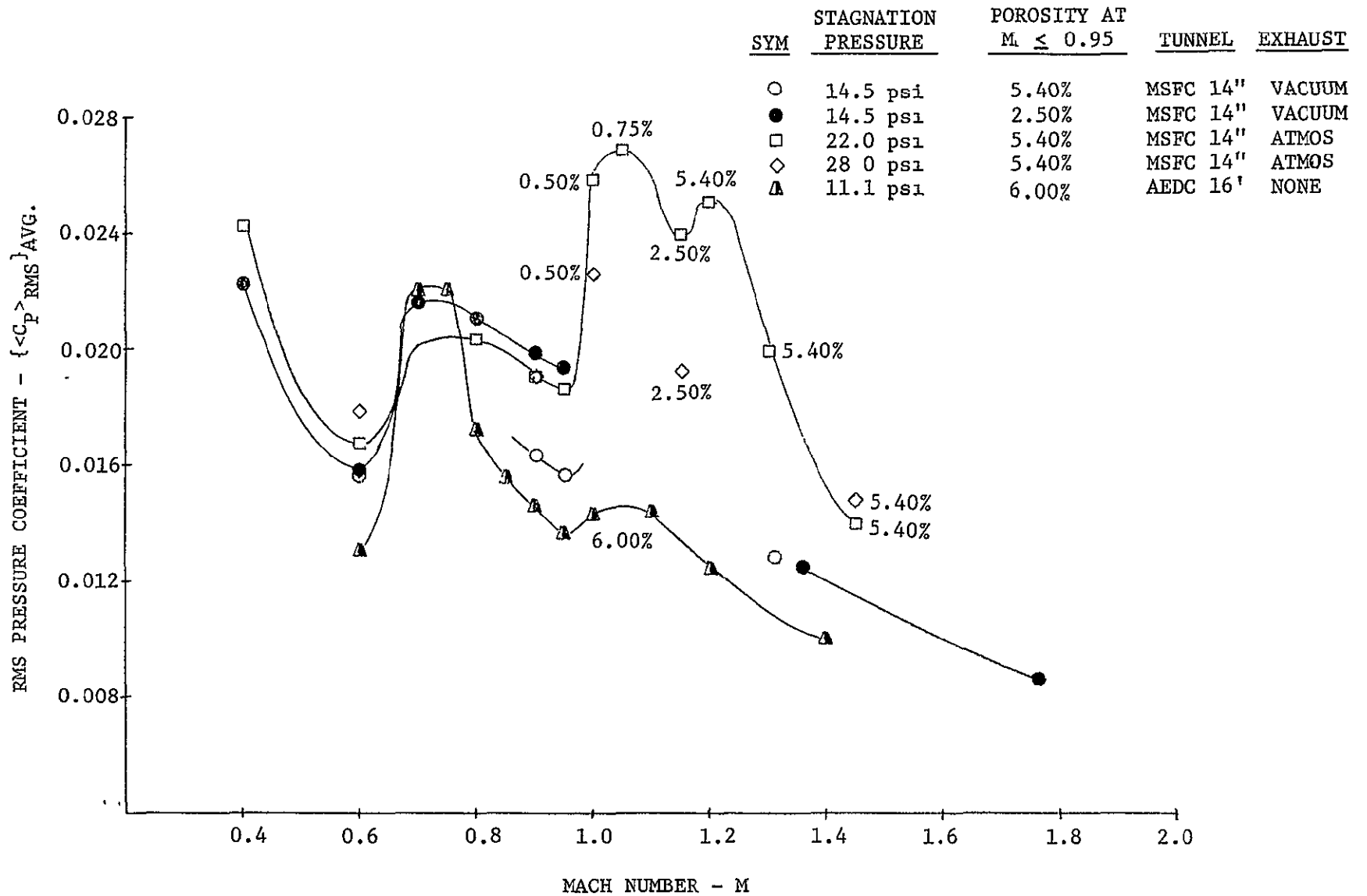
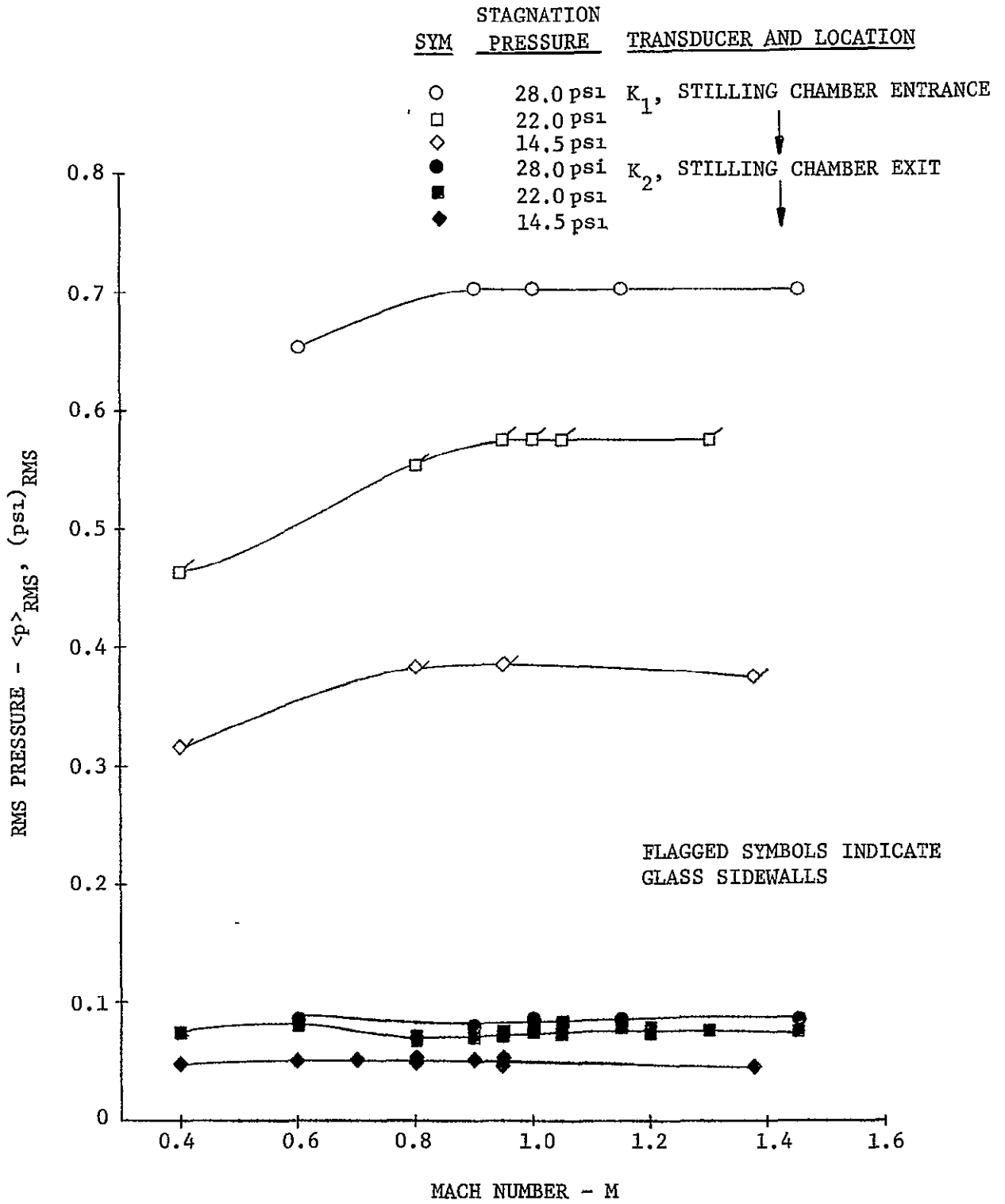FIGURE 6.1. EFFECTS OF STAGNATION PRESSURE AND POROSITY ON TEST SECTION FLUCTUATIONS

FIGURE 6.2. EFFECTS OF STAGNATION PRESSURE ON STILLING CHAMBER FLUCTUATIONS
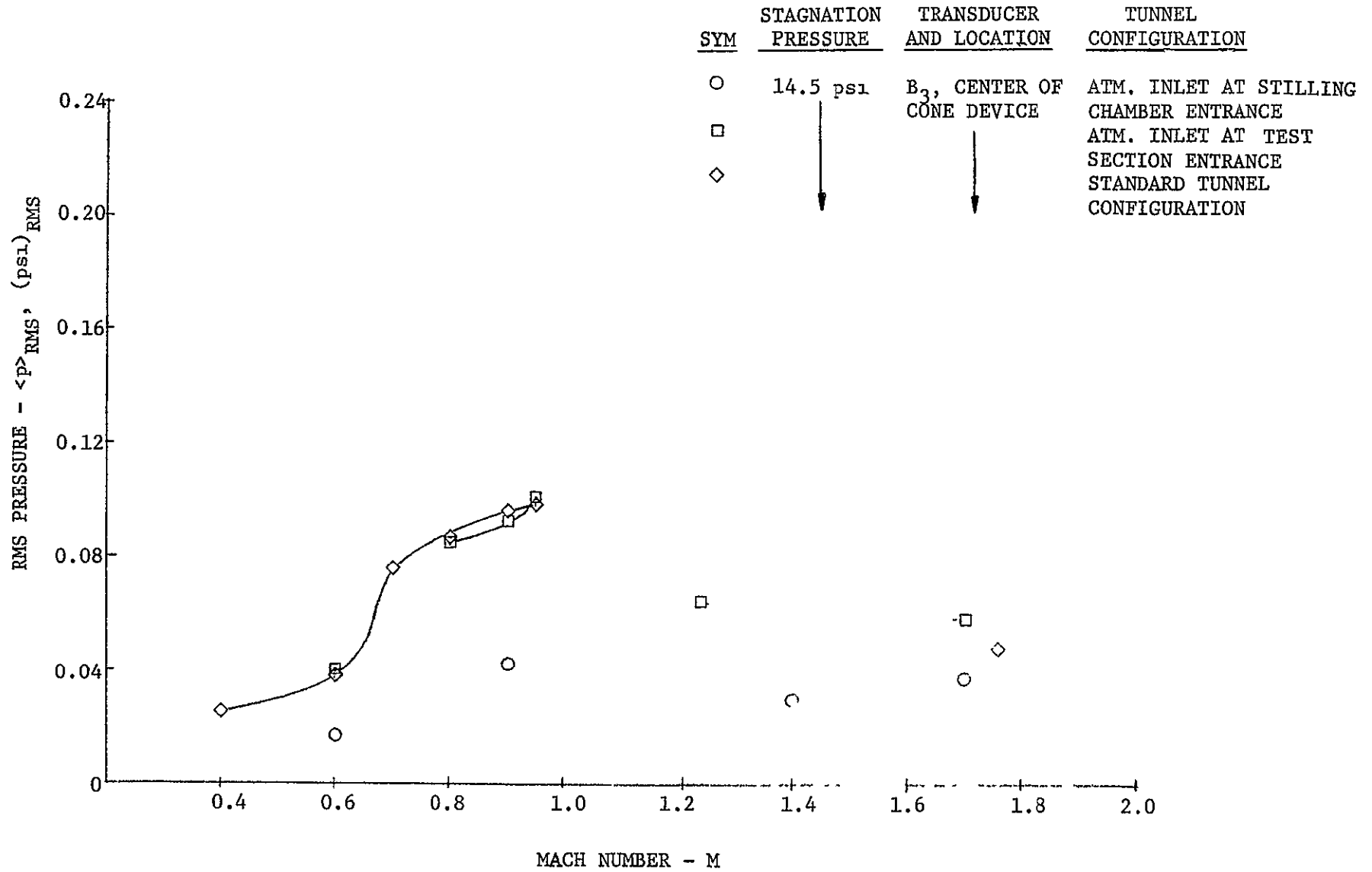
FIGURE 6.3. EFFECTS OF TUNNEL CONFIGURATION ON BACKGROUND

NOISE AT 2.5% POROSITY

operating configuration generates. However, atmospheric entrance to the stilling chamber reduces the fluctuation level to about half of that measured in the normal operation of the wind tunnel. This result is restricted to the regime in which these tests were conducted, which was below Mach 1.00 and above Mach 1.20.

A series of tests was conducted with the transonic test section to compare pressure fluctuations measured on a porous wall with those measured on the calibration cone in the approximate center of the test section. These results are shown in Figures 6.4 and 6.5. The wall measurements are approximately twice as great as those measured in the center of the tunnel. Figure 6.7 shows the accelerations of the porous wall that were measured near the pressure transducer. Extremely large accelerations were measured. These measurements follow the same trends as the measurements of the porous wall pressure fluctuations. Some runs were made during this series of tests with solid glass side walls, Figure 6.4 The solid glass walls are shown to increase the fluctuation level below Mach 1.00 and reduce it above Mach 1.00.

Measurements were made of the pressure fluctuations in the diffuser when the transonic test section was in operation. The rms pressures measured in the diffuser is given in Figure 6.7. A comparison with Figures 6.4 and 6.5 shows that these fluctuations follow the same trends as those measured in the test section. The magnitudes are about the same as those measured on the test section side wall, and they are about one half of those measured in the center of the test section.

A series of tests were made to determine the effects of stagnation temperature, or stilling chamber heating rate, on the test section fluctuations. The results of this series of tests are given in Figures 6.8 and 6.9. The data shows that the addition of a limited quantity of heat reduces the test section fluctuations. Beyond a given point, however, additional heating tends to increase the test section fluctuations.

Some of the key data that was obtained in the tests described above was reduced with a Princeton Applied Research, Model 100, Correlator. The correlation functions thus derived gives the mean square values of the fluctuations and also yields the primary frequency composition of the data. Figure 6.10 shows the correlation functions of the data measured with a cone mounted transducer in the transonic test section and with the wind tunnel in its standard operating configuration. The stagnation pressure was 22.0 psi. The correlator was set to reduce data from 7 cps to 100,000 cps. The transducer data above 20,000 cps is eliminated by instrumentation characteristics. This data corresponds to that shown by the level squares in Figures 6.2 and 6.4. The first two correlations in Figure 6.10 show random low level fluctuations for low Mach number operation of the wind tunnel. The correlation at Mach 0.80, which is the third correlation, shows a strong, narrow band, random oscillation at 10,000 cps. This strong oscillation is seen to persist up through Mach 1.30 as the narrow band frequency shifts to 12,000 cps. Figure 6.10 shows that the major portion of the test section fluctuations from Mach 0.80 to Mach 1.30 consists of a narrow band oscillation in the 10,000 to 12,000 cps range.
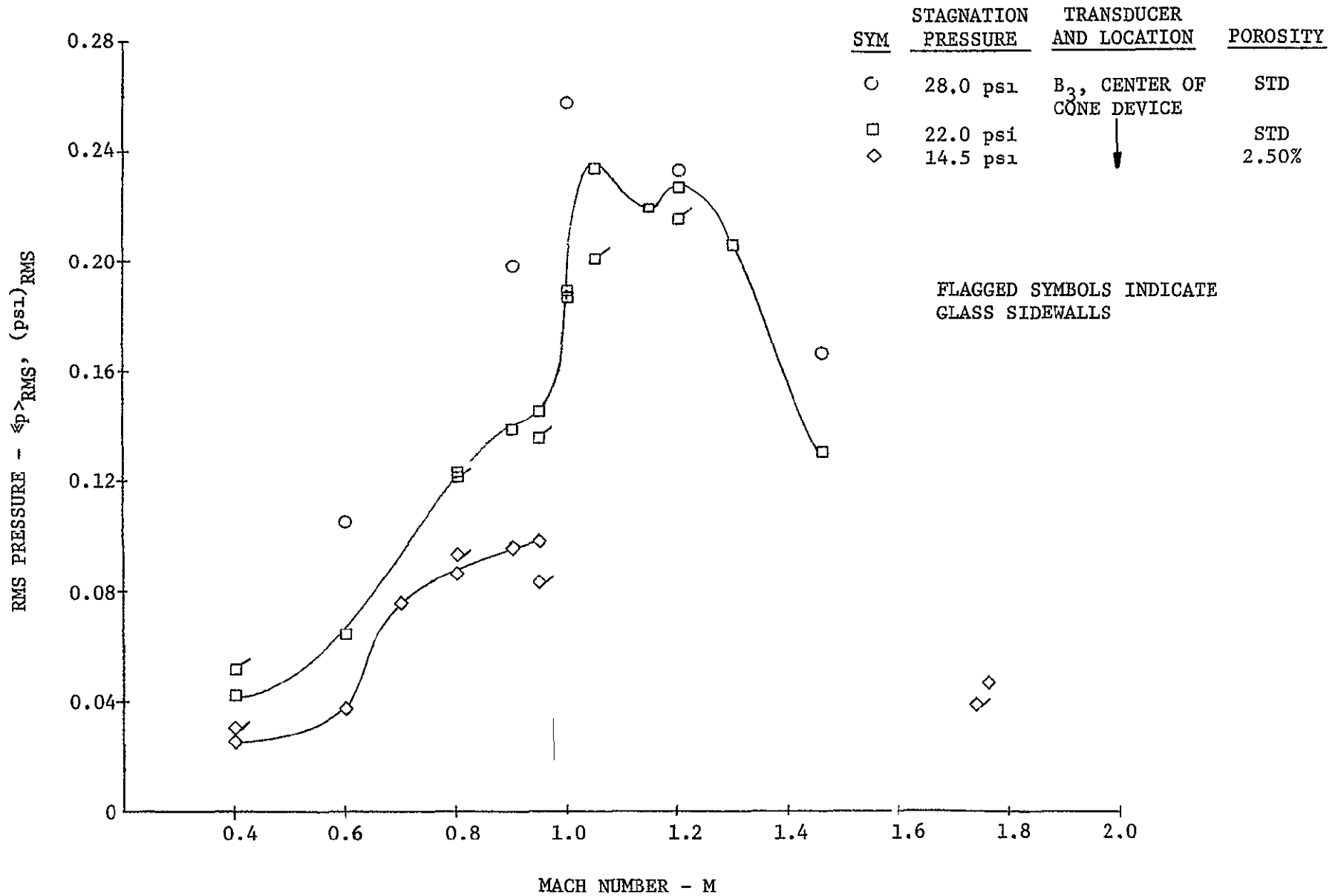
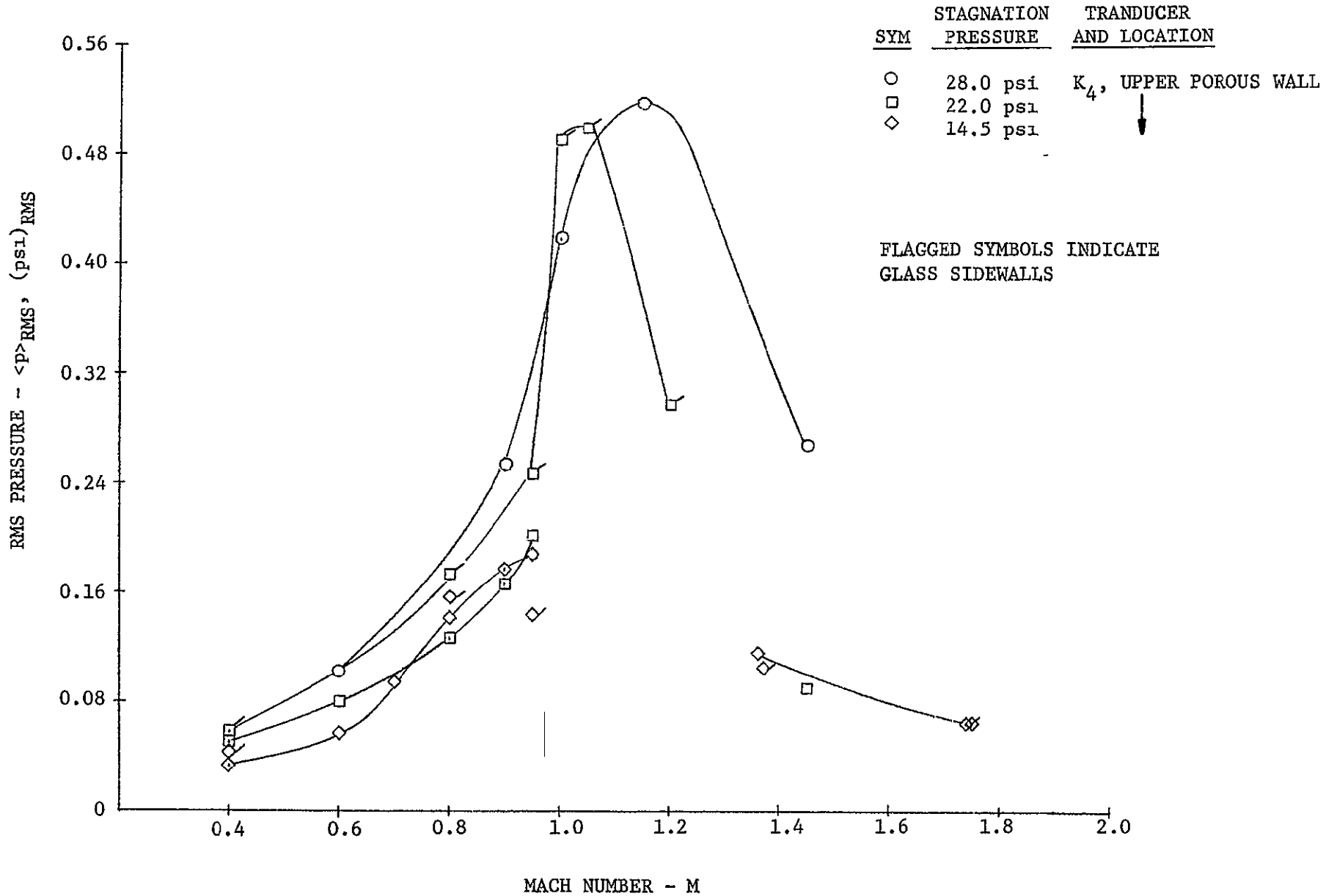FIGURE 6.4. CONE MOUNTED PRESSURE TRANSDUCER AT CONE MIDPOINT

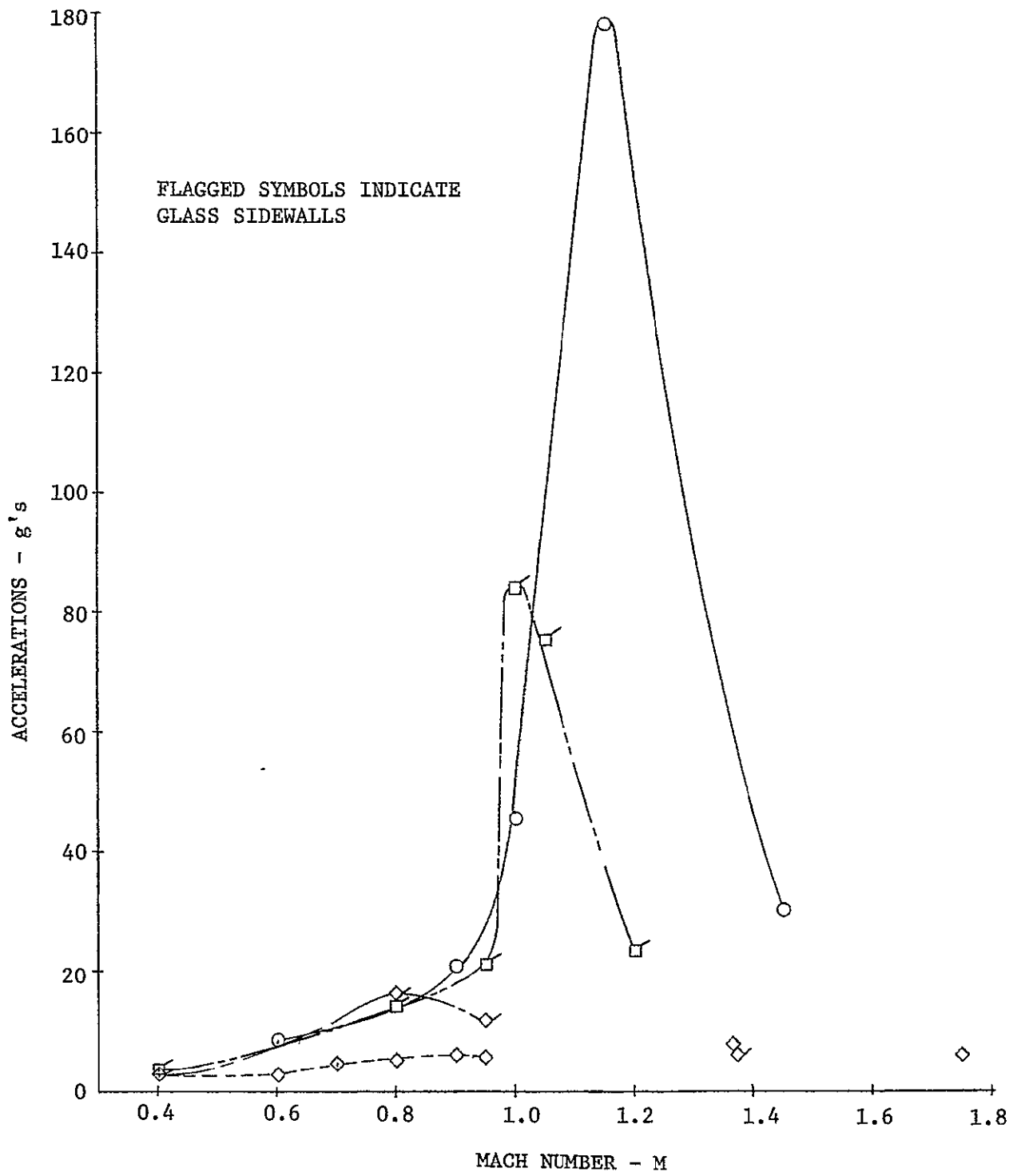FIGURE 6.5.   UPPER POROUS WALL MOUNTED PRESSURE TRANSDUCER
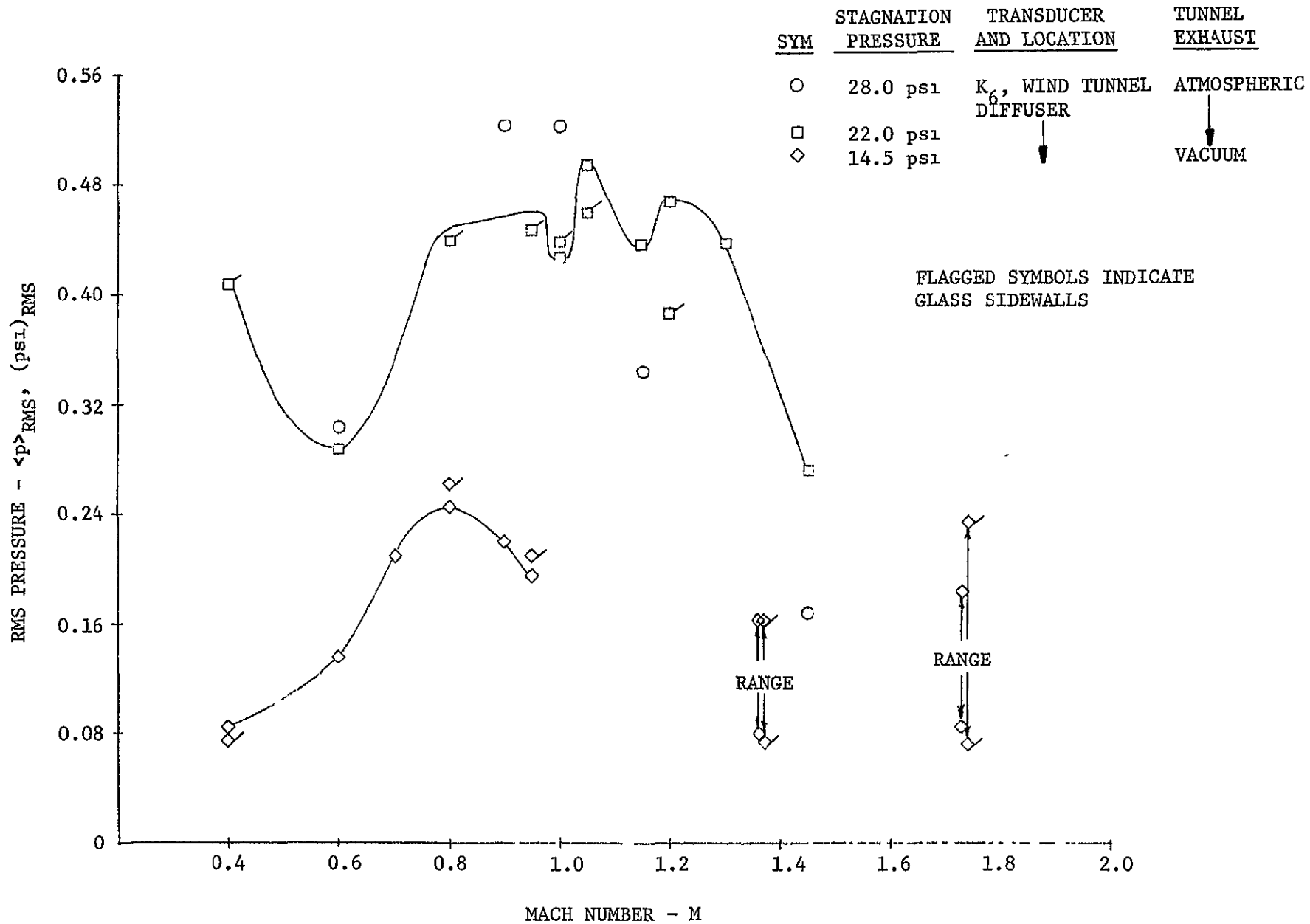
FIGURE 6.6. VIBRATION LEVEL MEASURED ON UPPER POROUS WALL

FIGURE 6.7.   MSFC 14 IN. TUNNEL DIFFUSER FLUCTUATIONS

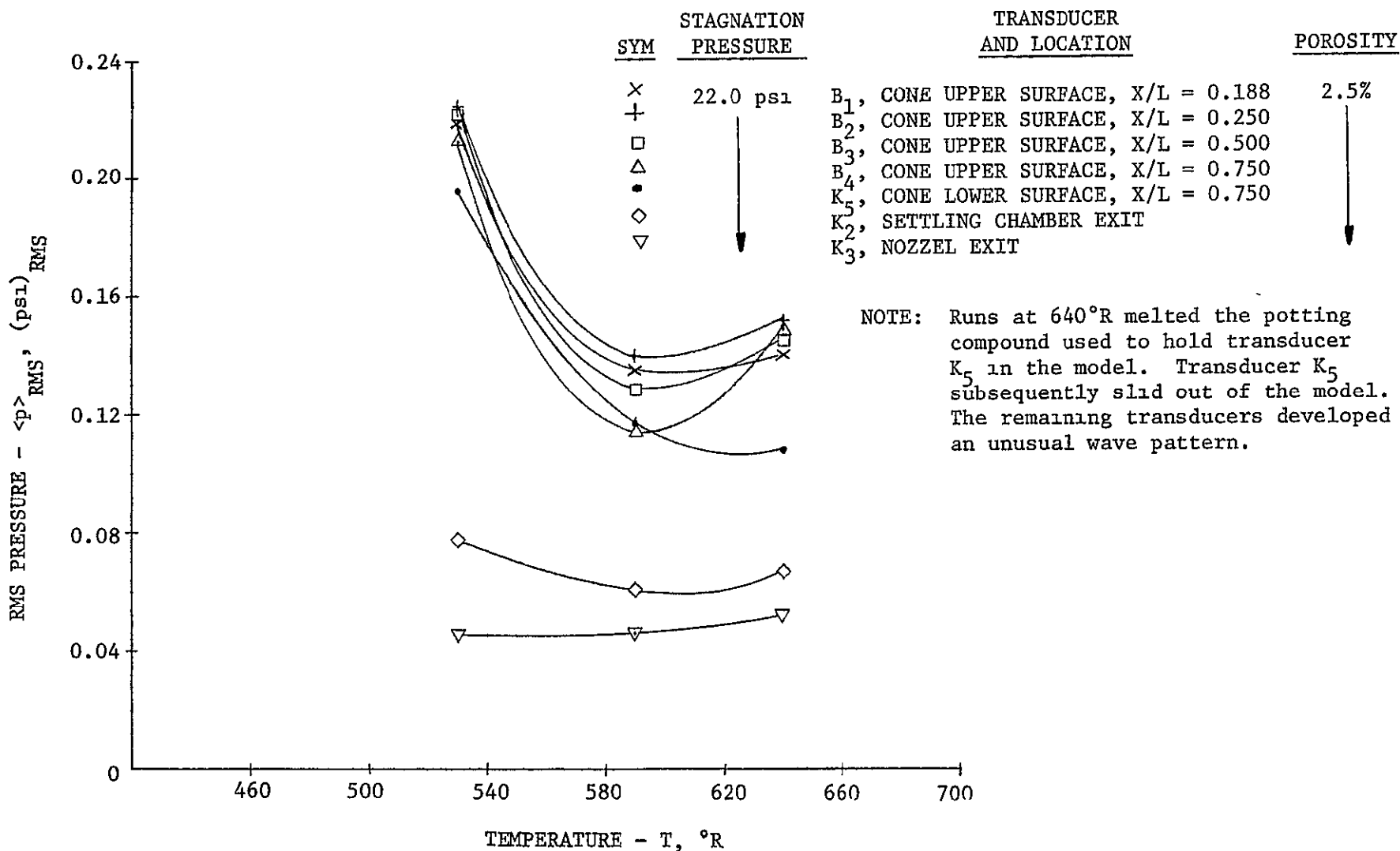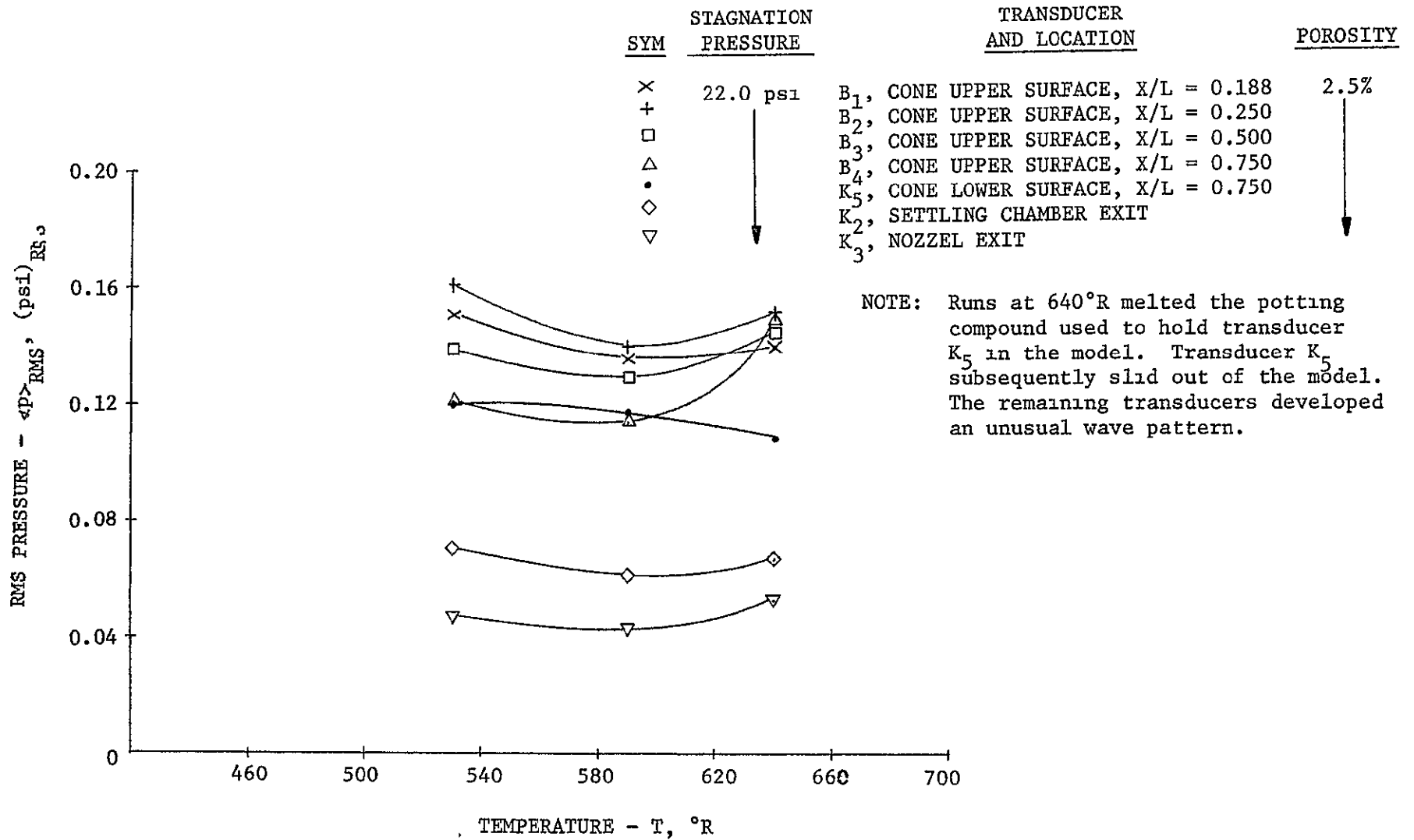FIGURE 6.8. TEMPERATURE EFFECTS ON FLUCTUATIONS AT MACH NUMBER OF 1.15

| | STAGNATION | TRANSDUCER | |
| SYM | PRESSURE | AND LOCATION | POROSITY |

× + □ △ • ◇ ▽   22.0 psi

B_1, CONE UPPER SURFACE, X/L = 0.188   2.5%
B_2, CONE UPPER SURFACE, X/L = 0.250
B_3, CONE UPPER SURFACE, X/L = 0.500
B_4, CONE UPPER SURFACE, X/L = 0.750
K_5, CONE LOWER SURFACE, X/L = 0.750
K_2, SETTLING CHAMBER EXIT
K_3, NOZZLE EXIT

NOTE: Runs at 640°R melted the potting compound used to hold transducer K_5 in the model. Transducer K_5 subsequently slid out of the model. The remaining transducers developed an unusual wave pattern.

FIGURE 6.9. TEMPERATURE EFFECTS ON FLUCTUATIONS AT MACH NUMBER 0.90
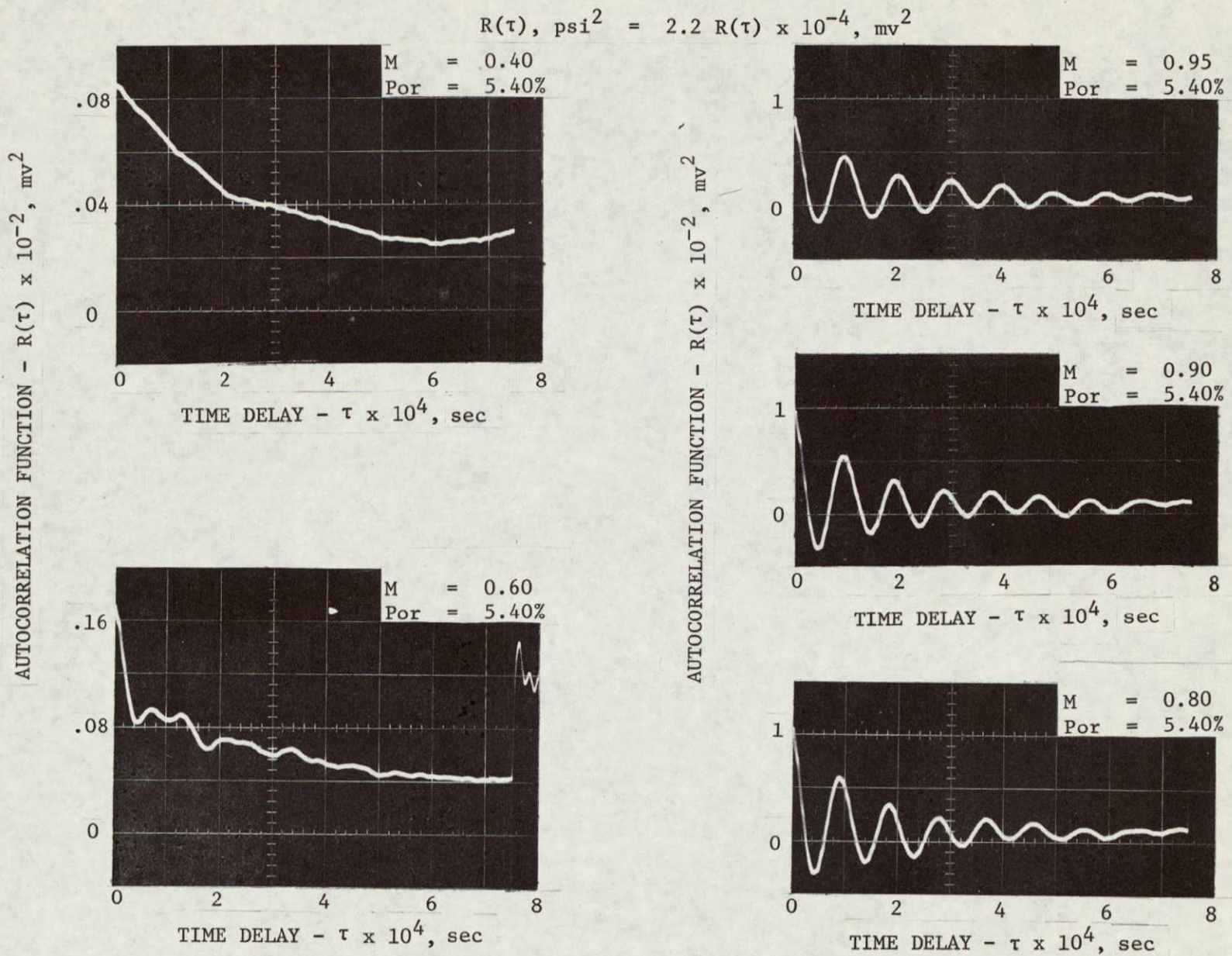
$$R(\tau), \text{ psi}^2 = 2.2\ R(\tau) \times 10^{-4}, \text{ mv}^2$$

FIGURE 6.10.   EFFECTS OF MACH NUMBER ON TRANSONIC TEST SECTION FLUCTUATIONS
(TRANSDUCER B_3, P_o = 22.0 psi, CONFIGURATION T_1, SONIC BLOCKS)

$$R(\tau), \text{psi}^2 = 2.2\ R(\tau) \times 10^{-4},\ \text{mv}^2$$

FIGURE 6.10. EFFECTS OF MACH NUMBER ON TRANSONIC TEST SECTION FLUCTUATIONS
(TRANSDUCER B_3, P_o = 22.0 psi, CONFIGURATION T_1, SONIC BLOCKS)

$$R(\tau), \text{psi}^2 \;=\; 2.2\; R(\tau) \times 10^{-4}, \text{mv}^2$$
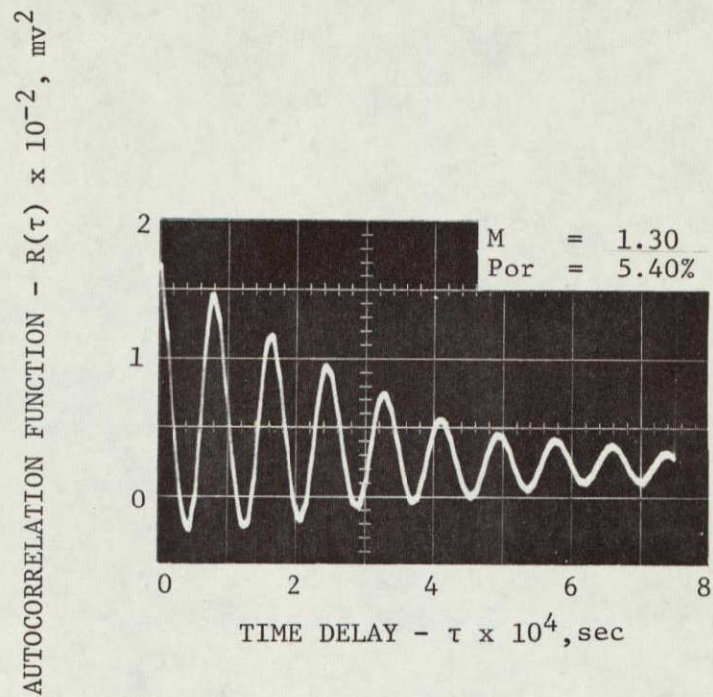
FIGURE 6.10. EFFECTS OF MACH NUMBER ON TRANSONIC TEST SECTION FLUCTUATIONS
(TRANSDUCER B_3, P_O = 22.0 psi, CONFIGURATION T_1, SONIC BLOCKS)

These 10,000 to 12,000 cps fluctuations obscured lower frequency oscilla-
tions. In order to observe these low frequency fluctuations, the correlator
was set to reduce data in the 8 to 2,000 cps range. (With this setting some
fluctuations between 2,000 cps and 8,000 cps may be sensed.) The same data
that was analyzed above was then reduced with these settings to establish its
low frequency composition. These results are shown in Figure 6.11. A narrow
band random oscillation is observed at Mach 0.40, 0.60, and 0.80. It rises in
frequency from 110 cps at Mach 0.40 to 160 cps at Mach 0.80. As the Mach num-
ber rises random fluctuations are superimposed on this narrow band oscillation.
It appears that the narrow band fluctuations die out at Mach 0.90.

Data was reduced on the correlator to determine the effects of variations
in porosity. This data reduction covers 8 cps through 100,000 cps. Again the
instrumentation blocks all fluctuations above 20,000 cps. The data of Figure
6.12 describes the frequency composition of the test section fluctuations meas-
ured on the calibration cone at Mach 0.60. As the porosity of the walls is in-
creased from 0.50% to 5.40%, the amplitude of the narrow band random fluctuations
decreased. The frequency of this narrow band noise rises from 6,000 cps at a
porosity of 0.50% to 10,000 cps at 5.40% porosity. A similar reduction was
applied to calibration cone data taken at a Mach number of 0.90. The results
are shown in Figure 6.13. As in the previous case, the amplitude of the nar-
row band fluctuations decreased with increasing porosity. The frequency of
these fluctuations increased from 8,800 cps at a porosity of 0.75% to 11,000
cps at a porosity of 5.40%.

Correlations were computed to determine the effects of variations of
porosity on the low frequency fluctuations. Data at Mach 0.6 from the cali-
bration cone was reduced between 8 cps and 2,000 cps. Figure 6.14 shows that
the amplitude of these fluctuations decreases with increasing porosity. It is
difficult to determine if the frequency of these narrow band fluctuations in-
crease with increasing porosity. The frequency of these fluctuations is about
130 cps.

Correlations of diffuser pressure fluctuations were also computed. The
objective of these calculations was to establish the behavior of the diffuser
fluctuations and to determine if there is any interaction between the diffuser
and test section fluctuations. The diffuser correlations were first established
for the standard operation of the wind tunnel. The diffuser data that was an-
alyzed by the correlator was obtained both upstream and downstream of the shock
wave. The correlations given on Figure 6.15 correspond to the test section data
given by the level squares in Figure 6.2 and 6.5. The correlator was set to
yield valid data between 8 cps and 20,000 cps. The instrumentation will not
transmit fluctuations above 20,000 cps. The maximum diffuser fluctuations
occur at Mach 0.80 rather than at Mach 1.15 which is the operating condition
for maximum test section fluctuations. From Mach 0.60 through Mach 1.30 the
diffuser fluctuations are periodic with some random oscillations superimposed.
The periodic fluctuations have a frequency of 555 cps at all Mach numbers.
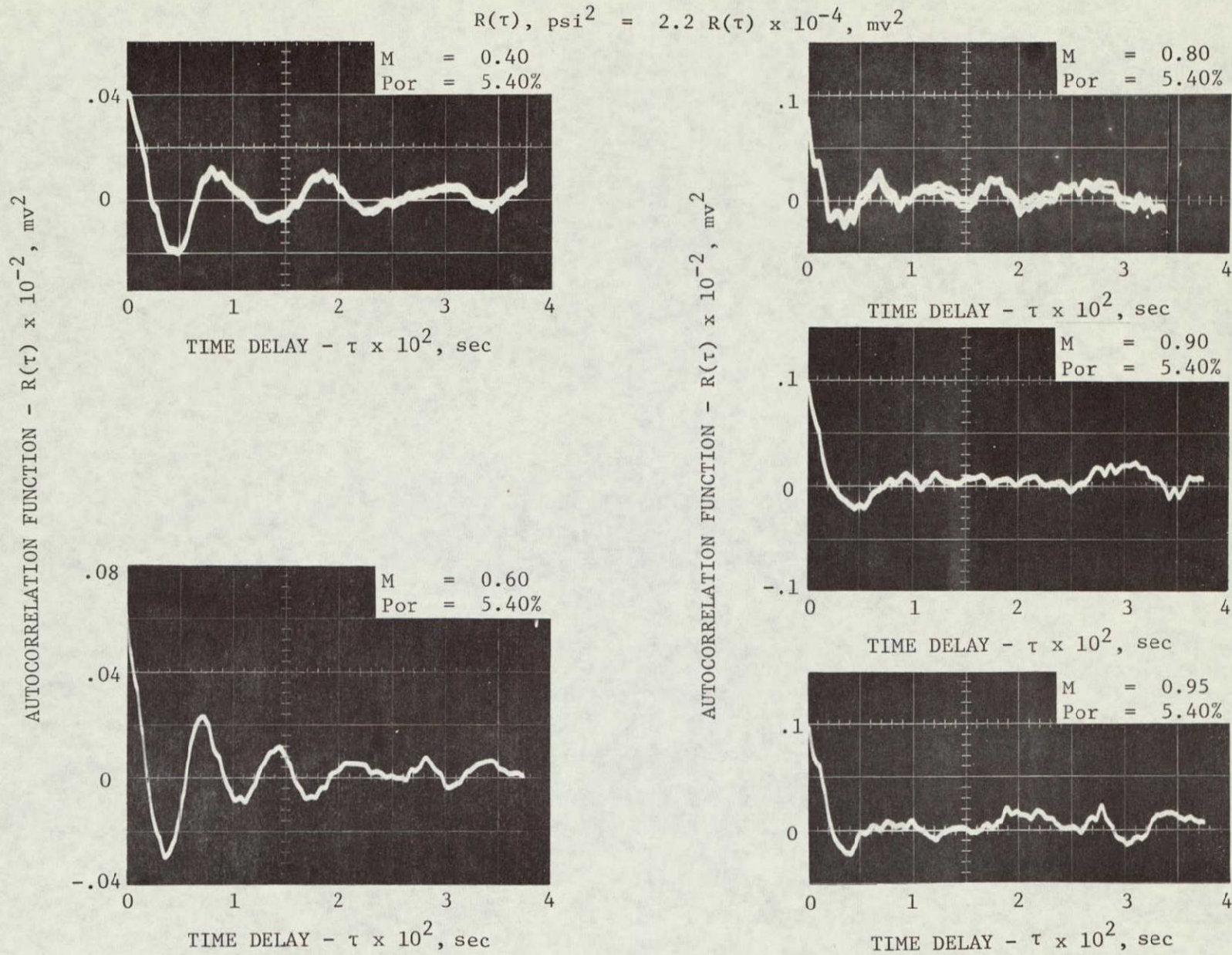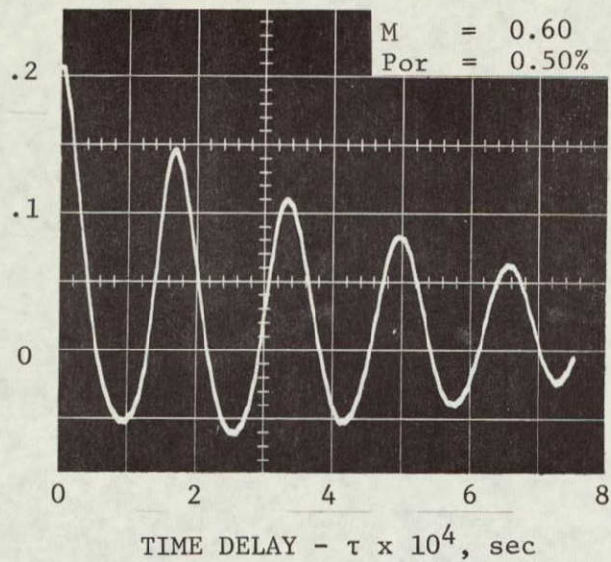Thus, the frequency is independent of Mach number and porosity of the wind tun-
nel.

$$R(\tau), \text{psi}^2 = 2.2\ R(\tau) \times 10^{-4}, \text{mv}^2$$

FIGURE 6.11. EFFECTS OF MACH NUMBER ON TRANSONIC TEST SECTION FLUCTUATIONS
(TRANSDUCER B_3, P_o = 22.0 psi, CONFIGURATION T_1, SONIC BLOCKS)

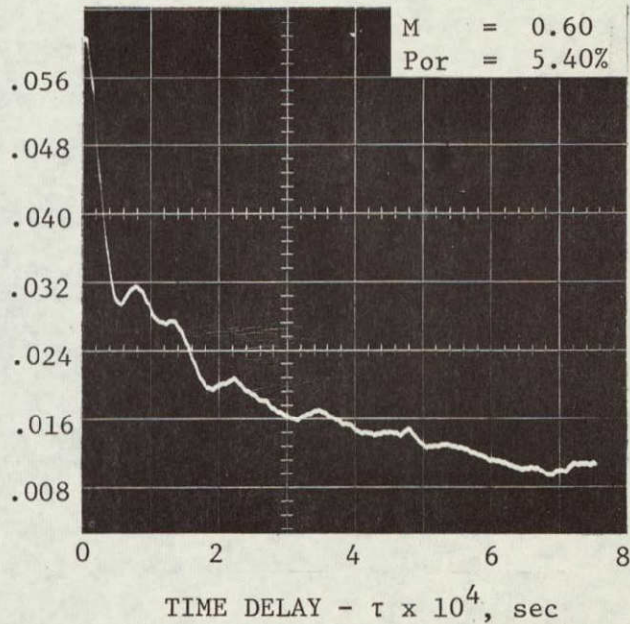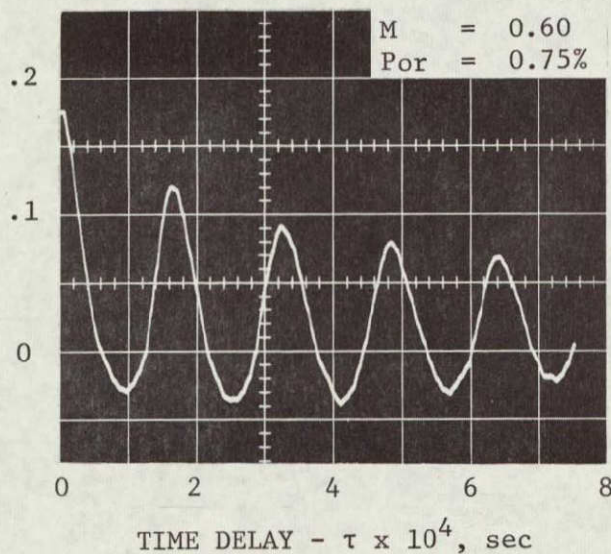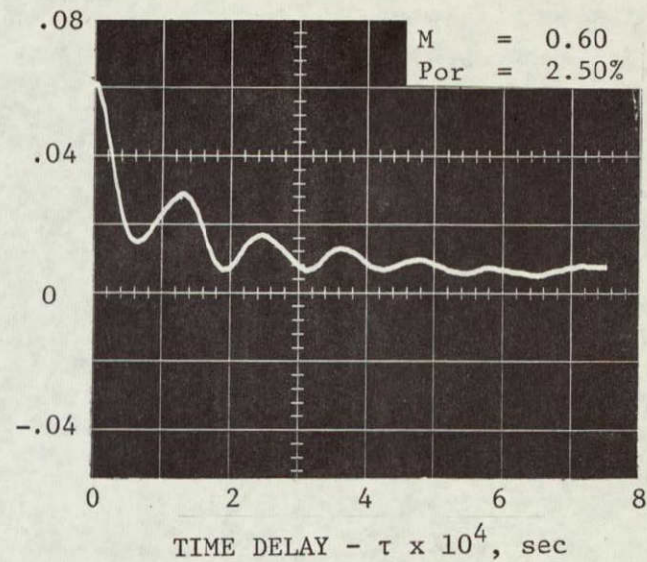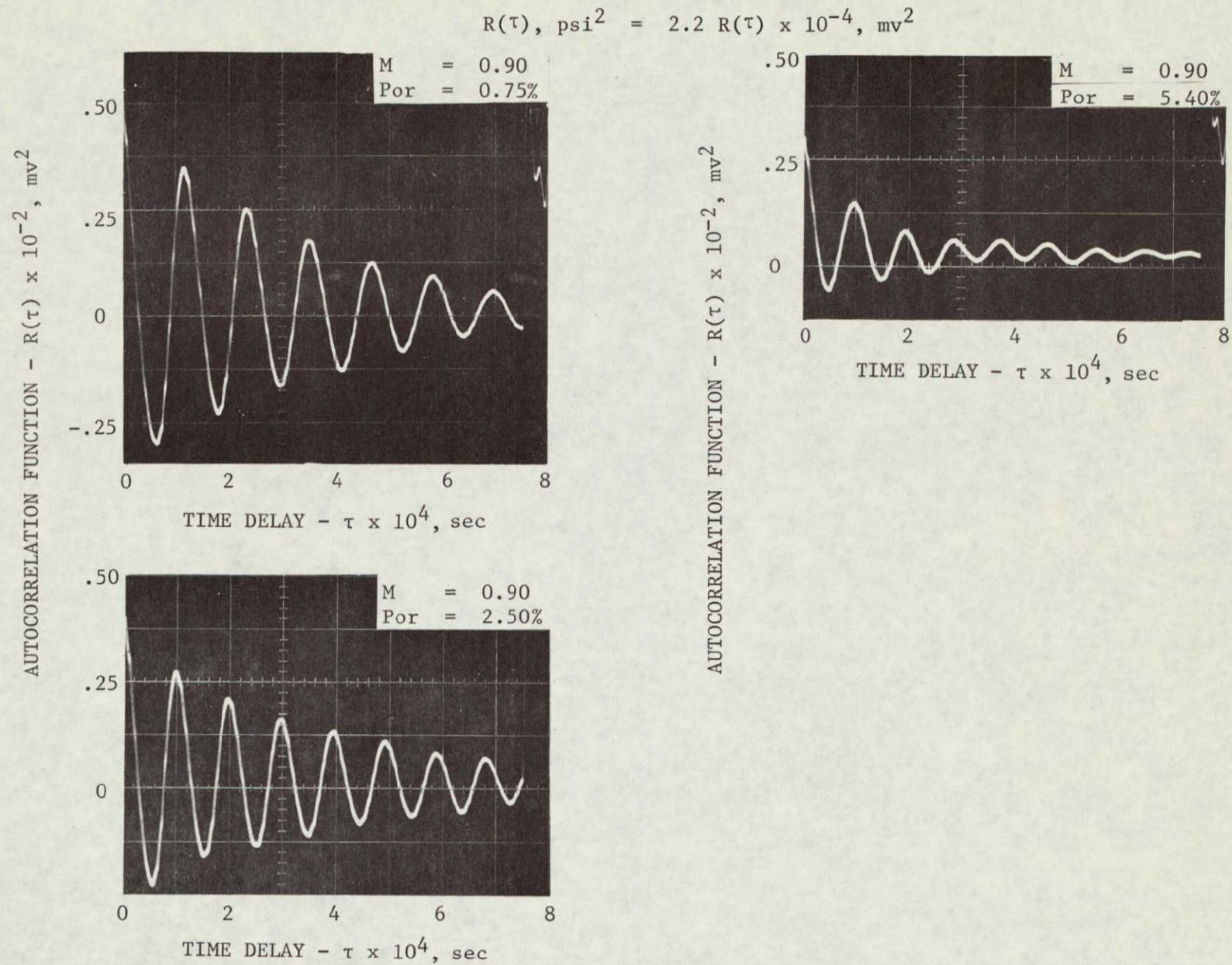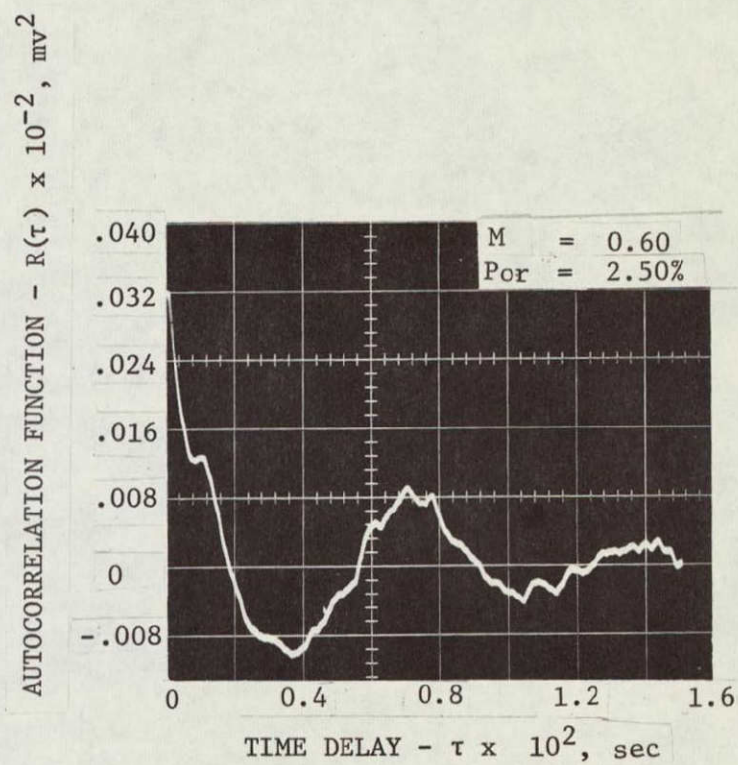$$R(\tau), \text{psi}^2 = 2.2\ R(\tau) \times 10^{-4}, \text{mv}^2$$

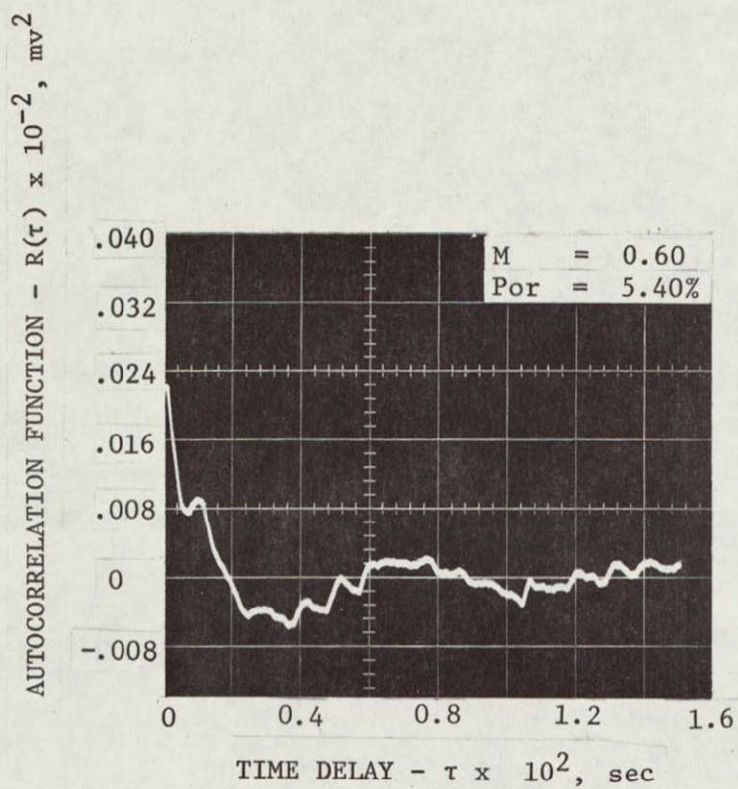FIGURE 6.12.   EFFECTS OF POROSITY ON TRANSONIC TEST SECTION FLUCTUATIONS
(TRANSDUCER B_3, P_o = 14.5 psi, CONFIGURATION T_1, SONIC BLOCKS)

$$R(\tau), \text{ psi}^2 = 2.2\ R(\tau) \times 10^{-4},\ \text{mv}^2$$

FIGURE 6.13.   EFFECTS OF POROSITY ON TRANSONIC TEST SECTION FLUCTUATIONS
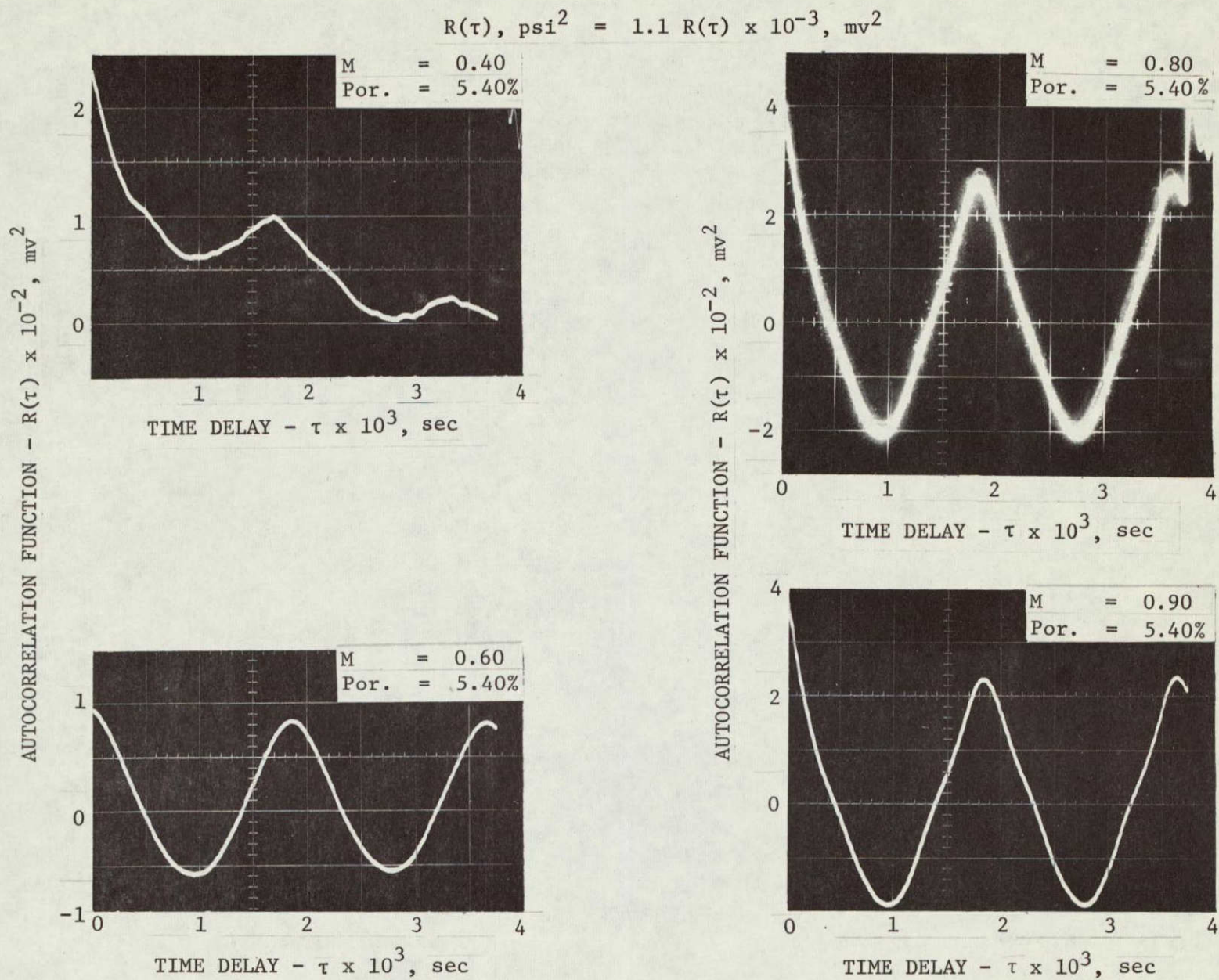(TRANSDUCER B_3, P_o = 14.5 psi, CONFIGURATION T_1, SONIC BLOCKS)

73

$$R(\tau), \ psi^2 \ = \ 2.2 \ R(\tau) \ x \ 10^{-4}, \ mv^2$$

FIGURE 6.14.   EFFECTS OF POROSITY ON TRANSONIC TEST SECTION FLUCTUATIONS
(TRANSDUCER B_3, P_o = 14.5 psi, CONFIGURATION T_1, SONIC BLOCKS)

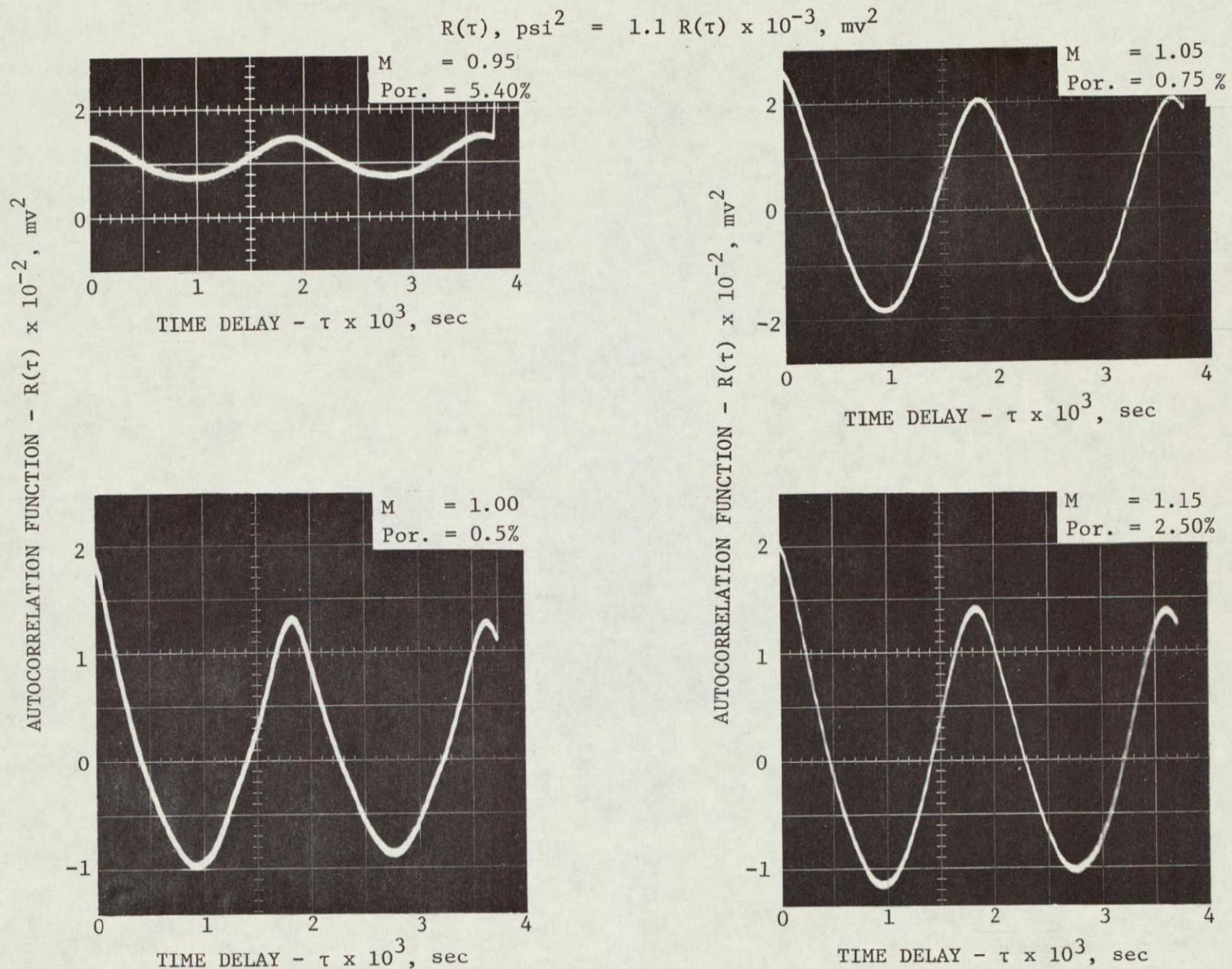$$R(\tau),\ psi^2\ =\ 1.1\ R(\tau)\ \times\ 10^{-3},\ mv^2$$

FIGURE 6.15. EFFECTS OF MACH NUMBER ON DIFFUSER FLUCTUATIONS
(TRANSDUCER K_6, P_O = 22.0 psi, CONFIGURATION T_1,
SONIC BLOCKS)

$$R(\tau), \text{psi}^2 = 1.1 \, R(\tau) \times 10^{-3}, \text{mv}^2$$

M = 0.95
Por. = 5.40%

M = 1.05
Por. = 0.75 %

TIME DELAY – $\tau \times 10^3$, sec

TIME DELAY – $\tau \times 10^3$, sec

M = 1.00
Por. = 0.5%

M = 1.15
Por. = 2.50%

AUTOCORRELATION FUNCTION – $R(\tau) \times 10^{-2}$, mv^2

AUTOCORRELATION FUNCTION – $R(\tau) \times 10^{-2}$, mv^2

TIME DELAY – $\tau \times 10^3$, sec

TIME DELAY – $\tau \times 10^3$, sec

FIGURE 6.15. EFFECTS OF MACH NUMBER ON DIFFUSER FLUCTUATIONS
(TRANSDUCER K_6, P_o = 22.0 psi, CONFIGURATION T_1,
SONIC BLOCKS)

76

$$R(\tau), \text{ psi}^2 = 1.1 \, R(\tau) \times 10^{-3}, \text{ mv}^2$$

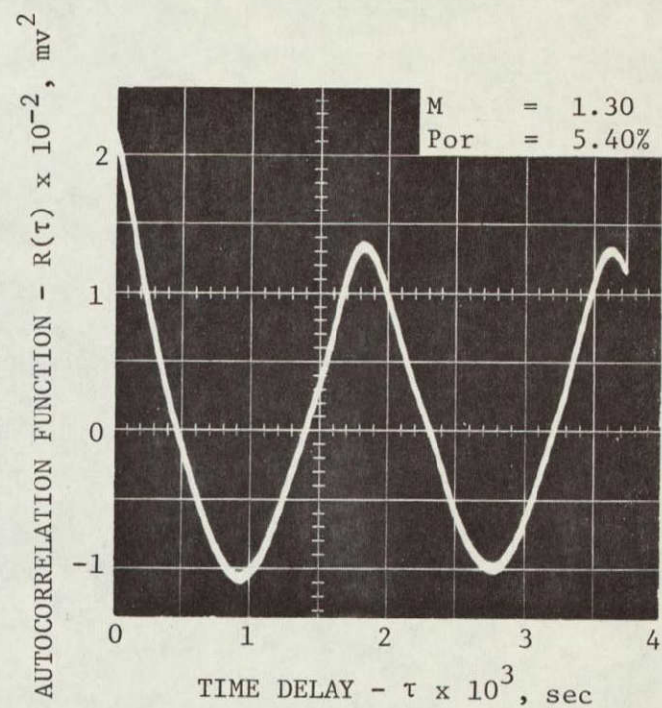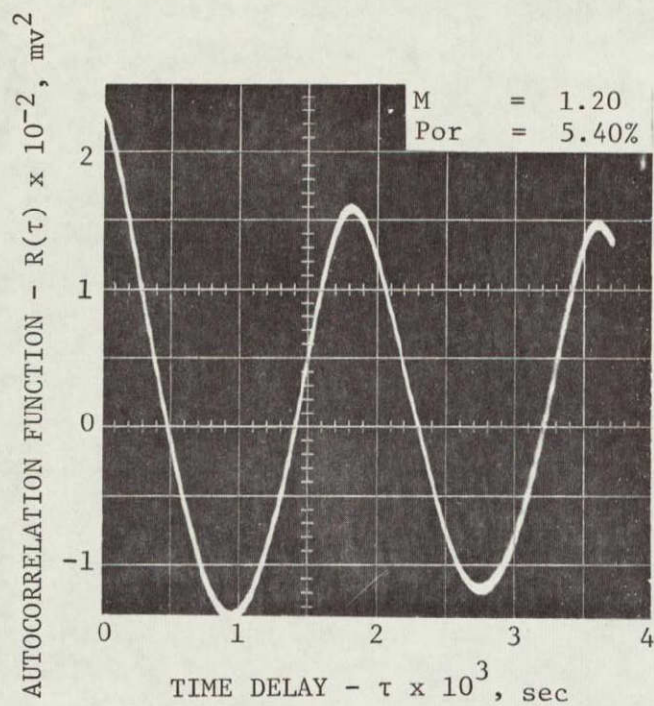
FIGURE 6.15. EFFECTS OF MACH NUMBER ON DIFFUSER FLUCTUATIONS
(TRANSDUCER K_6, P_o = 22.0 psi, CONFIGURATION T_1,
SONIC BLOCKS)

Figure 6.16 shows correlation of diffuser data obtained at Mach 0.90. It provides a comparison of the fluctuations measured during normal tunnel operation with those obtained with the stilling chamber removed. It also yields a comparison of the fluctuations measured during normal tunnel operation with those obtained with the stilling chamber in place, but with the high pressure supply and the control valve removed. In the first two tests solid walls were used. A porosity of 5.40% was used for the third test. The removal of the stilling chamber lowered the magnitude of the diffuse fluctuations in comparison with the standard operating diffuser fluctuations. Replacing the stilling chamber, but excluding the high pressure supply and control valve, again lowered these diffuser fluctuations. The frequency of these fluctuations was unaffected by the changes in wind tunnel configuration and porosity. It remained at a constant 555 cps.

Correlations were made of similar diffuser data obtained at higher Mach numbers with the Mach 1.46 nozzle blocks. The results of the data reduction are given in Figure 6.17. The diffuser fluctuations are about an order of magnitude lower than recorded at Mach 0.9. The data from the standard operating configuration indicates the fluctuations are random with a weak periodic component superimposed. This periodic component has a frequency of 1180 cps. When the tunnel is operated without the stilling chamber, and without the high pressure supply and control valve, the random fluctuations are greatly reduced, but a strong period fluctuation appears. Its frequency is 625 cps.

Additional correlations of diffuser data are given in Figure 6.18. The first correlation is for the transonic test section with the Mach 1.76 nozzle blocks. The tunnel was operated in the standard configuration. The results are comparable to the standard configuration data obtained at Mach 1.46 and shown in the previous figure. Also shown in Figure 6.18 is a correlation of diffuser data taken with the supersonic test section installed and operating at Mach 2.99. The magnitude of this data is greatly reduced and it appears to be completely random.

Correlations were also made of data obtained in the stilling chamber, though they are not shown in this report. The significant finding in this data is that the fluctuations in the stilling chamber are generally random. The only 10,000 to 12,000 cps fluctuations found in the data were in the down stream end of the stilling chamber and they were detected only during the subsonic operation of the wind tunnel. These fluctuations were found to be weak.

Additional correlations of fluctuation data, measured in the stilling chamber and test section, indicate the presence of a weak periodic fluctuation concentration. The frequency of these concentrations range from 600 to 1750 cps, depending on the configuration of the tunnel. These correlations are not given in this report. These fluctuations were never sensed in the diffuser. They may exist in the diffuser, but if they do they are masked by the 555 cps diffuser shock wave oscillation. These fluctuations have been determined to exist in the stilling chamber and test section under a wide variety of conditions. The amplitudes of these fluctuations in the test section are much less than that of the 6,000 to 12,000 cps fluctuations measured here.
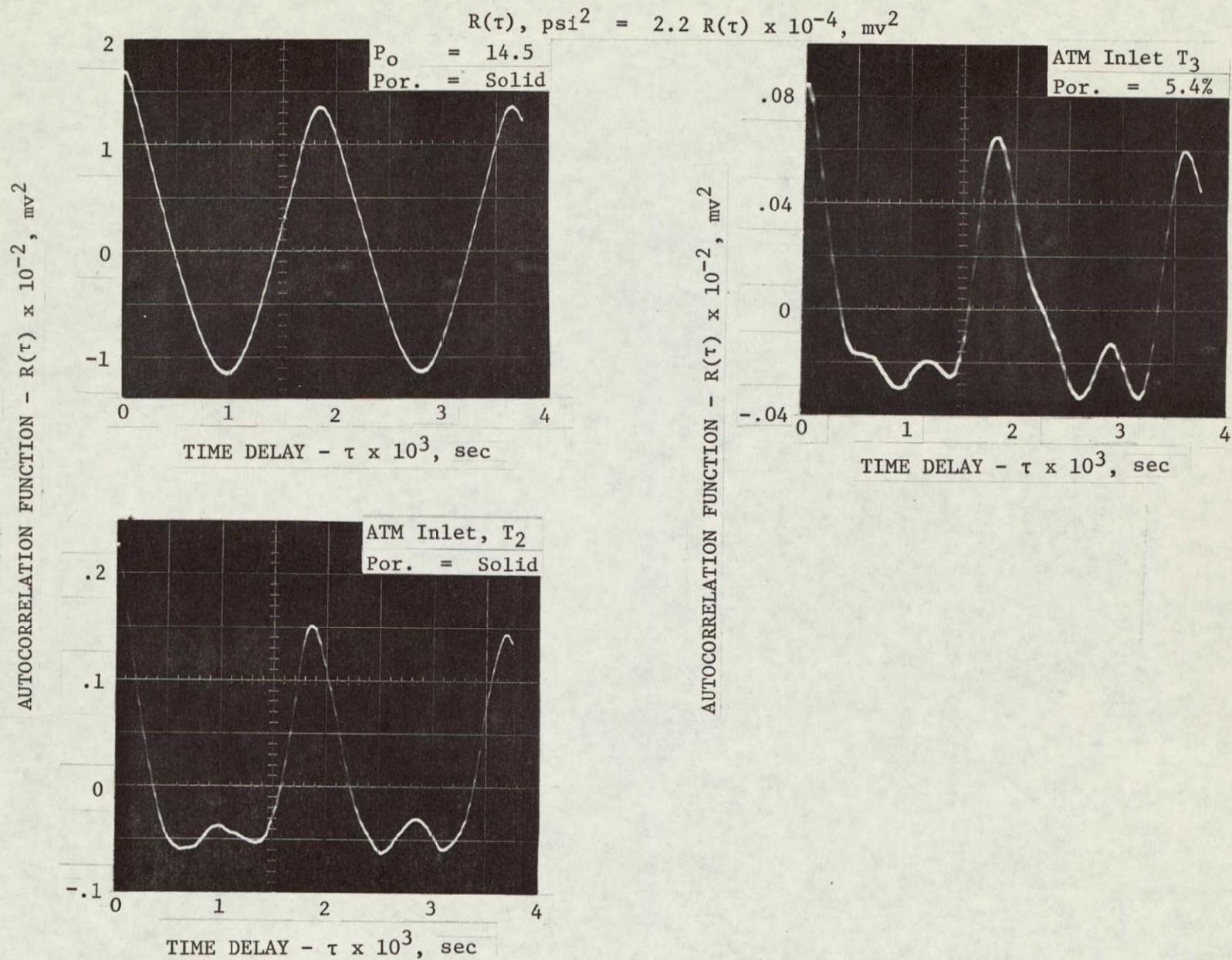
FIGURE 6.16.   EFFECTS OF UPSTREAM TURBULENCE ON DIFFUSER FLUCTUATIONS
(TRANSDUCER K_6, M = 0.9, SONIC BLOCKS)
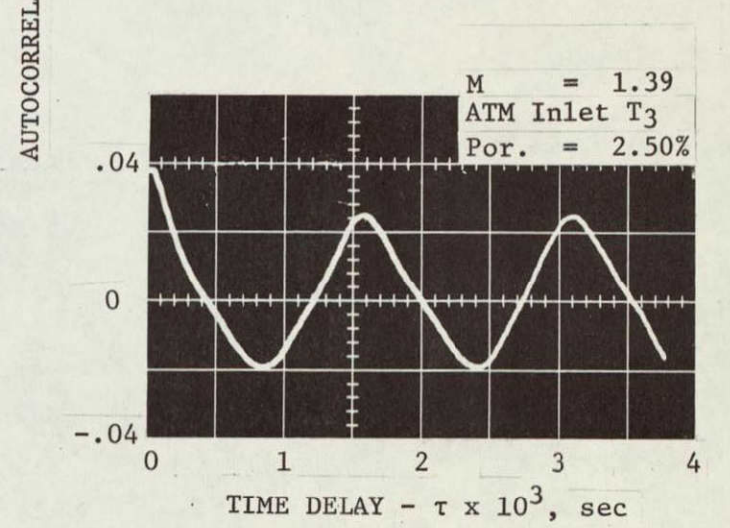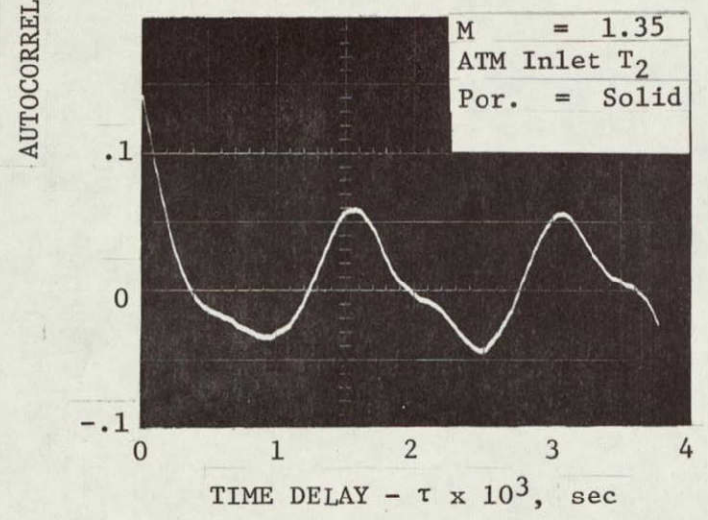
$R(\tau)$, psi^2 = 2.2 $R(\tau)$ x 10^{-4}, mv^2

M = 1.46
P_o = 14.5
Por = Solid

AUTOCORRELATION FUNCTION – $R(\tau)$ x 10^{-2}, mv^2

.2

.1

0

-.05

0   1   2   3   4

TIME DELAY – τ x 10^3, sec

$R(\tau)$, psi^2 = 1.1 $R(\tau)$ x 10^{-3}, mv^2

M = 1.36
ATM Inlet T_3
Por = 5.40%

.04

.02

0

-.02

0   1   2   3   4

TIME DELAY – τ x 10^3, sec

M = 1.35
ATM Inlet T_2
Por. = Solid

.1

0

-.1

0   1   2   3   4

TIME DELAY – τ x 10^3, sec

AUTOCORRELATION FUNCTION – $R(\tau)$ x 10^{-2}, mv^2

M = 1.39
ATM Inlet T_3
Por. = 2.50%
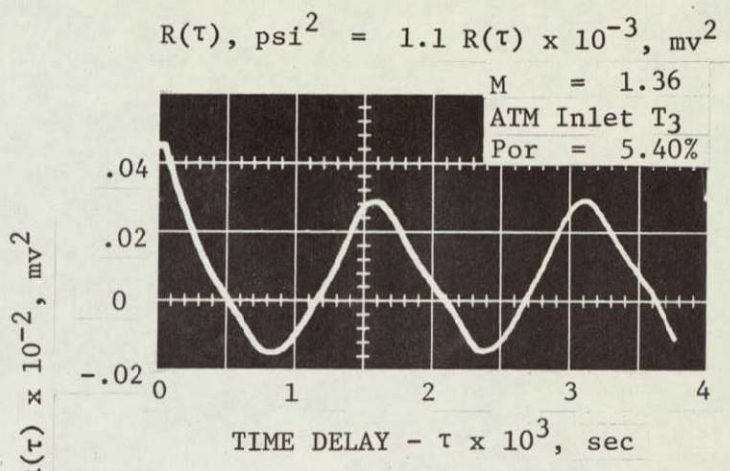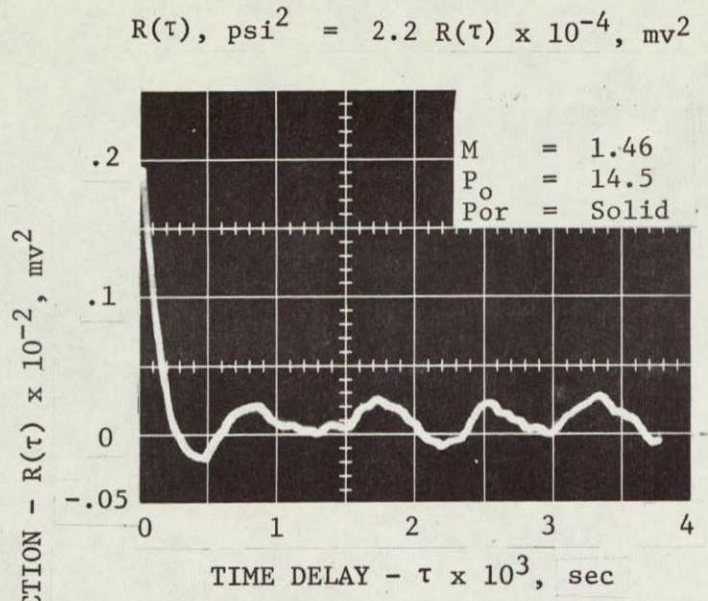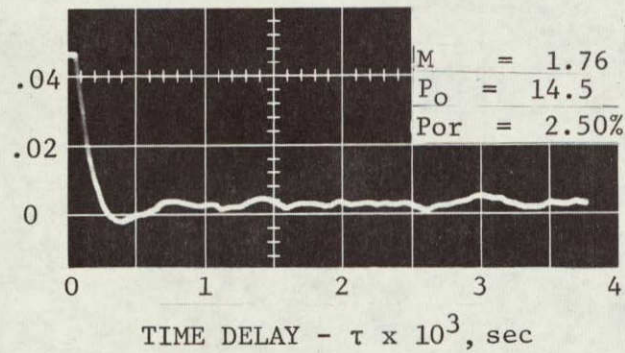
.04

0

-.04

0   1   2   3   4

TIME DELAY – τ x 10^3, sec

FIGURE 6.17.   EFFECTS OF UPSTREAM TURBULENCE ON DIFFUSER FLUCTUATIONS
(TRANSDUCER K_6, BLOCKS FOR MACH 1.46)

80

$$R(\tau), \text{ psi}^2 = 1.1 \, R(\tau) \times 10^{-3}, \text{ mv}^2$$
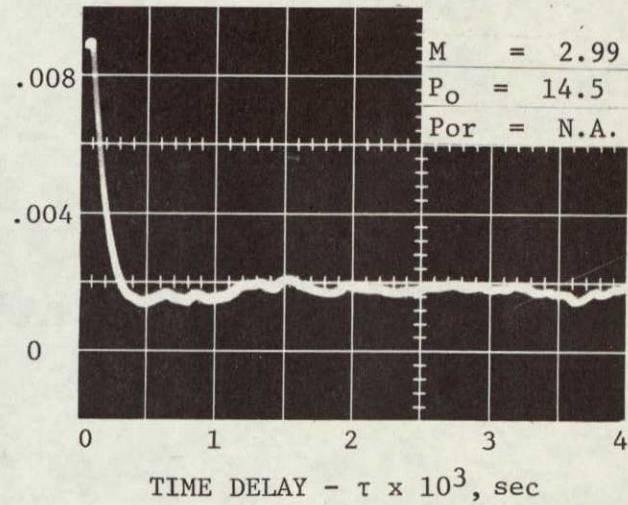
FIGURE 6.18. EFFECTS OF MACH NUMBER ON DIFFUSER FLUCTUATIONS
(TRANDUCER K_6, CONFIGURATION T_1, SUPERSONIC TEST
SECTION)

Several investigations of fluctuations in wind tunnels have been conducted throughout the world. Some of these investigations are described in the introduction of this report. For illustrative purposes, the results of these studies have been reduced to a common basis and presented in tabular form. This is shown in Figure 6.19. The supersonic tunnels are listed first and then followed by the subsonic tunnel. The results of the calibrations of the transonic wind tunnels are given last. The data in these tests was collected by a variety of instrumentation. This instrumentation responds over varying frequency ranges. The Mach number at which the tabulated data was gathered is listed. In each case this is the Mach number for the maximum reported fluctuations. The ratio of the stilling chamber rms pressure fluctuations to the stagnation pressure of the tunnel is given at these Mach numbers. Also given is the rms pressure coefficient in the test section. The results of the calibration of the standard configuration of the MSFC 14 in. wind tunnel is given in the last line at the Mach number of maximum fluctuations. The stilling chamber fluctuation ratio of 0.025 is for the upstream condition and the ratio of 0.003 is for the downstream condition.

A limited amount of frequency data is available from the calibrations reported in the above mentioned literature. The AEDC 16 ft transonic tunnel test data showed a concentration of fluctuations in the 500 to 600 cps range at low transonic Mach numbers. It is not known whether the frequency of these fluctuations changed with Mach number. The calibration of the ONERA 6 ft trisonic tunnel also showed a concentration of fluctuations from Mach 0.62 to Mach 0.85. The frequency of this concentration of fluctuations decreased as the Mach number increased. The oscillations were at 675 cps at Mach 0.62 and 530 cps at Mach 0.81. These fluctuations were virtually eliminated by reducing the porosity of the tunnel.

OPERATOR	LOCATION	CONFIGURATION	TEST SECTION SIZE	MACH NO RANGE	TYPE	WALLS	INSTRUMENTATION	DATA MACH NO	STILLING CHAMBER Prms/Po	TEST SECTION C_p rms
Johns Hopkins University	?	Standard	?	Super-sonic	Continuous Closed Circuit	Solid	Hot Wire	1 76	?	00092 00185
Jet Propulsion Laboratory	Pasadena, Calif	Standard	18x20 in	1 3/5 6	Continuous Closed Circuit	Solid	Hot Wire	1 6	?	0009
University of California	Berkeley Calif	Standard	6x16 in	1 8/2 8	Continuous Closed Circuit	Solid	Dynamic Pressure Transducer	2 4	?	00075
University of Michigan	Ann Arbor, Mich	Standard	6x6 in 8x8 in 12x12 in	Incom-pressible	Continuous Open Circuit	Solid	Hot Wire	Incom-pressible	?	?
National Physics Lab	England	Standard	15x10 in	Incom-pressible	Continuous Open Circuit	Solid	?	Incom-pressible	?	?
AEDC, PWT	Tullahoma, Tenn.	Standard	16x16 ft	0 5/1 6	Continuous Closed Circuit	Porous 6% Porosity	Dynamic Pressure Transducer	0 78	?	024
ONERA	Châtillon France	Standard	6x6 ft	0 2/1 3	Continuous Closed Circuit	Porous	Dynamic Pressure Transducer	0 62/0.91	?	?
ONERA	Châtillon France	1/2 Standard Porosity	6x6 ft	0 2/1 3	Continuous Closed Circuit	Porous	Dynamic Pressure Transducer	0 62/0 91	?	?
Douglas Aircraft Co	El Segundo, Calif	No Muffler	1x1 ft	0 2/1 8	Blowdown	Porous	Dynamic Pressure Transducer	0 75/1 0	025	058
Douglas Aircraft Co	El Segundo, Calif	With Muffler	1x1 ft	0 2/1 8	Blowdown	Porous	Dynamic Pressure Transducer	0 75/1 0	005	022
Douglas Aircraft Co	El Segundo, Calif	With Auxiliary Tanks	1x1 ft	0 2/1 8	Blowdown	Porous	?	?	?	?
National Aero Establishment	Canada	Standard	5x5 in	0 2/4 5	Blowdown	Porous	Dynamic Pressure Transducer	1 2	016	038
Marshall Space Flight Center	Huntsville, Ala	Standard	14x14 in	0 2/5 0	Blowdown	Porous	Dynamic Pressure Transducer	1 05	025/ 003	028

FIGURE 6 19   SUMMARY TABLE OF FLUCTUATING PRESSURE LEVELS IN VARIOUS SUBSONIC, TRANSONIC, AND SUPERSONIC WIND TUNNELS

83

7.0 CONCLUSIONS AND RECOMMENDATIONS

7.1 CONCLUSIONS FROM MSFC 14 IN. TRISONIC TUNNEL TEST

The following conclusions are based on the reduced data from the calibration tests of the MSFC 14 in. trisonic wind tunnel. These data are presented in the previous section. Calibration data from other tests are also used in forming the following conclusions:

- The maximum fluctuations that exist in MSFC 14 in. wind tunnel occur in the transonic flow regime. The rms pressure coefficients in Figure 6.1 and the rms pressures presented in Figures 6.2 through 6.7 illustrate this conclusion. Data in Figure 6.19 show that other transonic tunnels have pressure fluctuations of similar magnitude in this flow regime.

- The major portion of the transonic test section fluctuations consists of a narrow band random fluctuation concentration in the frequency range of 6,000 to 12,000 cps. These fluctuations are apparently generated by the porous walls. Correlation functions computed for this concentration of fluctuations are shown in Figures 6.10, 6.12, and 6.13. Data not presented in this report shows that this fluctuation concentration is transmitted into the stilling chamber for subsonic flow condition. It is also seen from Figures 6.15 through 6.18 that this fluctuation concentration is not detected in the tunnel diffuser. It may exist there but be masked by the large diffuser periodic noise.

- The frequency and magnitude of the 6,000 to 12,000 cps noise is affected by porosity, Mach number, and stagnation pressure. Examination of Figures 6.10, 6.12, and 6.13 shows the effects of Mach number and porosity. The stagnation pressure primarily affects the magnitude of these fluctuations.

- The strong test section fluctuations between 6,000 and 12,000 cps in the MSFC 14 in. tunnel is similar to fluctuation concentrations found in other wind tunnels. In the AEDC 16 ft wind tunnel a strong fluctuation between 500 and 600 cps is measured in the test section. Another concentration of fluctuations occurs between 1500 and 2500 cps in the AEDC 16 ft test section. In the ONERA 6 ft tunnel a strong fluctuation concentration between 500 and 800 cps is found in the test section. It is shown in Reference [13] that this frequency is a function of porosity. It is concluded that porous walls are a significant source of background noise in the ONERA tunnel.

- The 6,000 to 12,000 cps fluctuation concentration does not appear, under similar test conditions, in the wind tunnel test section when the solid walls are installed.

- The above fact leads to the conclusion that the 6,000 to 12,000 cps fluctuation concentration is a porous wall phenomena.

- It was also found that the porous wall vibrations shown in Figure 6.6 exist in the 6,000 to 12,000 cps frequency range.

- The upstream turbulence level has a significant effect on the magnitude of the 6,000 to 12,000 cps fluctuations. Examination of the fluctuation magnitudes for three separate tunnel configurations demonstrates this. Figure 6.3 shows the rms pressure in the test section for tunnel operations T_1, T_2, and T_3. Tunnel configuration T_2 is an atmospheric inlet at the nozzle entrance. This is a sharp lip inlet and considerable turbulence is generated. At Mach number 0.9 it is seen on Figure 6.3 that the overall test section fluctuations are approximately equal for high upstream turbulence cases T_1 and T_2. While in tunnel configuration T_3 (a low upstream turbulence level exist for this tunnel configuration), the test section noise has been significantly reduced for similar test conditions.

- Periodic fluctuations of 555 cps appear in the tunnel diffuser. These fluctuations are generated by the diffuser shock wave. The frequency of this shock wave oscillation is not effected by other tunnel parameters in the transonic flow regime. Figures 6.15 through 6.18 substantiate this conclusion.

- The 555 cps fluctuations are also significantly affected by upstream turbulence. Figure 6.16 shows the correlation function for similar test conditions for tunnel configurations T_1, T_2, and T_3. It is seen that there is almost an order of magnitude difference between T_1 and T_2 and between T_2 and T_3. The frequency is, however, unaffected

- Another fluctuation concentration exist in the test section, nozzle, and stilling chamber. These fluctuations are essentially periodic with frequencies from 500 to 1750 cps. The source of this is not known. It probably cannot be traced until the 6,000 to 12,000 cps and the 555 cps fluctuations are reduced or eliminated.

- The 500 to 1750 fluctuations exist under all tunnel operating configurations (i.e., T_1, T_2, T_3, $T_{1,4}$, and $T_{2,4}$). Therefore, it is difficult to isolate the source of these fluctuations.

7.2 RECOMMENDATIONS FOR IMPROVEMENT OF MSFC 14 IN. TUNNEL

It is apparent from the above discussion and the figures of Section 6.0 that there is a major source of noise in the wind tunnel test section and the diffuser. It is also shown in the previous discussion that the major test section noise is caused by the porous walls and that it is a function of porosity. It is therefore recommended that:

- A series of tests be conducted to determine the optimum porosity setting of the test section walls with reference to fluctuating pressures.

- A study be conducted into the effects of the porous wall hole angle, shape, and sizes with regard to the pressure fluctuations and test section relief.

- An investigation should be conducted into the possibility of using solid walls composed of a material with high permeability.

Previous discussion has shown that the upstream turbulence level affects the test section noise and the diffuser noise. It is therefore recommended that additional screening be installed in the tunnel stilling chamber to lower the broad band turbulence generated by the wind tunnel valve.

It is also shown in previous discussion that a contributor to the tunnel noise is the diffuser shock. It is recommended that:

- A shock wave stabilization device be designed to fit in the existing wind tunnel diffuser.

- During dynamic testing care should be taken in interpreting results in the frequency range near 550 cps in the subsonic flow regime.

7.3 OVERALL CONCLUSIONS AND RECOMMENDATIONS OF THE STUDY

It was found that the existing transonic wind tunnels all have an appreciable pressure fluctuation in their test sections. These fluctuations are generated by a variety of sources. Two of the more significant sources are the porous walls and the diffuser. It was also found that it is not necessary to accept the high fluctuating levels now existing in transonic wind tunnels. The test section fluctuations can be significantly reduced, in the transonic regime, by changing the wall porosity. The upstream turbulence was found to severely affect the fluctuations generated in the test section and diffuser. It is, therefore, concluded that reducing the magnitude of the broad band turbulence that exists forward of the test section will result in lower background fluctuations in the test section. Stabilizing the diffuser shock wave will also reduce the overall level of fluctuations in the wind tunnel.

REFERENCES

1. Uberoi, Mahinder S., "Effects of Wind-Tunnel Contraction on Free-Stream Turbulence," *Journal of the Aeronautical Sciences*, Vol. 23, No. 8, August 1956, pp. 754 - 764.

2 Morkovin, Mark V., "On Transition of Moderate Supersonic Speeds," *Journal of the Aeronautical Sciences*, Vol. 24, No. 7, July 1957, pp. 480 - 486.

3. Murphy, J. S., "Pressure Fluctuations in the Trisonic One-Foot Tunnel, Douglas Wind Tunnel Technical Memorandum Number 28, March 4, 1958, Douglas Aircraft Company, El Segundo, California.

4. Murphy, J. S., "Pressure Fluctuations in a Blowdown Wind Tunnel," *Journal of the Aero/Space Sciences*, Vol. 26, No. 1, January 1959, pp. 61 - 62.

5. Laufer, John, "Aerodynamic Noise in Supersonic Wind Tunnels," *Journal of the Aerospace Sciences*, Vol. 28, No. 9, September 1961, pp. 685 - 692.

6. Irani, P. A., and Iya Sridhar K., "Aerodynamic Noise in Aircraft and Wind Tunnels," N64-20438, Scientific Review No. SR-AE-2-63, August 1963, National Aeronautical Laboratory, Bangalore, India.

7. Murphy, J. S., Bies, D. A., and Speaker, W. W., "Wind Tunnel Investigation of Turbulent Boundary Layer Noise as Related to Design Criteria for High Performance Vehicles," NASA TN-D-2247, April 1964, National Aeronautics and Space Administration, Washington, D. C.

8. Bossel, Hartmut, "Flow Studies and Turbulence Measurements In the Hesse 6-Inch Supersonic Wind Tunnel," Report No. AS-67-2, February 1967, College of Engineering, University of California, Berkeley, California.

9. Unpublished Test Data, "Martin Company Titan III B/Agena 6% Pressure Model Test Data Obtained in the AEDC 16 ft Transonic Wind Tunnel," Obtained from P. Howard, NASA, MSFC, R-AERO-AU, Unsteady Aerodynamics Branch.

10. Riddle, C. D., "Investigation of Free-Stream Fluctuating Pressure in the 16 ft Tunnel of the Propulsion Wind Tunnel Facility," AEDC TR-67-167, August 1967, ARO, Inc., Tullahoma, Tennessee.

11. Boone, James R. and McCanless, George F., "Evaluation of the Acoustic Sources of Background Noise in Wind Tunnel Facilities," Technical Report HSM-R65-68, June 1968, Chrysler Huntsville Operations, Huntsville, Alabama.

12. Wills, J. A. B., "Spurious Pressure Fluctuations in Wind Tunnels," NPL AERO Report 1237, July 1967, <u>Aeronautical Research Journal, Noise Research Committee</u>.

13. Christopher, J. M. and Loniewski, J. M., "Reduction of Pressure Fluctuations in a Transonic Test Section," (ONERA, TP No. 567, 1968, Chatillon-sous-Begneux, Hauts-de Seine, France) April 22 – 23, 1968, <u>Supersonic Tunnel Association</u>, 29th Meeting, Silver Springs, Maryland.

14. Simon, Erwin, "Calibration Tests of the MSFC 14 x 14 Inch Trisonic Wind Tunnel," NASA TM X-53113, August 20, 1964, George C. Marshall Space Flight Center, Huntsville, Alabama.

15. Simon, Erwin, "The George C. Marshall Space Flight Center's 14 x 14 Inch Trisonic Wind Tunnel Technical Handbook," NASA TM X-53185, December 22, 1964, George C. Marshall Space Flight Center, Huntsville, Alabama.

16. Anonymous, "Arnold Center Test Facilities Handbook," January 1, 1961, Arnold Center, Arnold Air Force Station, Tennessee.

17. Van Driest, E. R., "Calculation of the Stability of the Laminar Boundary Layer in a Compressible Fluid on a Flat Plate with Heat Transfer," <u>Journal of the Aeronautical Sciences</u>, Vol. 19, No. 12, December 1952, pp. 801 – 812.

BACKGROUND PRESSURE FLUCTUATIONS

IN WIND TUNNELS

By: _James R. Boone_

By: _George F. McCanless, Jr._

Approved: _M. L. Bell_
Manager, Aero-Space Mechanics
Branch

Approved: _H. Bader, Jr._
Chief Engineer, Structures
and Mechanics Engineering
Department